Out-of-hospital ventricular fibrillation waveform analysis: Towards a multi-lead defibrillator for in-field detection of acute myocardial infarction

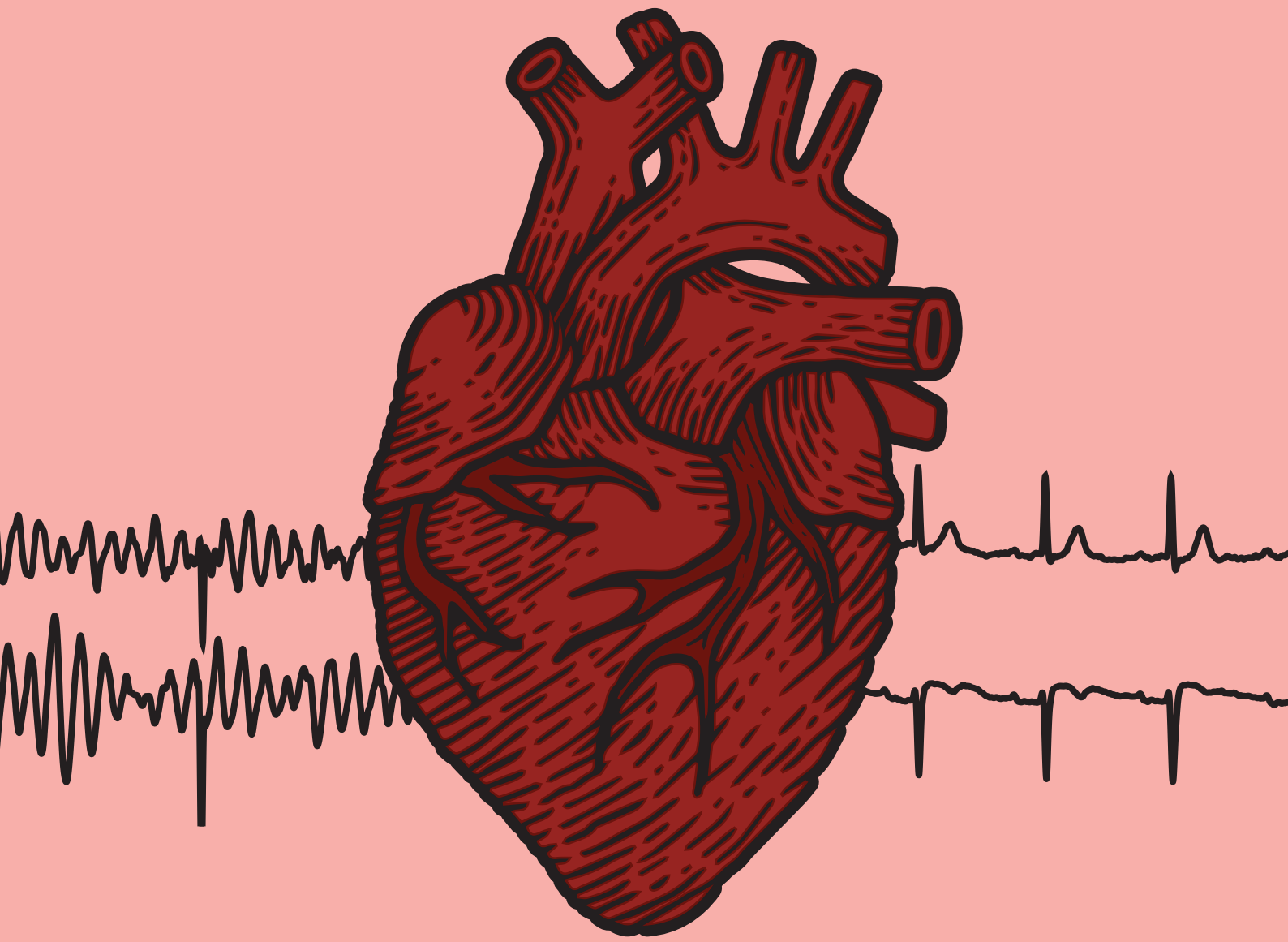

K.M. van der Sluijs

Out-of-hospital ventricular fibrillation waveform analysis: Towards a multi-lead defibrillator for in-field detection of acute myocardial infarction

---

Master Thesis Technical Medicine

September 29, 2020

Author
K.M. van der Sluijs (Koen)

Graduation committee

Chairman:	prof.dr. H.J. Zwart
Medical supervisor:	dr. M.A. Brouwer
Technical supervisor:	prof.dr. H.J. Zwart
Technical medicine supervisor:	J. Thannhauser, MSc
Process supervisor:	E.M. Walter, MSc
External member:	dr.ir. B.E. Westerhof

University of Twente, Enschede
Faculty: Science and Technology
Programme: Technical Medicine
Track: Medical Sensing & Stimulation

Radboud University Medical Center, Nijmegen
Department: Cardiology

UNIVERSITY OF TWENTE.

Radboudumc

Acknowledgements

Nijmegen, 29 september 2020

In juni 2018 kwam ik voor mijn tweede M2 stage terecht bij het Radboudumc in Nijmegen, bij de afdeling cardiologie. Door de goede ervaringen koos ik ervoor om mijn afstuderen op dezelfde plek te doen en mijn opleiding Technische Geneeskunde hier af te ronden. Uiteraard speelden mijn interesse in de cardiologie en het reanimatieonderzoek daarin mee, maar de gemoedelijke, toegankelijke en ontspannen sfeer hebben hier ook zeker aan bijgedragen. Inmiddels komt het eind van mijn afstuderen in zicht en kijk ik terug op een leuk en leerzaam jaar. Hiervoor wil ik een aantal mensen bedanken.

Jos, allereerst wil ik jou bedanken. Je bent enthousiast, toegankelijk en niet vies van een geintje. De prettige omgang die daaruit is voortgekomen heeft ervoor gezorgd dat ik me thuis heb gevoeld op de afdeling en dat ik met plezier naar stage ging. Toen dat laatste niet meer kon door COVID-19 zorgde jouw enthousiasme tijdens onze wekelijkse meetings steeds voor een dosis motivatie om door te blijven gaan. In de beginfase van mijn afstuderen was jouw hulp erg waardevol bij het opstellen van een concrete afstudeeropdracht. Zonder die sturing was ik nu waarschijnlijk nog bezig geweest met mijn werkplan ;). Daarnaast heb je me geleerd om stil te staan bij “waarom” iets is zoals het is, in plaats van het meteen voor waar aan te nemen en er niet verder over na te denken. Bedankt voor de fijne samenwerking en de intensieve begeleiding!

Marc, bedankt voor alle leerzame inzichten die je me gebracht hebt. “Hoe minder je me ziet, hoe beter het gaat met je onderzoek.” Op de weinige momenten dat we elkaar zagen kwam je altijd met nuttige toevoegingen en inspirerende gedachten vanuit jouw medische kijk naar het probleem. Ook in de kliniek heb ik veel van je kunnen leren, mede doordat je de moeite nam om daar tijd en ruimte voor vrij te maken.

Hans, bedankt voor uw rol als technisch begeleider en procesbewaker. Ik heb onze gesprekken altijd als prettig ervaren, fijn dat u daar steeds zoveel tijd voor wilde nemen. Door uw technische blik werd duidelijk dat niet al mijn plannen even realistisch waren. Bedankt voor uw begeleiding en het bijsturen en haalbaar houden van mijn afstudeeropdracht.

Elyse, bedankt voor de goede procesbegeleiding. Door jouw oprechte en betrokken houding heb je me uitgedaagd om mezelf op persoonlijk vlak te ontwikkelen en na te denken over wat ik wil in mijn leven. Jorik, bedankt voor de leuke, blikverruimende intervisiegesprekken en de feedback op alle reflectieverslagen.

Berend, bedankt voor het deelnemen in mijn afstudeercommissie als buitenlid.

Sarah, bedankt voor het zijn van een leuke collega. Alle koffie-, thee- en lunchpauzes samen met jou en de andere studenten zorgden voor de nodige ontspanning, alhoewel die soms juist extra werk bezorgden (COFFEE trial). Daarnaast was jij mijn eerste aanspreekpunt voor vragen, waarmee je me altijd graag wilde helpen.

Na zeven mooie jaren ga ik met een goed gevoel mijn studententijd afsluiten. Ik ben benieuwd wat de toekomst mij gaat brengen!

Koen van der Sluijs

Summary

Globally, 34.7 per 100,000 inhabitants suffer from out-of-hospital cardiac arrest (OHCA) each year, of which approximately 30% presents with a cardiac rhythm of ventricular fibrillation (VF). Less than 20% survives; the only available therapy is defibrillation, aimed at achieving a return of spontaneous circulation. The most frequent underlying cause of VF is acute myocardial infarction (AMI). In-field identification of AMI could individualise resuscitation care and improve survival.

The paddle electrocardiogram (ECG) recorded by the defibrillator provides unique, patient-specific information in an early phase of the arrest. Quantified using ventricular fibrillation waveform characteristics, the VF-waveform on the ECG can be analysed in real-time. Research suggests that VF-morphology is affected by old myocardial infarction (OMI) and even more by AMI. Studies have therefore focused on detecting OMI as a surrogate for AMI. A proof-of-concept machine learning study applying waveform analysis on 12-lead ECGs of VF induced for implantable cardioverter-defibrillator testing showed that lead II could identify OMI and that detection improved when twelve leads were used. This method lacked an optimisation of input features and did not combine specific leads.

The first aim of this thesis was to investigate the effect of established feature selection methods on the ability of support vector machines to discriminate between patients with (n=137) and without (n=105) OMI. Models of lead II, twelve leads and lead II + V_1 reached an area under the curve (AUC) of 0.58, 0.83 and 0.76 respectively. The results showed that feature selection and additional leads improved the detection of OMI. The main limitation was that VF was induced electrically, indicating that these methods require validation in the out-of-hospital setting with spontaneous VF and AMI.

The second aim was to assess the performances of similar models based on the paddle ECG in a real-world OHCA cohort to discriminate between patients with (n=62) and without (n=40) AMI. Models based on a single VF segment of the resuscitation reached AUCs of 0.74 and 0.72. A model including both segments had an AUC of 0.76. Incorporating the evolution of the VF-waveform over time and including organisation-related measures led to an acceptable detection of AMI using the paddle ECG.

Concluding, this thesis demonstrated that selecting relevant features of multiple ECG leads and segments improves the detection of myocardial infarction. Clinical implementation of multi-lead models that detect AMI during the arrest is the next step to facilitate individualised OHCA treatment and improve survival.

Samenvatting

Wereldwijd zijn er elk jaar 34.7 gevallen van een hartstilstand buiten het ziekenhuis per 100.000 inwoners, waarvan ongeveer 30% het hartritme ventrikelfibrilleren (VF) heeft. Minder dan 20% overleeft het; de enige beschikbare behandeling is defibrillatie, met als doel om de spontane circulatie te herstellen. De meest voorkomende onderliggende oorzaak van VF is een acuut hartinfarct (AHI). Het ter plaatse herkennen van een AHI zou de reanimatiezorg kunnen individualiseren en de overleving verbeteren.

Het defibrillator elektrocardiogram (ECG) biedt unieke, patiënt-specifieke informatie in de vroege fase van de hartstilstand. De golfvorm van het VF op het ECG kan worden gekwantificeerd met VF-golfvorm karakteristieken die *live* kunnen worden geanalyseerd. Onderzoek heeft aangetoond dat zowel een oud hartinfarct (OHI) als een AHI de VF-morfologie verandert. Studies hebben zich daarom in het verleden gericht op het herkennen van OHI als surrogaat voor AHI. Een *proof-of-concept* studie heeft met *machine learning* aangetoond dat VF-golfvorm analyse van afleiding II van het 12-afleidingen ECG een OHI kon detecteren en dat de detectie beter werd met het gebruik van twaalf afleidingen. Het VF werd hierbij elektrisch opgewekt tijdens het testen van implanteerbare cardioverter-defibrillatoren. Bij deze *machine learning* methode werd de invoer niet geoptimaliseerd en werden specifieke combinaties van afleidingen niet onderzocht.

Het eerste doel van deze thesis was om te onderzoeken wat het effect is van veelgebruikte invoerselectiemethoden op het vermogen van *support vector machines* om patiënten met OHI (n=137) te onderscheiden van patiënten zonder OHI (n=105). Modellen van afleiding II, twaalf afleidingen en afleidingen II + V_1 behaalden een oppervlakte onder de *receiver operating characteristic* van respectievelijk 0,58, 0,83 en 0,76. De resultaten lieten zien dat invoerselectie en het gebruik van extra afleidingen de detectie van OHI verbeterden. De hoofdlimitatie was dat VF elektrisch werd opgewekt, waardoor er validatie nodig is buiten het ziekenhuis aan de hand van spontaan VF en AHI.

Het tweede doel was om te onderzoeken wat het vermogen is van soortgelijke modellen om patiënten met AHI (n=62) te onderscheiden van patiënten zonder AHI (n=40), op basis van het defibrillator ECG in een cohort van patiënten met een hartstilstand buiten het ziekenhuis. Modellen op basis van één VF segment uit de reanimatie behaalden een oppervlakte onder de *receiver operating characteristic* van 0,74 en 0,72. Een model op basis van beide segmenten behaalde een oppervlakte onder de *receiver operating characteristic* van 0,76. Het meenemen van de VF-golfvorm veranderingen door de tijd en het toevoegen van organisatie-gerelateerde maten zorgde voor acceptabele detectie van AHI aan de hand van het defibrillator ECG.

Concluderend, in deze thesis is aangetoond dat het selecteren van relevante variabelen uit meerdere ECG afleidingen en segmenten de detectie van hartinfarcten verbetert. Klinische implementatie van modellen met meerdere afleidingen die AHI detecteren tijdens een hartstilstand buiten het ziekenhuis is de volgende stap om reanimatiezorg te individualiseren en overleving te verbeteren.

Contents

List of abbreviations

$\Delta_{1,2}$ differences between the VFWC of VF_1 and VF_2.

f_s sampling frequency.

ACS acute coronary syndrome.

AED automated external defibrillator.

AMI acute myocardial infarction.

AMSA amplitude spectrum area.

AP action potential.

AUC area under the curve.

BW bandwidth.

CAD coronary artery disease.

CAG coronary angiography.

CPR cardiopulmonary resuscitation.

CRT-D cardiac resynchronisation therapy-defibrillator.

DFA detrended fluctuation analysis.

ECG electrocardiogram.

EMS emergency medical services.

FD dominant frequency.

FFT fast Fourier transform.

flucmaa mean absolute amplitude of the upper envelope derivative.

flucmean mean of the upper envelope.

flucrms root-mean-square of the upper envelope derivative.

flucvar variance of the upper envelope.

FM median frequency.

ICD implantable cardioverter-defibrillator.

LL log-likelihood.

MAA mean absolute amplitude.

MI myocardial infarction.

MMC maximal margin classifier.

MS median slope.

MVR multivariate logistic regression.

NSTEMI non-ST-elevation myocardial infarction.

OHCA out-of-hospital cardiac arrest.

OHVF out-of-hospital ventricular fibrillation.

OI organisation index.

OMI old myocardial infarction.

PCI percutaneous coronary intervention.

PSA power spectrum area.

PSD power spectral density.

Radboudumc Radboud University Medical Center.

ROC receiver operating characteristic.

ROSC return of spontaneous circulation.

SCA sudden cardiac arrest.

SCD sudden cardiac death.

STEMI ST-elevation myocardial infarction.

SVC support vector classifier.

SVM support vector machine.

VF ventricular fibrillation.

VF_1 last segment before the first defibrillation shock.

VF_2 last segment before the second defibrillation shock.

VFWC ventricular fibrillation waveform characteristics.

VT ventricular tachycardia.

List of figures

List of tables

1 | Introduction

The global incidence rate of out-of-hospital cardiac arrest (OHCA) treated by the emergency medical services is estimated to be 34.7 per 100.000 person-years[1,2]. Nearly 30% of OHCA patients presents a cardiac rhythm of ventricular fibrillation (VF), of which 17.3% survives to hospital discharge, more than twice as much as the survival of patients with other rhythms[1,2]. Early cardiopulmonary resuscitation (CPR) at the scene of the arrest and use of automated external defibrillators are the cornerstone of cardiac arrest care and main contributors of favourable outcome[2–6]. A resuscitation attempt is currently protocolised and aimed at achieving a return of spontaneous circulation (ROSC)[7]. An individualised approach of treating patients before ROSC is achieved is therefore uncommon, yet it might for some patients improve survival chances.

The most frequent underlying cause of OHCA is acute myocardial infarction (AMI), as myocardial ischaemia induces phenomena that may initiate and perpetuate VF[7–13]. Eliminating ischaemia by means of intervention therefore seems important when attempting to terminate the arrhythmia and prevent its recurrence. Novel treatment pathways have been proposed for patients without ROSC using mechanical CPR devices and extracorporeal life support. Early transportation and intervention according to this method have recently shown to improve survival in patients with AMI as the underlying cause of refractory VF[10]. A method to effectively treat OHCA patients with AMI thus seems available. In-field identification of patients that may benefit from such an aggressive treatment strategy remains a challenge, however.

The paddle electrocardiogram (ECG) of the defibrillator provides unique, patient-specific information in an early phase of the arrest. The waveform on the ECG may be quantified using ventricular fibrillation waveform characteristics (VFWC). Animal studies suggest that VF-morphology is affected by old myocardial infarction (OMI) and even more by AMI. In both cases, presence of myocardial infarction (MI) was associated to lower amplitude and frequency characteristics[14–18]. In humans, similar VF-waveform changes have been described in presence of OMI and AMI[19–22]. Because of this similarity, OMI has previously been used as a surrogate when investigating the mechanism by which AMI affects the VF-waveform. VF-waveform analysis thus offers a way to detect AMI that is worth exploring. Chapter 3 presents a literature overview on the current status and future perspectives of VF-waveform analysis for the detection of AMI.

A study on 12-lead ECGs of VF obtained while testing implantable cardioverter-defibrillators has shown that MI-related waveform changes occur predominantly in the leads directed at the location of the MI[21]. Using multiple leads to register these local waveform changes might therefore improve the detection of MI. A recent proof-of-concept study used machine learning models to demonstrate that VFWC of twelve leads as input features could detect OMI more accurately than VFWC of a single lead[23]. The study lacked an optimised feature selection process and did not investigate models based on a combination of a few selected leads. The study in chapter 4 therefore aimed to investigate the effect of established feature selection methods on the ability of multi-lead machine learning models to detect OMI.

It is unknown whether the results described in the aforementioned proof-of-concept study on electrically induced VF in patients with OMI can be translated to the OHCA setting of spontaneous VF in patients with AMI. The study in chapter 5 therefore focused on identification of patients with AMI as the underlying cause of OHCA using the VF-waveform. The aim was to identify predictors and to assess the discriminative ability for detection of AMI using a machine learning approach similar to the method used in chapter 4.

Altogether, this thesis aimed to investigate and optimise machine learning methods for the detection of MI using VF-waveform analysis. This will pave the way for future implementation of a smart defibrillator that can detect AMI as the underlying cause of OHCA to facilitate individualised treatment strategies and improve survival chances.

References

[1] Jocelyn Berdowski, Robert A. Berg, Jan G P Tijssen, and Rudolph W. Koster. "Global incidences of out-of-hospital cardiac arrest and survival rates: Systematic review of 67 prospective studies". In: *Resuscitation* 81.11 (Nov. 2010), pp. 1479–1487. ISSN: 03009572. DOI: 10.1016/j.resuscitation.2010.08.006.

[2] Comilla Sasson, Mary A.M. Rogers, Jason Dahl, and Arthur L. Kellermann. "Predictors of survival from out-of-hospital cardiac arrest a systematic review and meta-analysis". In: *Circulation: Cardiovascular Quality and Outcomes* 3.1 (Jan. 2010), pp. 63–81. ISSN: 19417713. DOI: 10.1161/CIRCOUTCOMES.109.889576.

[3] Reinier A. Waalewijn, Marië A. Nijpels, Jan G. Tijssen, and Rudolph W. Koster. "Prevention of deterioration of ventricular fibrillation by basic life support during out-of-hospital cardiac arrest". In: *Resuscitation* 54.1 (July 2002), pp. 31–36. ISSN: 03009572. DOI: 10.1016/S0300-9572(02)00047-3.

[4] I. G. Stiell et al. "Modifiable factors associated with improved cardiac arrest survival in a multicenter basic life support/defibrillation system: OPALS study phase I results". In: *Annals of Emergency Medicine* 33.1 (Jan. 1999), pp. 44–50. ISSN: 01960644. DOI: 10.1016/S0196-0644(99)70415-4.

[5] Ingela Hasselqvist-Ax et al. "Early cardiopulmonary resuscitation in out-of-hospital cardiac arrest". In: *New England Journal of Medicine* 372.24 (June 2015), pp. 2307–2315. ISSN: 15334406. DOI: 10.1056/NEJMoa1405796.

[6] J. Nas et al. "Changes in automated external defibrillator use and survival after out-of-hospital cardiac arrest in the Nijmegen area". In: *Netherlands Heart Journal* 26.12 (Dec. 2018), pp. 600–605. ISSN: 18766250. DOI: 10.1007/s12471-018-1162-9.

[7] Jasmeet Soar et al. "European Resuscitation Council Guidelines for Resuscitation 2015 Section 3. Adult advanced life support on behalf of the Adult advanced life support section Collaborators 1". In: *Resuscitation* 95 (2015), pp. 100–147. DOI: 10.1016/j.resuscitation.2015.07.016.

[8] Robert J. Myerburg and Agustin Castellanos. "Cardiac Arrest and Sudden Cardiac Death". In: *Braunwald's Heart Disease: A Textbook of Cardiovascular Medicine*. Ed. by Robert O. Bonow, Douglas L. Mann, Douglas P. Zipes, and Peter Libby. 9th ed. Elsevier Saunders, 2012. Chap. 41, pp. 845–884. DOI: 10.1016/b978-1-4377-0398-6.00041-x.

[9] Guillaume Debaty et al. *Prognostic factors for extracorporeal cardiopulmonary resuscitation recipients following out-of-hospital refractory cardiac arrest. A systematic review and meta-analysis*. Mar. 2017. DOI: 10.1016/j.resuscitation.2016.12.011.

[10] Demetris Yannopoulos et al. "Coronary Artery Disease in Patients With Out-of-Hospital Refractory Ventricular Fibrillation Cardiac Arrest". In: *Journal of the American College of Cardiology* 70.9 (Aug. 2017), pp. 1109–1117. ISSN: 15583597. DOI: 10.1016/j.jacc.2017.06.059.

[11] José M. Di Diego and Charles Antzelevitch. "Ischemic ventricular arrhythmias: Experimental models and their clinical relevance". In: *Heart Rhythm* 8.12 (Dec. 2011), pp. 1963–1968. ISSN: 15563871. DOI: 10.1016/j.hrthm.2011.06.036.

[12] K. Ramaswamy and M. H. Hamdan. "Ischemia, metabolic disturbances, and arrhythmogenesis: Mechanisms and management". In: *Critical Care Medicine* 28.10 SUPPL. (Oct. 2000), N151–7. ISSN: 00903493. DOI: 10.1097/00003246-200010001-00007.

[13] R E Klabunde. *Cardiovascular Physiology Concepts*. Lippincott Williams & Wilkins/Wolters Kluwer, 2003, p. 243. ISBN: 1451113846.

[14] Julia H. Indik, Richard L. Donnerstein, Robert A. Berg, Ronald W. Hilwig, Marc D. Berg, and Karl B. Kern. "Ventricular fibrillation frequency characteristics are altered in acute myocardial infarction". In: *Critical Care Medicine* 35.4 (Apr. 2007), pp. 1133–1138. ISSN: 00903493. DOI: 10.1097/01.CCM.0000259540.52062.99.

[15] Julia H. Indik et al. "The influence of myocardial substrate on ventricular fibrillation waveform: A swine model of acute and postmyocardial infarction". In: *Critical Care Medicine* 36.7 (July 2008), pp. 2136–2142. ISSN: 15300293. DOI: 10.1097/CCM.0b013e31817d798c.

[16] Julia H. Indik et al. "Predictors of resuscitation outcome in a swine model of VF cardiac arrest: A comparison of VF duration, presence of acute myocardial infarction and VF waveform". In: *Resuscitation* 80.12 (Dec. 2009), pp. 1420–1423. ISSN: 03009572. DOI: 10.1016/j.resuscitation.2009.08.023.

[17] Julia H. Indik et al. "Predictors of resuscitation in a swine model of ischemic and nonischemic ventricular fibrillation cardiac arrest: Superiority of amplitude spectral area and slope to predict a return of spontaneous circulation when resuscitation efforts are prolonged". In: *Critical Care Medicine* 38.12 (Dec. 2010), pp. 2352–2357. ISSN: 15300293. DOI: 10.1097/CCM.0b013e3181fa01ee.

[18] Julia H. Indik, Daniel Allen, Michael Gura, Christian Dameff, Ronald W. Hilwig, and Karl B. Kern. "Utility of the ventricular fibrillation waveform to predict a return of spontaneous circulation and distinguish acute from post myocardial infarction or normal swine in ventricular fibrillation cardiac arrest". In: *Circulation: Arrhythmia and Electrophysiology* 4.3 (June 2011), pp. 337–343. ISSN: 19413149. DOI: 10.1161/CIRCEP.110.960419.

[19] Theresa M. Olasveengen, Trygve Eftestøl, Kenneth Gundersen, Lars Wik, and Kjetil Sunde. "Acute ischemic heart disease alters ventricular fibrillation waveform characteristics in out-of hospital cardiac arrest". In: *Resuscitation* 80.4 (Apr. 2009), pp. 412–417. ISSN: 03009572. DOI: 10.1016/j.resuscitation.2009.01.012.

[20] Judith L. Bonnes et al. "Characteristics of ventricular fibrillation in relation to cardiac aetiology and shock success: A waveform analysis study in ICD-patients". In: *Resuscitation* 86 (Jan. 2015), pp. 95–99. ISSN: 18731570. DOI: 10.1016/j.resuscitation.2014.10.003.

[21] Judith L. Bonnes et al. "Ventricular fibrillation waveform characteristics differ according to the presence of a previous myocardial infarction: A surface ECG study in ICD-patients". In: *Resuscitation* 96 (Nov. 2015), pp. 239–245. ISSN: 18731570. DOI: 10.1016/j.resuscitation.2015.08.014.

[22] Michiel Hulleman et al. "Predictive value of amplitude spectrum area of ventricular fibrillation waveform in patients with acute or previous myocardial infarction in out-of-hospital cardiac arrest". In: *Resuscitation* 120 (Nov. 2017), pp. 125–131. ISSN: 18731570. DOI: 10.1016/j.resuscitation.2017.08.219.

[23] Jos Thannhauser et al. "Computerized analysis of the ventricular fibrillation waveform allows identification of myocardial infarction: a proof-of-concept study for smart defibrillator applications in cardiac arrest". In: *Journal of the American Heart Association* (2020).

2 | Background

2.1 Clinical background

2.1.1 Sudden cardiac arrest, coronary artery disease and ventricular fibrillation

The term sudden cardiac death (SCD) is used to describe a natural death from cardiac cause, heralded by an abrupt loss of consciousness within one hour of the onset of an acute change in cardiovascular status[1]. Severe atherosclerosis of the coronary arteries is known to be the most common cause of SCD or sudden cardiac arrest (SCA) when not fatal; for approximately half of the patients it is the first manifestation of the disease[2,3]. Numerous reviews have estimated this disease to be present in 70-80% of SCD victims[3–6]. Early evidence for this was found in autopsy studies[7–10]. Later studies that included clinical evaluation of SCA survivors further affirmed this estimation[11–13]. Although the underlying disease is the same, it is interchangeably referred to in literature as coronary artery disease (CAD), coronary heart disease and ischaemic heart disease; here the term CAD will be used.

SCA may present itself as a tachyarrhythmia or bradyarrhythmia. The former includes pulseless ventricular tachycardia (VT) and ventricular fibrillation (VF). SCAs that occur as a result of myocardial ischaemia due to CAD most commonly present as tachyarrhythmias[1,14,15]. The percentage of out-of-hospital cardiac arrest (OHCA) patients with a rhythm of VF upon arrival of the emergency medical services is approximately 30%[16]. This includes both initial VF rhythms and VTs that have deteriorated into VF. In a significant portion of patients, OHCA is therefore thought to be related to CAD.

The pathophysiological changes caused by CAD-related myocardial ischaemia result in electrical instability which can trigger these lethal arrhythmias. These mechanisms will be elaborated upon in section 2.1.2. As the rhythmic electrical activity is lost, the coordinated myocardial contraction stops. This results in a loss of pumping function and haemodynamic collapse that will ultimately lead to death without adequate treatment in the form of defibrillation[17,18].

2.1.2 Acute myocardial ischaemia and ventricular fibrillation

Electrical activation of the myocardium occurs through the propagation of action potentials (APs) caused by consecutive ionic currents across the cell membrane. Regulation of adequate intracellular and extracellular ion concentrations is needed in order to establish rhythmic AP generation. This is a complex process, involving different ion channels that are influenced by a range of factors.[18–20]

Acute ischaemia induces changes in both the intracellular and extracellular environment that evolve over the course of the ischaemia. Among other things it leads to a rise of the extracellular K^+ concentration, depolarising the membrane potential. This partially inactivates the Na^+ channels that are responsible for the rapid upstroke of the AP, thereby suppressing the excitability of myocytes and slowing the AP propagation. These are two examples of the multitude of changes caused by ischaemia, each affecting the shape and duration of APs and subsequently their ability to propagate through the myocardium. Figure 2.1 displays typical changes that occur to the ventricular myocyte AP as a result of ischaemia. Altogether, these AP changes caused by myocardial ischaemia increase the likelihood of events that may trigger tachyarrhythmias such as VF.[14,21–24]

The two major mechanisms of VF initiation are reentry excitation and presence of extrasystoles; both may be the result of myocardial ischaemia[14]. As a consequence of ischaemia, tissue may become less excitable or inexcitable, splitting the wavefront of an approaching AP into two pathways. Ischaemia might furthermore cause a unidirectional block to occur in either of the

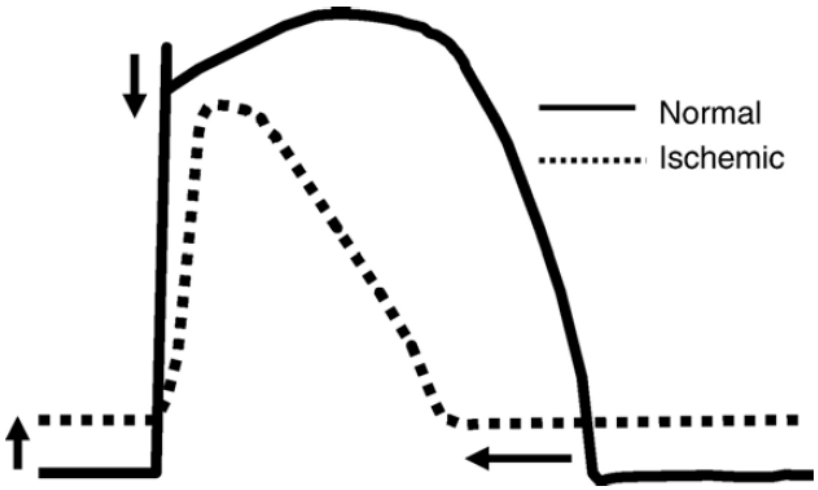

Figure 2.1: A schematic depiction of the slowing of the upstroke, amplitude decrease and shortening of the ventricular action potential and depolarisation of the membrane potential as a result of ischaemia. Adapted from "Regulation of ion channels and arrhythmias in the ischemic heart", J.G. Akar, 2007, Journal of Electrocardiology, 40.[22]

pathways, as well as alter the conduction velocity. If the conduction around the inexcitable region is slow enough, reentry excitation may occur. This might start out as VT, but may degenerate into VF.[14,17,18,21]

Extrasystoles may occur due to early or delayed afterdepolarisations or abnormal automaticity. Early afterdepolarisation can occur when the AP duration is prolonged and Ca^{2+} channels reactivate during the repolarisation phase. This increases the membrane potential to its firing threshold and generates a new AP prematurely. High intracellular Ca^{2+} levels may furthermore lead to a transient inward current, evoking an AP via a process called delayed afterdepolarisation.[24–26] Abnormal automaticity occurs when otherwise non-pacemaker cells such as ventricular cells begin depolarising automatically, creating extrasystoles. In case of ischaemia, this is usually caused by currents of injury which will be elaborated upon in section 2.1.4. When abnormal automaticity causes repetitive fast depolarisation, it might overdrive the automaticity of the sinoatrial node, thereby inducing arrhythmia.

Thus, electrical instability due to myocardial ischaemia related changes may give rise to phenomena that induce tachyarrhythmias such as VF.[14,21,24,27,28]

2.1.3 The basics of electrocardiography

An important diagnostic tool in cardiology is the electrocardiogram (ECG). Surface electrodes measure the compound electrical activity produced by all myocytes during the cardiac cycle. Clinical ECGs are normally recorded using ten electrodes: four limb electrodes placed on each wrist and foot and six thorax electrodes placed on the anterior and left lateral side of the thorax. These electrodes can be used to compute the potential difference in twelve directions. Each direction is called a lead, from which the term 12-lead ECG is derived.

The potential at the right wrist, left wrist and left foot are called v_A, v_B and v_C respectively, with the right foot electrode being the reference. These produce the frontal leads I, II, and III, as is shown in figure 2.2.[18] They are derived in the following way:

$$\mathrm{I} = v_B - v_A \tag{2.1}$$

$$\mathrm{II} = v_C - v_A \tag{2.2}$$

$$\mathrm{III} = v_C - v_B \tag{2.3}$$

The three augmented frontal leads aVR, aVL and aVF are described by:

$$\text{aVR} = v_{\text{A}} - \frac{1}{2}(v_{\text{B}} + v_{\text{C}}) = -\frac{1}{2}(\text{I} + \text{II}) \tag{2.4}$$

$$\text{aVL} = v_{\text{B}} - \frac{1}{2}(v_{\text{A}} + v_{\text{C}}) = \frac{1}{2}(\text{I} - \text{III}) \tag{2.5}$$

$$\text{aVF} = v_{\text{C}} - \frac{1}{2}(v_{\text{A}} + v_{\text{B}}) = \frac{1}{2}(\text{II} + \text{III}) \tag{2.6}$$

These six leads divide the frontal plane into twelve 30° segments; each lead pointing in one direction or the opposite way. Figure 2.3 shows the six frontal leads with their respective angle.[18,29,30]

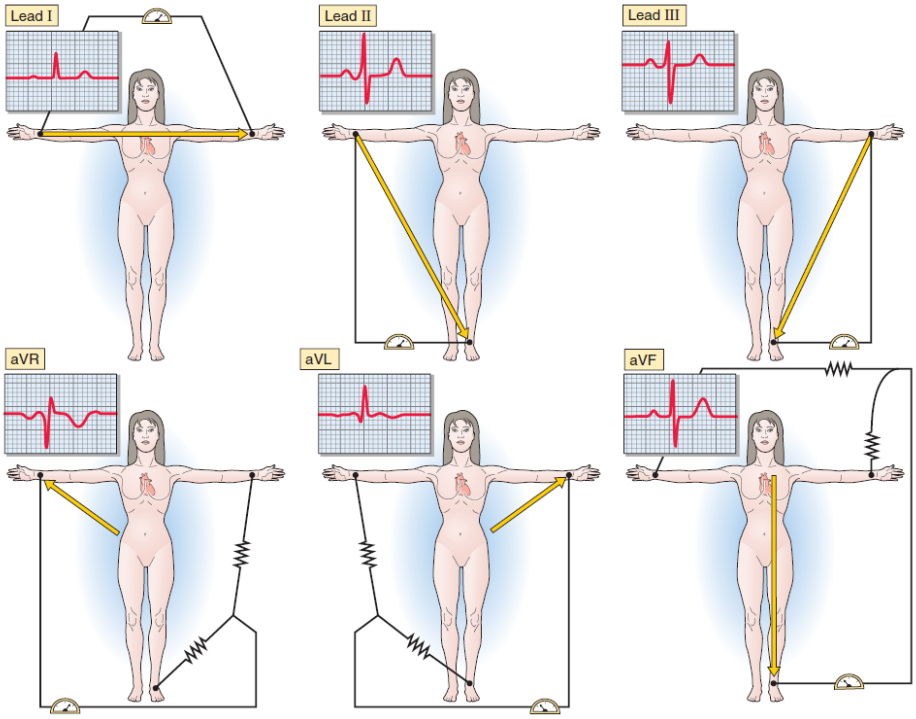

Figure 2.2: The six frontal ECG leads. Adapted from Medical Physiology (p. 516), W. Boron and E. Boulpaep, 2012.[18]

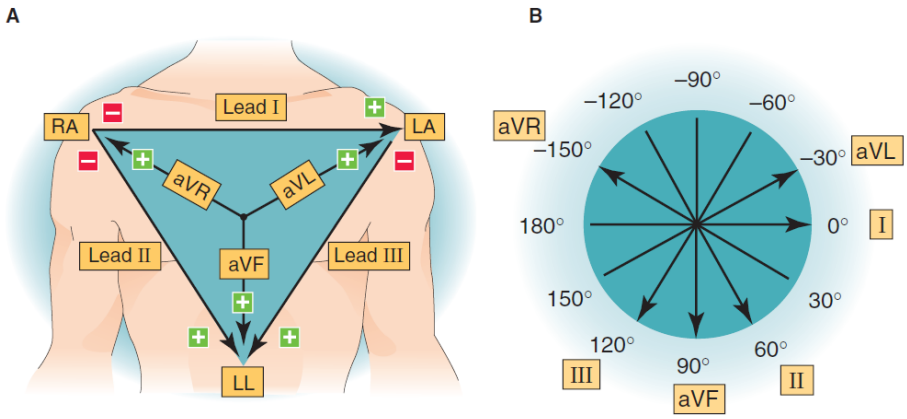

*Figure 2.3: **A)** Directions of the six frontal leads. **B)** The angle of the leads. Adapted from Medical Physiology (p. 517), W. Boron and E. Boulpaep, 2012.*[18]

In order to evaluate the electrical activity in a plane other than the frontal plane, the six thorax electrodes are used to compute the six precordial leads V_1, V_2, V_3, V_4, V_5 and V_6 that lie in the transverse plane. They represent the potential difference between one of the thorax electrodes (v_i) and the electrical average of the three limb electrodes:

$$V_i = v_i - \frac{1}{3}(v_A + v_B + v_C) \tag{2.7}$$

with $i \in \{1, 2, ..., 6\}$. Figure 2.4 shows the location of the six thorax electrodes and the precordial leads in the transverse plane that are derived from them.[18,29–31]

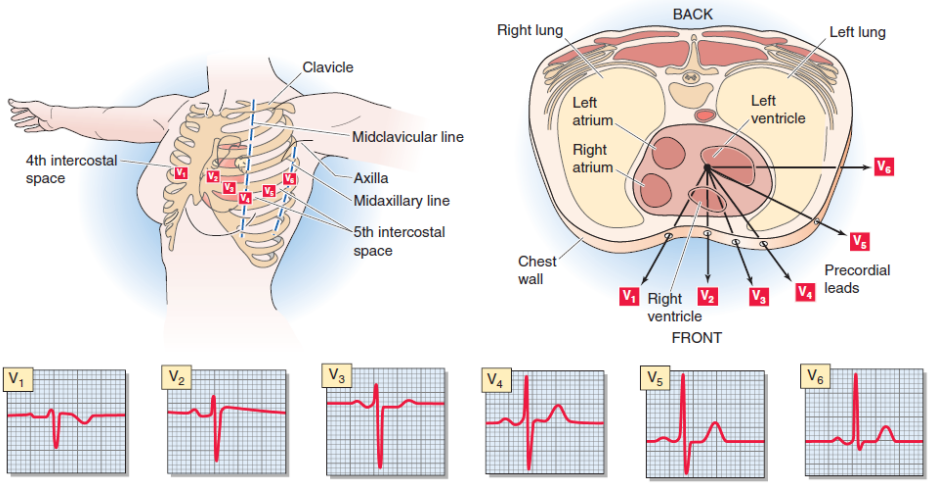

Figure 2.4: The locations of the six precordial electrodes and leads derived from them. Adapted from Medical Physiology (p. 516), W. Boron and E. Boulpaep, 2012.[18]

2.1.4 The electrocardiogram of sine rhythm

The normal heart

The 12-lead ECG is one of the most common diagnostic tools in cardiology as it is cheap, quick to make and can provide a lot of information about a patient's cardiac status. Arrhythmias can be recognised by investigating the underlying rhythm and other abnormalities can be traced back to a specific myocardial region by looking at the phase of the cardiac cycle and the leads in which they occur. The cardiac cycle is the result of the consecutive depolarisation and repolarisation of the myocardium as the AP travels along the conduction pathways. Figure 2.5 schematically visualises these conduction pathways[18]. The cardiac cycle of a normal heart is composed of several phases. The P wave occurs first, the Q, R and S waves which make up the QRS complex follow and the T wave marks the end of the cycle. Figure 2.6 shows the cardiac cycle of a normal heart.[18,29,30]

P wave

The cardiac cycle starts with activation by the pacemaker cells of the sinoatrial node, located in the superior posterolateral wall of the right atrium. The atria depolarise as the AP travels through the internodal pathways to the atrioventricular node. The atrial depolarisation is represented on the ECG by the P wave. The AP is delayed shortly by the atrioventricular node and then travels on through the fast-conducting Purkinje fibres in the bundle of His which splits into the left and right bundle branches. As the propagation through this part of the conduction system does not depolarise myocardial tissue, an electrical silence is visible on the ECG between the P wave and QRS complex, which is termed the PR segment. The P wave and PR segment together compose the PR interval which normally lasts between 0.12 and 0.20 second.[18,19,29,30]

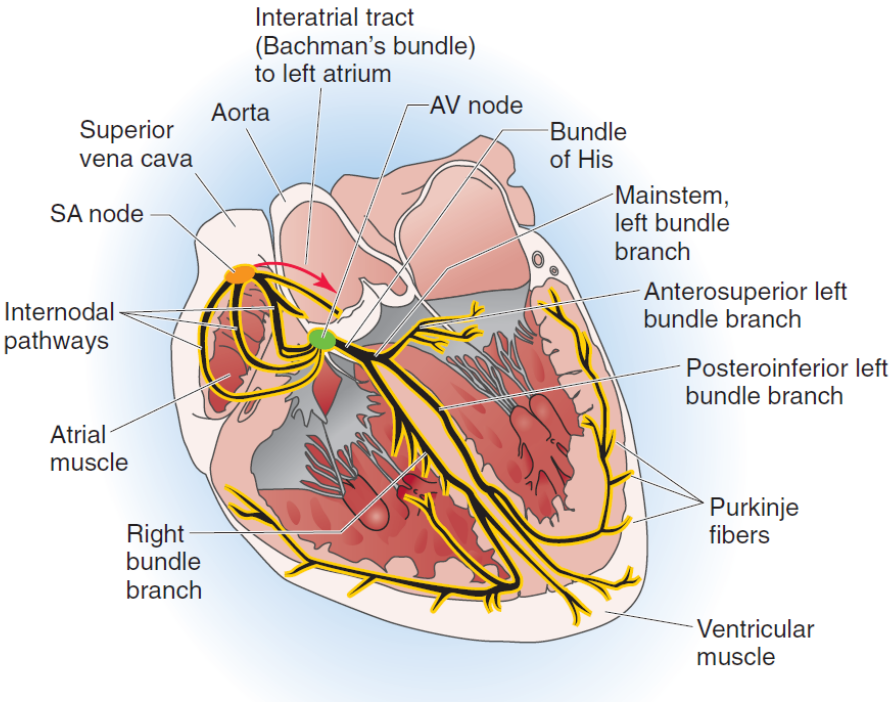

Figure 2.5: The conduction pathways mapped onto a cross-section of the long heart axis. SA: sinoatrial, AV: atrioventricular. Adapted from Medical Physiology (p. 505), W. Boron and E. Boulpaep, 2012.[18]

QRS complex

As the Purkinje fibres of the bundle branches split into smaller bundles, they ultimately become continuous with the ventricular muscle fibres. Ventricular depolarisation starts once the AP reaches these fibres. The large number of depolarising cells results in a peak of electrical activity represented by the QRS complex on the ECG. The depolarisation front moves from the ventricular septum along the endocardial surface and finally spreads through the muscle to the outside of the heart. Because the depolarisation occurs in a successive way, the electrical vector changes direction over time. This causes the QRS complex to consist of multiple waves in opposite directions instead of a single large wave. The exact configuration of the QRS complex depends on the direction in which it is viewed and is therefore different for each ECG lead. The QRS complex normally has a duration of less than 0.10 second. Conduction is considered to be delayed when the QRS complex lasts longer than 0.12 second. The J-point occurs directly after the QRS complex and represents the electrical baseline, since the entire ventricular mass is depolarised at that instant.[18–20,29,30]

T wave

Repolarisation of the ventricles begins shortly after they have been depolarised. It begins with the outer ventricular surface that was the last to depolarise; the endocardial areas repolarise last. Ventricular repolarisation is visible as the T wave on the ECG. The QT interval spans from the beginning of the QRS complex to the end of the T wave and is influenced by the heart rate. Its corrected version, the QTc interval, is derived by dividing the QT interval by the square root of the heart rate. A normal QTc interval is shorter than 0.45 or 0.46 second for men and women respectively. Once repolarisation has finished, the normal cardiac cycle is complete and will start over.[18–20,29,30]

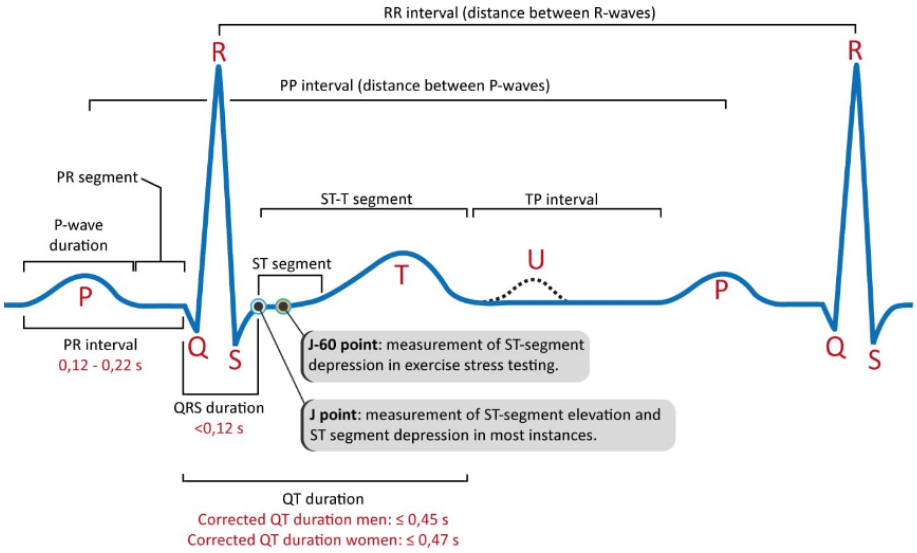

Figure 2.6: The waves and intervals of a normal electrocardiogram. Adapted from Braunwald's Heart Disease: A Textbook of Cardiovascular Medicine, chapter 13, (p. 132), D. Mirvis, and A. Goldberger, 2012.[30]

U wave

A U wave is usually not present in the normal ECG. Since figure 2.6 shows a U wave it is addressed anyway for the sake of completeness. The origin of the U wave is uncertain, though several theories exist[30,32]. The electromechanical hypothesis is that it is caused by stretch-induced delayed afterdepolarisations occurring as a result of ventricular wall distension during rapid filling[32]. Other theories suggest that it is caused by electrical potential gradients within the ventricular myocardium or between the myocardium and the His-Purkinje system[30].

The ischaemic heart

The electrophysiological changes caused by acute ischaemia can be monitored with the ECG, making it an important diagnostic tool. The most common cause of acute ischaemia in CAD patients is coronary occlusion by a thrombus after atherosclerotic plaque disruption. If this leads to SCA, the defibrillator ECG advises whether or not defibrillation is required by distinguishing between bradyarrhythmia and tachyarrhythmia. In most cases however, acute myocardial ischaemia does not lead to SCA but rather leads to the clinical presentation of acute coronary syndrome (ACS). The ECG plays an important role in differentiating between the three types of ACS known as unstable angina, ST-elevation myocardial infarction (STEMI) and non-ST-elevation myocardial infarction (NSTEMI).[33–35]

The effect of acute ischaemia on the normal electrocardiogram

The least severe type of ACS occurs when the ischaemia is reversible and of short duration such that no myocardial necrosis occurs; it is referred to as unstable angina. Longer lasting ischaemia causes tissue necrosis known as myocardial infarction (MI), which is accompanied by the release of the cardiac biomarker troponin[34]. Elevation of the ST-segment on the ECG is used to further categorise acute myocardial infarction (AMI) into STEMI or NSTEMI.

A NSTEMI tends to occur when the coronary artery is not fully occluded. The ischaemia may therefore be short-lived or affect only a small area. A STEMI is generally a more severe MI that lasts longer and affects a larger myocardial volume; it is often caused by complete and persistent coronary occlusions.[33–38] The ECG-based distinction between STEMI and NSTEMI is relevant

because of a difference in treatment strategy. Current European and American guidelines both recommend to perform immediate coronary angiography (CAG) and percutaneous coronary intervention (PCI) in case of a STEMI when ischaemic symptoms have been present for less than twelve hours[39,40]. A NSTEMI does not require equally aggressive treatment, as immediate CAG and PCI were not found to be superior to delayed CAG and PCI in terms of 90 day survival[41].

This illustrates the diagnostic value of the ECG in the setting of ACS when an organised rhythm is present. Numerous changes besides ST-segment elevation may occur in the ischaemic ECG, usually in a sequential manner.

Hyperacute T waves

The first electrocardiographic sign of acute ischaemia is usually the presence of tall, hyperacute T waves. The T wave describes ventricular repolarisation; hyperacute T waves are thought to arise as a result of slow repolarisation of ischaemic areas. Other pathologies may show hyperacute T waves as well, so in the absence of other clinical evidence they are not specific for myocardial ischaemia. Hyperacute T waves may occur as soon as two minutes after the onset of ischaemia and often evolve into ST-segment deviations after approximately thirty minutes.[42,43]

ST-segment deviation

Appearing twenty minutes to several hours after onset of ischaemia, deviation of the ST-segment is usually the first noticed ECG sign in the emergency department. ST-segment deviation is the result of a current of injury. The formation of this current can be explained by two theories; there is no scientific consensus on which theory is correct. Both types, the diastolic and systolic current of injury, arise because of an electrical potential gradient between ischaemic and healthy tissue.[20,30,42]

The diastolic current can be explained by a potential gradient caused by the inability of ischaemic tissue to maintain polarisation. This potential difference disappears together with the current immediately after cardiac depolarisation, which corresponds to the the J-point on the normal ECG, as shown in figure 2.6[18,20,30,42]. The current reappears once the myocardium repolarises, indicated by the TP-interval on the ECG. A potential difference between depolarisation (the J-point) and repolarisation (the TP-interval) therefore indicates the presence of a diastolic current of injury. With the TP-interval as electrical baseline, the current manifests as a depression or elevation of the J-point and ST-segment relative to this interval. As the current flows away from the ischaemic zone, the ECG lead pointing towards this zone will show the negative of this current. The TP-interval in this lead will therefore be negative compared to the J-point, which characterises as ST-elevation. Conversely, the ECG lead follows the current when it points away from the ischaemic zone. This makes the TP-interval positive compared to the J-point and the ECG will therefore exhibit ST-depression.[18,20,30,42]

The systolic current of injury is thought to arise because of a potential gradient between the ischaemic and healthy tissue during systole. This gradient occurs because of altered depolarisation in ischaemic tissue caused by changes in AP shape and duration. It results in current flow towards the ischaemic area, which causes primary ST-elevation in the ECG leads pointing in this direction.[30,42]

Both the diastolic and systolic current theories explain how ischaemia may cause ST-elevation and reciprocal ST-depression and in which ECG leads these phenomena occur. In contrast to these theories, leads aimed towards an area of ischaemia may show ST-depression rather than ST-elevation, which is suspicious for NSTEMI. This may occur when the ischaemia is subendocardial rather than transmural, resulting in a current of injury flowing in the opposite direction.[30]

An example ECG of STEMI is shown in figure 2.7. It illustrates how a large anterolateral AMI may show ST-elevation in leads I, aVL and V_1-V_6 pointing anteriorly and laterally. Additionally, leads pointing in the opposite direction such as III, aVR and aVF may display reciprocal ST-depression.[30]

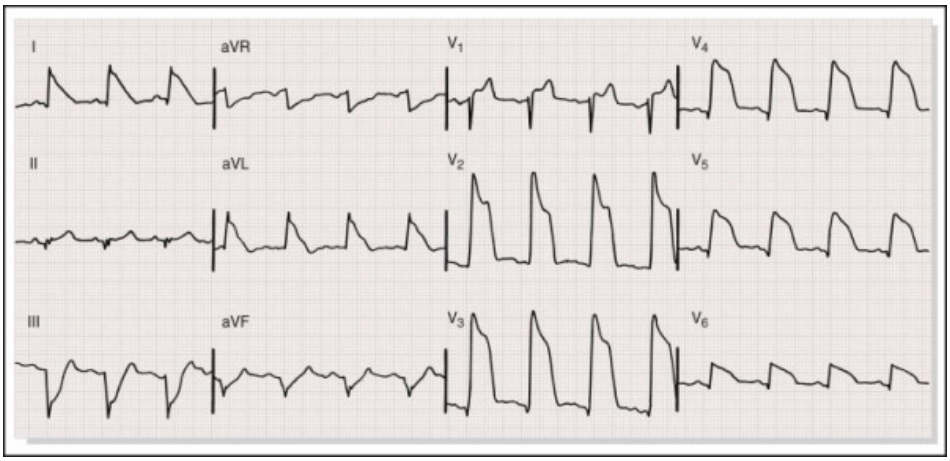

Figure 2.7: Acute anterolateral myocardial infarction, showing ST-elevation in anterolateral leads I, aVL and V_1-V_6 and reciprocal ST-depression in III, aVR and aVF. Adapted from Braunwald's Heart Disease: A Textbook of Cardiovascular Medicine, chapter 13, (p. 149-158), D. Mirvis, and A. Goldberger, 2012.[30]

Pathologic Q wave formation

An ECG of AMI may develop abnormal or pathologic Q waves within minutes to several hours after the onset of ischaemia. Appearing in the direction of the infarction, pathologic Q waves represent an electrical silence as necrotic myocardium is no longer able to propagate APs. Therapy aimed at coronary reperfusion may still be of benefit for the patient once pathologic Q waves appear, since some of the ischaemic tissue may be salvageable. Q waves caused by small MIs may disappear over time as the size of myocardial scar reduces. Extensive MIs will result in permanent Q waves.[30,42,43]

T wave inversion

Inversion of the T wave is one of the latest signs of an evolving MI and may be seen hours to days after onset. Similar to hyperacute T waves in the first phase of MI, T wave inversion is caused by alterations of ventricular repolarisation. The repolarisation vector will flip as epicardial repolarisation delays, now moving from endocardium to epicardium instead of the opposite way. T wave inversion indicates the MI is transmural since the compromised area must include the epicardium. They may remain inverted permanently or may revert after a few months, which is indicative of good myocardial recovery with higher left ventricular ejection fractions.[30,42–44]

ST-segment normalisation

ST-segment deviations are usually the longest lasting electrocardiographic changes of a STEMI and will begin to normalise approximately twelve hours after onset. The potential gradient between the ischaemic and healthy tissue that caused the current of injury decreases as the ischaemic tissue necroses and loses electrical activity. ST-elevation diminishes gradually, which may take approximately two weeks for inferior MIs but much longer for anterior MIs. ST-elevation may normalise after successful reperfusion therapy. This is generally a good prognostic sign, indicating that the myocardial microcirculation is restored properly.[42,43]

2.2 Technical background

2.2.1 Quantifying the ventricular fibrillation waveform

During VF, the rhythmic electrical activity that coordinates myocardial contraction becomes disorganised. This results in a loss of pumping function and haemodynamic collapse. Since the 1980s, many different ventricular fibrillation waveform characteristics (VFWC) have been introduced as a means to objectify the seemingly chaotic and unstructured waveform[45,46]. These VFWC may describe signal properties in the time or frequency domain, or may describe the organisation of the signal. Here, an overview is presented of how the VFWC used in this thesis were computed. The formulas include numbers and indexing based on the data analysed in chapter 4 to clarify the computational steps. The VFWC analysed in chapter 5 were computed using the same formulas but with different indexing, appropriate for the data. First, an explanation is given of how the data were acquired.

Data acquisition

Electrically induced ventricular fibrillation

The VF analysed in chapter 4 was recorded during implantable cardioverter-defibrillator testing with a 12-lead surface ECG using the BARD® LabSystem™ Pro (Lowell, MA, USA) with a sampling frequency (f_s) of 1000 Hz and a 16 bit A/D converter. Approximately thirty seconds were recorded, including a period before VF induction and after VF termination.

The data were analysed using MATLAB® (version 2020a, MathWorks®, Natick, MA, USA). The 4.1-second segment of VF prior to first shock delivery was selected manually and pre-processed with a fourth order Butterworth bandpass filter with cut-off frequencies of 1 and 48 Hz. Visually identified artefacts were removed and replaced by linear interpolation. This resulted in the time domain signal x_n with $n \in \{1, 2, ..., N\}$ and a number of samples $N = 4096$.

An overview of the VFWC computed from these time domain signals is presented below. Seventeen regular VFWC were computed of all twelve leads, amounting to $12 * 17 = 204$ regular VFWC. Furthermore, the differences between the VFWC of each lead and the corresponding VFWC of lead V_1 were computed, resulting in an additional $11 * 17 = 187$ features named the ΔV_1 VFWC. As such, a total of $204 + 187 = 391$ VFWC was acquired per patient.

Spontaneous ventricular fibrillation

The VF analysed in chapter 5 was recorded during OHCA with the paddles of a LIFEPAK 12 defibrillator (Physio-Control, Redmond, WA, USA) with an f_s of 125 Hz.

The data were analysed using MATLAB® (version 2020a, MathWorks®, Natick, MA, USA). The data were pre-processed with a fourth order Butterworth bandpass filter with cut-off frequencies of 1 and 48 Hz. A graphical user interface was developed to review each ECG and select a three-second segment of VF without chest compressions before the first, and if available, the second defibrillation shock. This resulted in one or two time domain signals x_n with $n \in \{1, 2, ..., N\}$ and a number of samples $N = 375$.

Seventeen VFWC were computed from each time domain signal. Additionally, the differences between the VFWC of the two segments were computed, resulting in seventeen extra VFWC. Patients with a two or more defibrillation shocks therefore had a total of $3 * 17 = 51$ VFWC while patients with one shock had 17.

Time domain characteristics

Mean absolute amplitude (mV)

The mean absolute amplitude (MAA) is acquired by taking the mean of the absolute values of the segment:

$$MAA = \frac{1}{N}\sum_{i=1}^{N}|x_i|. \tag{2.8}$$

Median slope (mVs^{-1})

The median slope (MS) is acquired by computing the difference between subsequent samples in the VF segment. The absolute value of this difference vector is then taken and multiplied by the sampling frequency. The median of the resulting vector is the MS:

$$MS = median(|x_i - x_{i-1}| \cdot f_s) \tag{2.9}$$

for $2 \leq i \leq 4096$.

Frequency domain characteristics

To acquire the frequency domain characteristics, the time domain signal is transformed into the frequency domain by *fast Fourier transform (FFT)* without windowing. This results in a vector of $N = 4096$ coefficients $\hat{x}_0, \hat{x}_1, ..., \hat{x}_{N-1}$. The absolute values of the first $N/2 + 1 = 2049$ indices that correspond to the positive frequencies $f_i = i \cdot f_s/N$ with $i \in \{0, 1, ..., N/2\}$ are kept. Since the frequencies between 2 and 48 Hz are of interest, only indices $9 \leq i \leq 196$ so that $2 < f_i < 48$ Hz are used to compute the frequency characteristics. The total area of the amplitude spectrum within this frequency range is approximated via trapezoidal integration:

$$Area_{total} = \Delta f(\sum_{i=9}^{196}|\hat{x}_i|^2 - \frac{|\hat{x}_9|^2 + |\hat{x}_{196}|^2}{2}), \quad [Area_{total}] = mV^2 \tag{2.10}$$

where $\Delta f = f_s/N$ is the frequency step size. This factor was falsely assumed to be equal to 1 in this thesis and was therefore omitted in calculations. This resulted in an overestimation of the total area by a factor of approximately four since the frequency step size was $f_s/N = 1000/4096$. Since the area was only used for the computation of the median frequency, as will be explained in the next paragraph, this mistake did not have any consequences.

Median frequency (Hz)

The median frequency (FM) is the smallest frequency f_k for which the area of the partial spectrum it encloses between boundaries 2 Hz and f_k is more than 50% of the total area. Here, $f_k = k \cdot f_s/N$ and $k \in \{9, 10, ..., 196\}$, and the partial spectrum area is approximated by trapezoidal integration:

$$Area_{partial} = \Delta f(\sum_{i=9}^{k}|\hat{x}_i|^2 - \frac{|\hat{x}_9|^2 + |\hat{x}_k|^2}{2}), \quad [Area_{partial}] = mV^2. \tag{2.11}$$

Dominant frequency (Hz)

The dominant frequency (FD) is the frequency f_i for which $|\hat{x}_i^2|$ is maximal, with $9 \leq i \leq 196$.

Amplitude spectrum area (mVHz)

The amplitude spectrum area (AMSA) is the normalised sum of the absolute values of the frequencies multiplied by the corresponding Fourier coefficients:

$$AMSA = \frac{1}{N/2+1} \sum_{i=9}^{196} |\hat{x}_i * f_i|. \tag{2.12}$$

Low frequency AMSA (mVHz)

The low frequency AMSA ($AMSA_{lf}$) is the AMSA computed for frequencies $2 < f_i < 12$ Hz, meaning $9 \leq i \leq 49$.

High frequency AMSA (mVHz)

The high frequency AMSA ($AMSA_{hf}$) is the AMSA computed for frequencies $12 < f_i < 48$ Hz, meaning $50 \leq i \leq 196$.

AMSA ratio

The AMSA ratio is the ratio between high and low frequency AMSA:

$$AMSA_{ratio} = \frac{AMSA_{hf}}{AMSA_{lf}}. \tag{2.13}$$

Power spectrum area (mV^2Hz)

The power spectral density (PSD) is a measure of the power present in the signal per unit of frequency. It is estimated by: $PSD_i \approx \beta_i |\hat{x}_i|^2$ with $i \in \{0, 1, ..., N/2\}$ and

$$\beta_i = \begin{cases} 2\dfrac{1}{f_s N} & i \in \{1, 2, ..., N/2 - 1\}, \\ \dfrac{1}{f_s N} & i = 0 \text{ or } i = N/2. \end{cases}$$

The power spectrum area (PSA) is derived from the PSD estimate as follows:

$$PSA = \frac{f_s}{N} \sum_{i=9}^{196} |PSD_i \cdot f_i|. \tag{2.14}$$

Organisation characteristics

Bandwidth (Hz)

Similar to how the median frequency is derived, the frequencies f_k for which the partial spectrum areas are 25% and 75% of the total spectrum area are computed. The difference between these frequencies is the bandwidth (BW).

Envelope characteristics

The fluctuation of the time domain signal is quantified using four VFWC describing the shape of the upper envelope of the VF. The original, unfiltered VF segment is passed through a fourth order low pass Butterworth filter with a cut-off frequency of 20 Hz to remove noise. It is then normalised so that the amount of fluctuation can be compared in an equivalent manner between different patients. Next, the upper envelope of the segment is computed using the MATLAB® function *envelope*. Envelope calls the *findpeaks* function which finds local maxima in the VF segment constrained by a minimal peak height of 0 and a minimal peak prominence of 0.5.

Furthermore, a minimal distance between two peaks is ensured to be $2/3$ of the dominant frequency, defined earlier. The *envelope* function then connects the peaks using linear interpolation to construct the upper envelope of the VF segment.

The settings for linear interpolation and each of the *findpeaks* arguments were optimised iteratively by visually assessing the goodness of the envelope fit. In this process, the 12-lead VF recordings of thirty patients were inspected using different settings, resulting in the final combination mentioned here.

Four new VFWC have been created to describe the fluctuation of the upper envelope e_n with $n \in \{1, 2, ..., N\}$ and the number of samples $N = 4096$. The mean of the upper envelope (flucmean) and variance of the upper envelope (flucvar) are defined as:

$$flucmean = \frac{1}{N}\sum_{i=1}^{N} e_i, \quad [flucmean] = mV, \tag{2.15}$$

$$flucvar = \frac{1}{N}\sum_{i=1}^{N} [e_i - \mu]^2, \quad [flucvar] = mV^2 \tag{2.16}$$

with μ the average value as defined by flucmean. The root-mean-square of the upper envelope derivative (flucrms) and mean absolute amplitude of the upper envelope derivative (flucmaa) describe how the upper envelope changes over time. They quantify this change using the time derivative e'_n:

$$e'_n = \frac{e_n - e_{n-1}}{T_s} \tag{2.17}$$

for $2 \leq n \leq 4096$ and with time step $T_s = 1/f_s$. In this thesis, a mistake was made in defining this derivative. $2T_s$ was used for the denominator rather than T_s. The magnitude of the derivative was therefore a factor 2 smaller as well as the magnitudes of the flucrms and flucmaa which were computed by taking the root-mean-square and the mean absolute amplitude of the derivative:

$$flucrms = \sqrt{\frac{1}{N-1}\sum_{i=1}^{N-1} [e'_i]^2}, \quad [flucrms] = mVs^{-1}, \tag{2.18}$$

$$flucmaa = \frac{1}{N-1}\sum_{i=1}^{N-1} |e'_i|, \quad [flucmaa] = mVs^{-1}. \tag{2.19}$$

Organisation index

The organisation index (OI) describes the ratio between the power of the dominant frequency and its harmonics combined and the total power given by the PSD estimate. The power of the dominant frequency and its harmonics is defined as the area of the PSD estimate around the peak with a bandwidth such that the border frequencies have an amplitude as large as 25% of the peak itself.

Figure 2.8 shows an example of how the OI is computed. The first and highest peak of the spectrum is the dominant frequency. The subsequent peaks represent its harmonics. The dark coloured regions represent the areas around the peaks. The borders of the shaded areas are those frequencies for which the amplitude is less than 25% of the peak amplitude. The ratio between the sum of the shaded areas and the total area of the spectrum is the OI.

Detrended fluctuation analysis

Detrended fluctuation analysis (DFA) was first described by Peng *et al.* and offers a way to analyse long-range correlations within a time series[48,49]. In contrast to conventional time or frequency domain analysis, this method is well-suited to analyse non-stationary data such as the ECG.

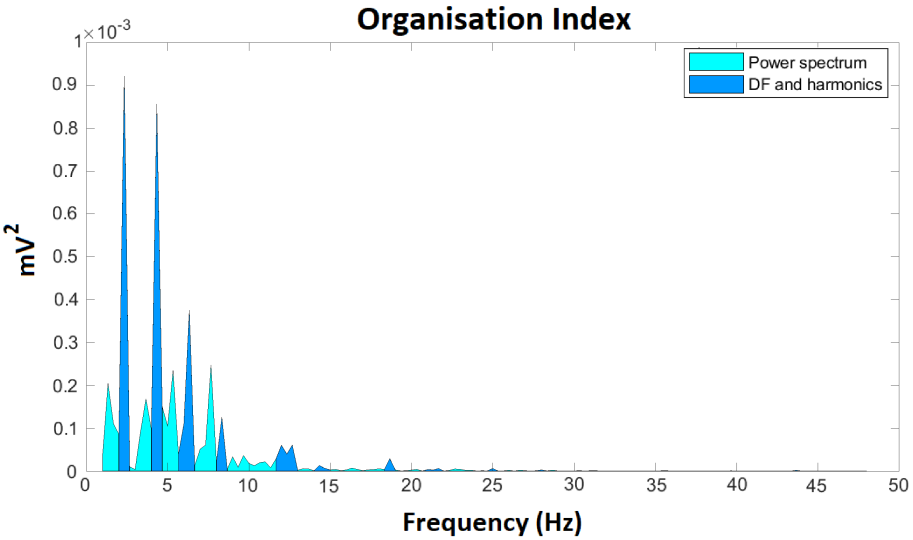

Figure 2.8: Power spectrum density estimate of a segment of ventricular fibrillation. The organisation index is defined as the ratio between the shaded area and the total area of the spectrum. DF: dominant frequency. Adapted from "Computerized analysis of the ventricular fibrillation waveform allows identification of myocardial infarction: a proof-of-concept study for smart defibrillator applications in cardiac arrest", by J. Thannhauser et al, 2020, Journal of the American Heart Association.[47]

DFA is performed according to the following steps and illustrated by figure 2.9. The offset is corrected by subtracting the mean from the original time domain signal x_n after which it is integrated by taking the cumulative sum:

$$y_n = \sum_{i=1}^{N} [x_i - x_{mean}] \tag{2.20}$$

where x_i is the i^{th} sample of x_n, x_{mean} its mean, y_n the integrated signal and N the signal length in samples. This is shown in the upper three panels (0), (1) and (2) of figure 2.9. Then, the integrated signal y_n is divided into equally sized boxes of sample length b, with $b \in \{2^1, 2^2, ..., 2^{12}\}$. A least-squares line is fit to the data in each box to compute the local trend z_n. The detrended signal is then created by subtracting the local trend from the integrated signal y_n. The local trend in each box and the corresponding detrended signal is shown twice in the lower panels (3) and (4) of figure 2.9, for two different box sizes. The fluctuation F as a function of box size b is calculated by taking the root-mean-square of the detrended signal:

$$F(b) = \sqrt{\frac{1}{N} \sum_{i=1}^{N} [y_n - z_n]^2}. \tag{2.21}$$

The fluctuation $F(b)$ is plotted against b using logarithmic axes, as can be seen in panel (5) of figure 2.9. The DFA scaling exponent α is the slope of the trend line estimated using linear regression. Two trend lines can be used instead of one to ensure a better fit. This study uses DFA scaling exponent 1 (DFAα1) and DFA scaling exponent 2 (DFAα2) as VFWC. Each α represents the DFA on a different time scale. DFAα1 was created using small box sizes and therefore describes the DFA on a short time scale between 0.002 and 0.064 seconds. DFAα2 was created using large box sizes and covers the larger time scale between 0.128 and 4.096 seconds.

In general, the larger the value of α, the smoother the original signal. Hence, a small value for α indicates that the signal fluctuates a lot while a large value suggests a smooth signal.[48,49]

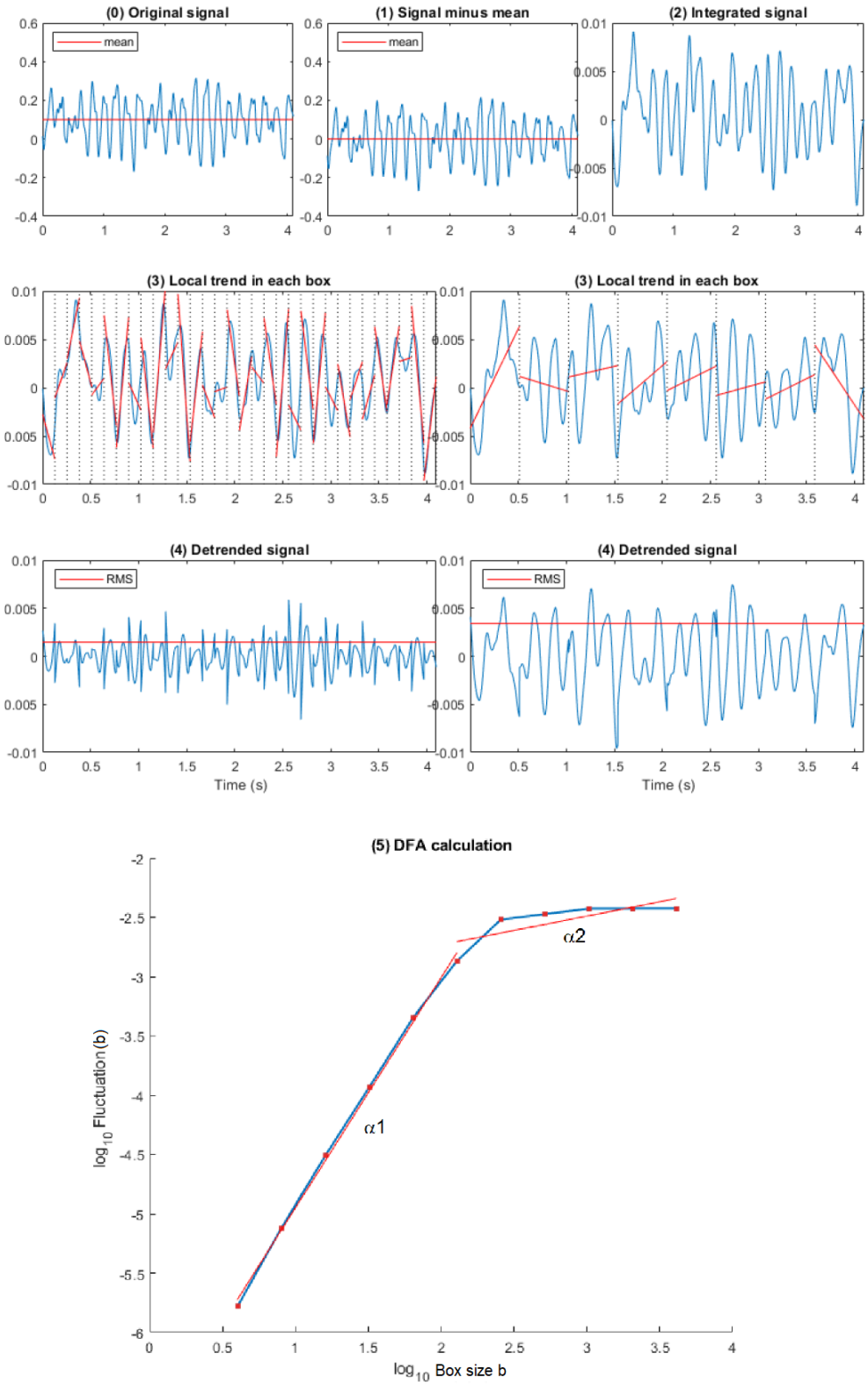

Figure 2.9: The steps used in detrended fluctuation analysis. (0) The original signal over time. (1) The original signal minus its mean. (2) The integrated signal. (3) The integrated signal divided into equally sized boxes and their local trends. (4) The integrated signal minus the local trends, creating the detrended signal. (3) and (4) are shown twice for two different box sizes. (5) The fluctuation of the detrended signal as a function of box size on logarithmic scales, quantified by the scaling exponents $\alpha 1$ and $\alpha 2$. DFA: detrended fluctuation analysis, RMS: root-mean-square. Adapted from "Computerized analysis of the ventricular fibrillation waveform allows identification of myocardial infarction: a proof-of-concept study for smart defibrillator applications in cardiac arrest", by J. Thannhauser et al, 2020, Journal of the American Heart Association.[47]

2.2.2 Analysing the ventricular fibrillation waveform

Using the aforementioned VFWC, the VF-waveform has been analysed for many different purposes over the last years[46]. It has been associated to several clinical outcomes and has been able to predict some as well, such as shock success[50–58]. Another relevant application is the use of VFWC to diagnose underlying diseases. Of particular importance for this thesis is the influence of old myocardial infarction (OMI) and AMI on the VF-waveform. This effect has been described numerously; an overview of these studies is given in the following section. The succeeding sections will elaborate on two prediction methods applied in this thesis for the detection of MI using VFWC.

The influence of myocardial infarction on the ventricular fibrillation waveform

Provided that an organised rhythm is present, QRS-T segment changes on the ECG allow for the identification of a STEMI and in some cases a NSTEMI. The absence of this segment during VF complicates the recognition of AMI. Hence, alternative methods of identifying AMI on the ECG during VF are required.

Analysis of the VF-waveform seems to offer possibilities. Several studies on animals and humans have suggested that MI alters VFWC. AMI induced in swine models by inserting a steel plug in one of the coronary arteries resulted in decreased amplitude and frequency characteristics of the subsequently induced VF[59,60]. Similarly, human studies showed that AMSA was reduced in patients with AMI[61,62]. An OMI seems to affect VFWC in a similar way. The VFWC in OMI swine were not altered as much as in AMI swine, but similar trends were described[63,64]. Supporting these findings, human studies comparing patients with OMI to patients without MI showed significant decreases in VFWC such as the MAA, MS, FM, FD and AMSA[47,65,66]. Table 2.1 shows an overview of animal and human studies that investigated VFWC changes caused by MI.

Table 2.1: Overview of animal and human studies on the influence of old or acute myocardial infarction on the ventricular fibrillation waveform. The arrows behind the waveform characteristics indicate the effect of myocardial infarction.

Author	Year	Study population	Controls	Old MI	Acute MI
Animal studies					
Indik et al.[67]	2006	19 rats	No MI	AMP, FM & FD ↓ BW ↑	-
Indik et al.[59]	2007	27 swine	No MI	-	Fmean, FM, FD & BW ↓
Indik et al.[63]	2008	37 swine	No MI	Fmean, FM, FD & BW ↓	Fmean, FM, FD & BW ↓
Indik et al.[60]	2009	60 swine	No MI	-	MS & AMSA ↓
Indik et al.[68]	2010	20 swine	No MI	-	MS & AMSA ↓
Indik et al.[64]	2011	30 swine	No MI	No significant differences	MS & AMSA ↓
McGovern et al.[69]	2015	48 swine	No MI	-	AMSA ↓
Human studies					
Sanchez-Munoz et al.[70]	2008	61 induced VF	No controls	Frequency changes at MI location	-
Olasveengen et al.[61]	2009	101 OHVF	No MI	-	MS & AMSA ↓
Bonnes et al.[65]	2015	186 induced VF	No MI	FD & OI ↓	-
Bonnes et al.[66]	2015	190 induced VF	No MI	MAA, FM, FD & AMSA ↓ BW ↑	-
Hidano et al.[71]	2016	430 OHVF	No MI	-	No significant differences
Hulleman et al.[62]	2017	716 OHVF	No MI	No significant differences	AMSA ↓
Thannhauser et al.[47]	2020	206 induced VF	No MI	MAA, MS, AMSA, PSA & OI ↓	-

AMP: amplitude, AMSA: amplitude spectrum area, BW: bandwidth, FD: dominant frequency, FM: median frequency, Fmean: mean frequency, MAA: mean absolute amplitude, MI: myocardial infarction, MS: median slope, OHVF: out-of-hospital ventricular fibrillation OI: organisation index, PSA: power spectrum area, VF: ventricular fibrillation.

Multivariate logistic regression

The main principle

Multivariate logistic regression (MVR) is a traditional statistical method that uses multiple variables to create a regression model that predicts categorical outcomes. Continuous outcomes can be estimated by linear regression. Categorical outcomes require logistic regression, the most common form being binary logistic regression which distinguishes between two outcomes that are coded 0 and 1.

Logistic regression estimates the probability of an outcome $Y \in \{0, 1\}$ occurring given p predictor variables $X_1, X_2, ..., X_p$ according to the expression:

$$P(Y) = \frac{1}{1 + e^{-(b_0 + b_1 X_1 + b_2 X_2 + ... + b_p X_p)}} \tag{2.22}$$

where $P(Y)$ is an abbreviation of the probability $P(Y = 1|X)$, with e the base of the natural logarithm, b_0 a constant and b_i the regression coefficient of the corresponding predictor variable X_i with $i \in \{1, 2, ..., p\}$. This is a logarithmic transformation of the linear regression equation. It allows the non-linear relationship between predictor variables and a categorical outcome to be expressed in a linear way.

The regression coefficients b_i are fitted to minimise the log-likelihood (LL) of the model:

$$LL = \sum_{i=1}^{N} [Y_i \ln(P(Y_i)) + (1 - Y_i) \ln(1 - P(Y_i))] \tag{2.23}$$

with N the number of cases and ln the natural logarithm. This measure quantifies how close a predicted outcome $P(Y_i)$ is compared to the actual outcome Y_i, summed for all N cases. The closer a predicted value is to the actual outcome, the smaller the LL and the more accurate the regression model. The LL is often multiplied by -2 so it approximates a χ^2 distribution.[72–75]

Variable entry

Multivariate regression implies that multiple predictor variables are used to construct the model. All available variables are included when using the forced entry method. A stepwise entry method includes only a selection of variables. The forward stepwise method based on the likelihood ratio is used in this thesis and will be explained next.

The regression model begins with the constant b_0 and without any predictor variables. Then a stepwise process begins that adds a variable to the model in each step. Roa's efficient score statistic is computed for all variables that are not in the model at the beginning of each step. This statistic resembles the likelihood ratio statistic but is less intensive to compute. A large score statistic indicates that adding the variable to the model will increase its performance; the variable with the largest score statistic and a *p*-value of <0.1 is added to the model. This results in a decrease of the model's -2LL, approximately the size of the Roa's score statistic of that variable, indicating that the model has become more accurate. The step ends by evaluating the contribution of the already included variables. The difference between the original model and the models in which one of the variables is removed is quantified by the likelihood ratio. The statistical significance of this ratio can be retrieved from the χ^2 distribution. If there is no significant difference at a *p*-value of <0.1 between the model with and the model without the variable, that specific variable is removed. Then the next step begins and the process is repeated until no more variables are added or removed.[72,73]

The forward stepwise method of variable entry is an example of a wrapper type of feature selection, where the performance of models with different input features is compared to determine the best combination[76,77].

Interpretation of the model

When stepwise variable inclusion has finished, the final model is acquired. The model is defined by a series of parameters for each of the included predictor variables.

The regression coefficients b_i and constant b_0 of equation (2.22) determine the role of each predictor variable in that equation. The standard error SE of the constant and each regression coefficient is computed as well, from which the Z_0 statistic can be computed:

$$Z_0 = \frac{b}{SE} \tag{2.24}$$

with b representing a regression coefficient b_i or constant b_0. This statistic follows an asymptotic standard-normal distribution under most circumstances[78]. The Wald statistic is then defined as its square:

$$Wald = Z_0^2. \tag{2.25}$$

The square of a normal distribution has a χ^2 distribution with one degree of freedom[78]. Therefore, the significance of the corresponding predictor variable can be computed. Variables usually contribute significantly when they have been included in a stepwise fashion.

Besides the regression coefficient itself, $exp(b)$ and its 95% confidence interval are computed as well. This represents the odds ratio of the predictor variable which gives it a meaningful interpretation. A unit increase of the variable means the odds of the outcome occurring are multiplied by the odds ratio. An odds ratio <1 therefore represents a negative correlation between the variable and the outcome whereas an odds ratio >1 indicates a positive correlation.[72]

Support vector machine

A support vector machine (SVM) is a binary classification technique that was developed mostly in the 1990s[79]. An SVM relies on using a hyperplane to divide the feature space of observations into two. The classification of an unseen test observation follows from the side of the hyperplane on which it resides. Details on how the hyperplane is defined, how it acts as a classifier and how it generalises to the concept of the SVM are explained in the following section.

Hyperplane

An $n \times p$ matrix $\mathbf{X}$ of n observations with p features can be described in a p-dimensional feature space. Each observation $x_i = (x_{i1}, x_{i2}, ..., x_{ip})$ has a class $y_i \in \{-1, 1\}$. For instance, $\mathbf{X}$ might be a 20×2 matrix. It then contains 20 observations with 2 features such as age and weight, of which some observations belong to the class of patients with an MI ($y = 1$) while others belong to the class of patients without an MI ($y = -1$). This data set can be described in a 2-dimensional plane, as is depicted in figure 2.10. The 1-dimensional line that divides the plane into two separated spaces can be considered a hyperplane.

More generally, a hyperplane is defined as a $(p-1)$-dimensional subset of the p-dimensional feature space described by the equation:

$$\beta_0 + \beta_1 x_1 + \beta_2 x_2 + ... + \beta_p x_p = 0. \tag{2.26}$$

If the equation holds for a point $x = (x_1, x_2, ..., x_p)$ it means that this point is located on the hyperplane. If a point x is located on either side of the hyperplane, the left side of equation (2.26) will be less or greater than 0, depending on the side of the hyperplane on which the point resides. A hyperplane that completely separates the observations in $\mathbf{X}$ according to their class labels y is called a separating hyperplane.

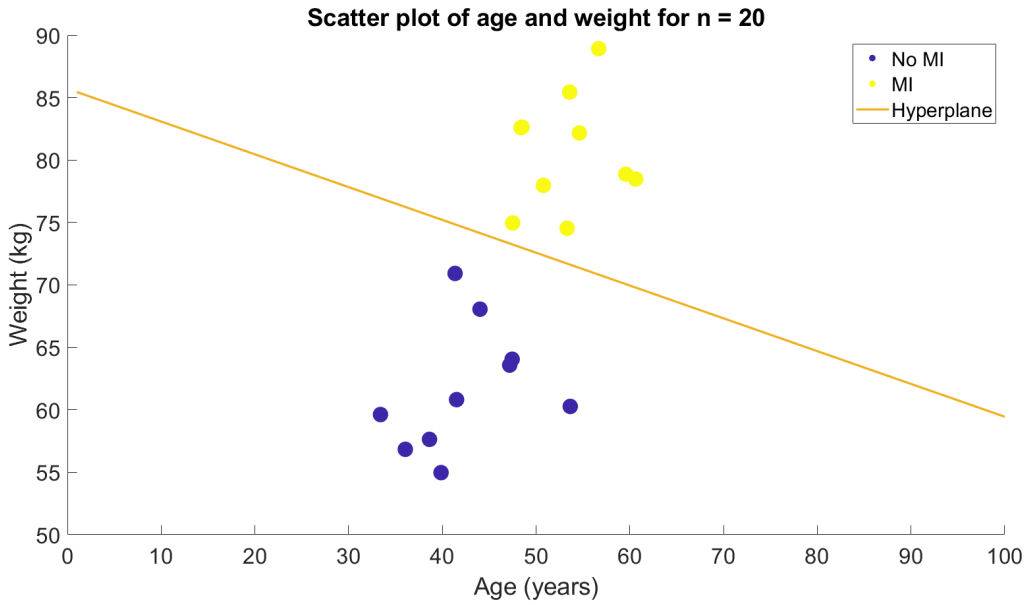

Figure 2.10: 2-dimensional scatter plot of a data set with 20 observations and the two features age and weight. The hyperplane is a 1-dimensional line that completely separating the two classes 'No MI' and 'MI'.

This means that

$$\beta_0 + \beta_1 x_{i1} + \beta_2 x_{i2} + ... + \beta_p x_{ip} > 0, \text{ if } y_i = 1, \tag{2.27}$$

$$\beta_0 + \beta_1 x_{i1} + \beta_2 x_{i2} + ... + \beta_p x_{ip} < 0, \text{ if } y_i = -1. \tag{2.28}$$

This can alternatively be written as

$$y_i(\beta x_i^T + \beta_0) > 0 \tag{2.29}$$

for all $i = 1, 2, ..., n$, with x_i the i^{th} row vector of $\mathbf{X}$ and $\beta = (\beta_1, \beta_2, ..., \beta_p)$. The separating hyperplane can then be used as a classifying function $f(x)$:

$$f(x) = \beta x^T + \beta_0. \tag{2.30}$$

A positive outcome means the test observation x belongs to the positive class $y = 1$; a negative outcome means it belongs to the negative class $y = -1$.[74,75]

Maximal margin classifier

For data sets such as the one shown in figure 2.10, infinitely many hyperplanes can be defined that completely separate the two classes. The optimal hyperplane is the one with the largest perpendicular distance, or margin M, to the nearest observations. A classifier based on the optimal hyperplane is therefore called the maximal margin classifier (MMC).

Maximising M is an optimisation problem defined by:

$$\begin{aligned} &\max_{\beta, \beta_0} M \\ &\text{subject to } \frac{1}{\|\beta\|} y_i(\beta x_i^T + \beta_0) \geq M \end{aligned} \tag{2.31}$$

with $i = 1, 2, ..., n$. The factor $1/\|\beta\|$ ensures that the distance of an observation to the hyperplane is expressed by the left side of the inequality. Any positively scaled multiples of β_0 and β

satisfy equation (2.31), so they can be chosen such that$\|\beta\| = 1/M$. Rephrasing the optimisation problem as a minimisation of $\|\beta\|$ rather than a maximisation of M:

$$\begin{gathered}\min_{\beta,\beta_0} \frac{1}{2}\|\beta\|^2 \\ \text{subject to } y_i(\beta x_i^T + \beta_0) \geq 1\end{gathered} \tag{2.32}$$

with $i = 1, 2, ..., n$. Multiplying $\|\beta\|$ by $1/2$ and squaring it is done for convenience as it makes the problem easier to solve. The problem can be solved by quadratic programming; this will not be explained here. The solution will give values for β and β_0 that define the optimal hyperplane.[74,75,80]

Support vector classifier

In most real-world applications, classes cannot be separated completely so an MMC does not work. Even if a separating hyperplane can be found, it might result in overfitting of the training data and thus yield a low accuracy for test data. An extension to the MMC is the support vector classifier (SVC). It allows some training observations to be classified incorrectly so the hyperplane can separate the rest of the observations with a larger margin. The observations that are on the margin or on the wrong side of the margin thereby define the position of the hyperplane. These are known as the support vectors.

The corresponding optimisation is similar to the MMC problem but with added terms:

$$\begin{gathered}\min_{\beta,\beta_0} \frac{1}{2}\|\beta\|^2 + C\sum_{i=1}^{N} \epsilon_i \\ \text{subject to } \epsilon_i \geq 0, y_i(\beta x_i^T + \beta_0) \geq 1 - \epsilon_i,\end{gathered} \tag{2.33}$$

with $i = 1, 2, ..., n$. The slack variables $\epsilon = (\epsilon_1, \epsilon_2, ..., \epsilon_n)$ are introduced to allow observations to be misclassified. Correct classification of observation x_i is quantified by $\epsilon_i = 0$, classification on the wrong side of the margin by $0 < \epsilon_i < 1$ and classification on the wrong side of the hyperplane by $\epsilon_i > 1$. C is non-negative parameter that dictates to what extent misclassification is allowed. It is called the cost or the box constraint. As such, a high value of C allows for few misclassifications and a narrow margin. For the limit $C \to \infty$ the classifier becomes an MMC. A low value of C results in more misclassifications and a wider margin. The SVC will therefore have a lower accuracy on training data but will generalise better to unseen data.[74,75,80,81]

Support vector machine

The SVC generally performs better than the MMC as it allows a soft margin. As it is a linear classifier, its application is limited to linearly separable data sets, however. Non-linear data sets cannot be separated properly with a linear classifier. A solution to this problem is enlarging the original feature space by introducing polynomial terms of x_i such as $x_{i1}^2, x_{i2}^2, ..., x_{ip}^2$, or even higher orders. The hyperplane of the classifier will be linear in the enlarged feature space but non-linear in the original feature space, which allows for boundaries that fit the data in a better way. An SVC with this extension is called an SVM.

The solution $\hat{\beta}$ of the SVC optimisation problem given by equation (2.33) can be expressed in the following way:

$$\hat{\beta} = \sum_{i=1}^{N} \hat{\alpha}_i y_i x_i \tag{2.34}$$

with $0 < \hat{\alpha}_i < C$[75,80,81]. Using equation (2.34), the solution $\hat{f}(x)$ of the classifying function given by equation (2.30) can be written as

$$\hat{f}(x) = \sum_{i \in S} \hat{\alpha}_i y_i x_i x^T + \hat{\beta}_0 \tag{2.35}$$

in which $\hat{\beta}_0$ is the optimised value for β_0 and collection S contains the indices i with $\hat{\alpha}_i > 0$. These indices represent the support vectors and as such they are the only observations needed to define the classifying function $\hat{f}(x)$. Leaving out the other observations decreases the computational cost which makes SVMs attractive.

A more general notation can be acquired by replacing $x_i x^T$ by a kernel function $K(x, x_i)$:

$$\hat{f}(x) = \sum_{i \in S} \hat{\alpha}_i y_i K(x, x_i) + \hat{\beta}_0. \tag{2.36}$$

When the kernel function is the inner product such as in equation (2.35), the classifying function is the linear SVC. An SVM can have other kernel functions as well. Popular alternative kernel functions are the polynomial function $K(x, x_i) = (1 + x_i x^T)^d$ with $d \geq 2$ or the radial basis function $K(x, x_i) = \exp(-\gamma \|x - x_i\|^2)$ also known as the Gaussian. Such alternatives extend the functionality of the SVM to classification of non-linear data.[74,75,80,81]

2.2.3 Support vector machine for the detection of myocardial infarction

Model creation

VF-waveform analysis using an SVM was performed using the function *fitcsvm* in MATLAB® (version 2020a, MathWorks®, Natick, MA, USA). This function creates an SVM model based on the $n \times p$ predictor matrix, the $n \times 1$ outcome vector with class labels and a set of hyperparameters. These hyperparameters include the box constraint C and kernel function $K(x, x_i)$. For Gaussian kernel functions the kernel scale can be chosen; for polynomial kernel functions the polynomial order can be chosen. Additionally, the option to standardise the predictor matrix is given. Finally, the misclassification cost can be altered so that false-positive predictions are penalised heavier or lighter than false-negative predictions.

Quantifying model performance

The performance of the SVM can be quantified using the function *crossval*. This returns the predictions and validation scores based on *k*-fold cross-validation which was for this thesis set to $k = 5$. The validation scores and true class labels of the observations can then be entered into the function *perfcurve*, which creates a receiver operating characteristic (ROC)-curve. For this thesis, an additional input argument 'NBoot' $= 1000$ was used to perform bootstrapping in order to compute the 95% confidence interval of the ROC-curve. The area under the curve (AUC) was used as a measure of model performance, as well as the sensitivity at the level of 80% specificity.

Hyperparameter optimisation

The hyperparameters of the SVM can be optimised automatically via the *fitcsvm* function which uses a Bayesian optimisation algorithm. The algorithm attempts to minimise the five-fold cross-validation loss by varying all aforementioned hyperparameters except for the misclassification cost. A maximum of 250 iterations was used to find the optimum for this thesis. Since Bayesian optimisation is not reproducible, the above optimisation procedure was repeated ten times for each SVM to evaluate the variation in the proposed hyperparameters between optimisation attempts. The set of hyperparameters that reached the highest AUC was considered optimal. This final combination was then used to train and cross-validate six SVMs with false-positive misclassification costs of 1, 2.5, 5, 10, 15 and 20 respectively, keeping the false-negative cost at 1. The misclassification cost that resulted in the highest AUC was chosen.

In this way, each set of input features led to a unique combination of hyperparameters and a misclassification cost. These settings were used to create the SVMs described in chapters 4 and 5. An overview of the steps of the hyperparameter optimisation procedure is given in figure 2.11.

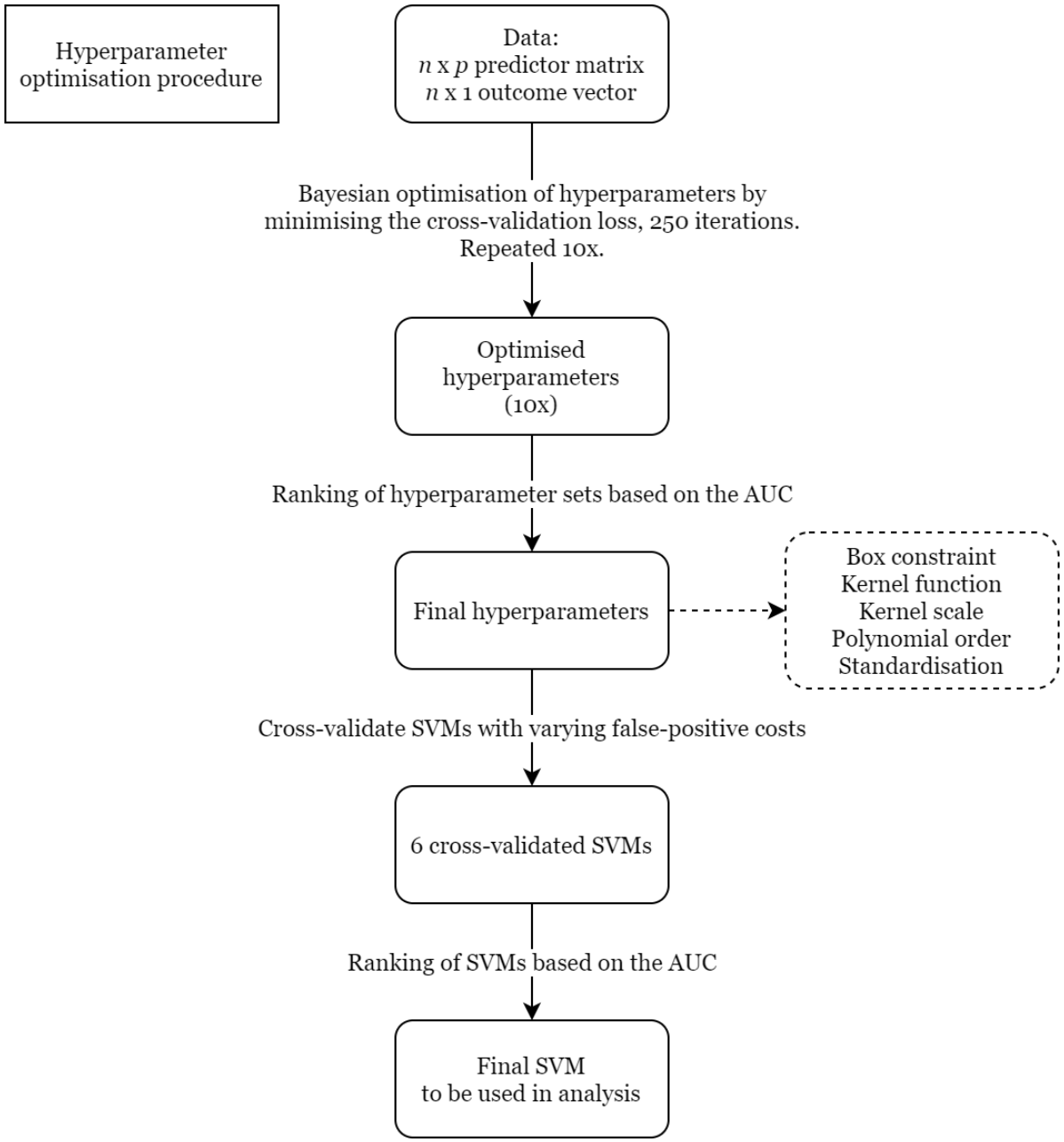

Figure 2.11: Overview of the hyperparameter optimisation procedure. AUC: area under the curve, SVM: support vector machine.

References

[1] Robert J. Myerburg and Agustin Castellanos. "Cardiac Arrest and Sudden Cardiac Death". In: *Braunwald's Heart Disease: A Textbook of Cardiovascular Medicine*. Ed. by Robert O. Bonow, Douglas L. Mann, Douglas P. Zipes, and Peter Libby. 9th ed. Elsevier Saunders, 2012. Chap. 41, pp. 845–884. DOI: 10.1016/b978-1-4377-0398-6.00041-x.

[2] Jacqueline J.M. De Vreede-Swagemakers et al. "Out-of-hospital cardiac arrest in the 1990s: A population-based study in the Maastricht area on incidence, characteristics and survival". In: *Journal of the American College of Cardiology* 30.6 (Nov. 1997), pp. 1500–1505. ISSN: 07351097. DOI: 10.1016/S0735-1097(97)00355-0.

[3] Robert J Myerburg, Alberto Interian, Raul M Mitrani, Kenneth M Kessler, and Agustin Castellanos. "Frequency of sudden cardiac death and profiles of risk". In: *American Journal of Cardiology* 80.5 B (Sept. 1997), 10F–19F. ISSN: 00029149. DOI: 10.1016/S0002-9149(97)00477-3.

[4] Douglas P. Zipes and Hein J.J. Wellens. "Sudden cardiac death". In: *Circulation* 98.21 (Nov. 1998), pp. 2334–2351. ISSN: 00097322. DOI: 10.1161/01.CIR.98.21.2334.

[5] A. Selcuk Adabag, Russell V. Luepker, Véronique L. Roger, and Bernard J. Gersh. "Sudden cardiac death: Epidemiology and risk factors". In: *Nature Reviews Cardiology* 7.4 (Apr. 2010), pp. 216–225. ISSN: 17595002. DOI: 10.1038/nrcardio.2010.3.

[6] Meiso Hayashi, Wataru Shimizu, and Christine M. Albert. "The Spectrum of Epidemiology Underlying Sudden Cardiac Death". In: *Circulation Research* 116.12 (June 2015), pp. 1887–1906. ISSN: 15244571. DOI: 10.1161/CIRCRESAHA.116.304521.

[7] R. R. Liberthson, E. L. Nagel, J. C. Hirschman, S. R. Nussenfeld, B. D. Blackbourne, and J. H. Davis. "Pathophysiologic observations in prehospital ventricular fibrillation and sudden cardiac death". In: *Circulation* 49.5 (May 1974), pp. 790–798. ISSN: 00097322. DOI: 10.1161/01.CIR.49.5.790.

[8] J K Madsen. "Ischaemic heart disease and prodromes of sudden cardiac death: Is it possible to identify high risk groups for sudden cardiac death?" In: *British Heart Journal* 54.1 (July 1985), pp. 27–32. ISSN: 00070769. DOI: 10.1136/hrt.54.1.27.

[9] Andrew Farb, Anita L. Tang, Allen P. Burke, Laura Sessums, Youhui Liang, and Renu Virmani. "Sudden coronary death: Frequency of active coronary lesions, inactive coronary lesions, and myocardial infarction". In: *Circulation* 92.7 (Oct. 1995), pp. 1701–1709. ISSN: 00097322. DOI: 10.1161/01.CIR.92.7.1701.

[10] Allen P. Burke, Andrew Farb, Gray T. Malcom, You Hui Liang, John Smialek, and Renu Virmani. "Coronary risk factors and plaque morphology in men with coronary disease who died suddenly". In: *New England Journal of Medicine* 336.18 (May 1997), pp. 1276–1282. ISSN: 00284793. DOI: 10.1056/NEJM199705013361802.

[11] Christian M. Spaulding et al. "Immediate coronary angiography in survivors of out-of-hospital cardiac arrest". In: *New England Journal of Medicine* 336.23 (June 1997), pp. 1629–1633. ISSN: 00284793. DOI: 10.1056/NEJM199706053362302.

[12] Guillaume Geri et al. "Etiological diagnoses of out-of-hospital cardiac arrest survivors admitted to the intensive care unit: Insights from a French registry". In: *Resuscitation* 117 (Aug. 2017), pp. 66–72. ISSN: 18731570. DOI: 10.1016/j.resuscitation.2017.06.006.

[13] Demetris Yannopoulos et al. "Coronary Artery Disease in Patients With Out-of-Hospital Refractory Ventricular Fibrillation Cardiac Arrest". In: *Journal of the American College of Cardiology* 70.9 (Aug. 2017), pp. 1109–1117. ISSN: 15583597. DOI: 10.1016/j.jacc.2017.06.059.

[14] K. Ramaswamy and M. H. Hamdan. "Ischemia, metabolic disturbances, and arrhythmogenesis: Mechanisms and management". In: *Critical Care Medicine* 28.10 SUPPL. (Oct. 2000), N151–7. ISSN: 00903493. DOI: 10.1097/00003246-200010001-00007.

[15] Janna P. Kauppila et al. "Association of initial recorded rhythm and underlying cardiac disease in sudden cardiac arrest". In: *Resuscitation* 122 (Jan. 2018), pp. 76–78. ISSN: 18731570. DOI: 10.1016/j.resuscitation.2017.11.064.

[16] Jocelyn Berdowski, Robert A. Berg, Jan G P Tijssen, and Rudolph W. Koster. "Global incidences of out-of-hospital cardiac arrest and survival rates: Systematic review of 67 prospective studies". In: *Resuscitation* 81.11 (Nov. 2010), pp. 1479–1487. ISSN: 03009572. DOI: 10.1016/j.resuscitation.2010.08.006.

[17] Arthur C. Guyton and John E. Hall. "Cardiac Arrhythmias and Their Electrocardiographic Interpretation". In: *Textbook of Medical Physiology*. Ed. by Arthur C. Guyton and John E. Hall. 11th ed. Elsevier Saunders, 2006. Chap. 13, pp. 147–157.

[18] W. J. Lederer. "Cardiac Electrophysiology and the Electrocardiogram". In: *Medical Physiology*. Ed. by Walter F. Boron and Emile L. Boulpaep. 2nd ed. Elsevier Saunders, 2009. Chap. 22, pp. 504–528.

[19] Arthur C. Guyton and John E. Hall. “Rhythmical Excitation of the Heart”. In: *Textbook of Medical Physiology*. Ed. by Arthur C. Guyton and John E. Hall. 11th ed. Elsevier Saunders, 2006. Chap. 10, pp. 116–122.

[20] Arthur C. Guyton and John E. Hall. “Electrocardiographic Interpretation of Cardiac Muscle and Coronary Blood Flow Abnormalities: Vectorial Analysis”. In: *Textbook of Medical Physiology*. Ed. by Arthur C. Guyton and John E. Hall. 11th ed. Elsevier Saunders, 2006. Chap. 12, pp. 131–146.

[21] Edward Carmeliet. “Cardiac ionic currents and acute ischemia: From channels to arrhythmias”. In: *Physiological Reviews* 79.3 (July 1999), pp. 917–1017. ISSN: 00319333. DOI: 10.1152/physrev.1999.79.3.917.

[22] Joseph G. Akar and Fadi G. Akar. “Regulation of ion channels and arrhythmias in the ischemic heart”. In: *Journal of Electrocardiology* 40.6 SUPPL. 1 (Nov. 2007), S37–S41. ISSN: 00220736. DOI: 10.1016/j.jelectrocard.2007.05.020.

[23] Nazar Luqman, Ruey J. Sung, Chun Li Wang, and Chi Tai Kuo. “Myocardial ischemia and ventricular fibrillation: Pathophysiology and clinical implications”. In: *International Journal of Cardiology* 119.3 (July 2007), pp. 283–290. ISSN: 01675273. DOI: 10.1016/j.ijcard.2006.09.016.

[24] Valentlno Ducceschi, Gianluca Di Micco, Berardo Sarubbi, Biancamaria Russo, Lucio Santangelo, and Aldo Iacono. “Ionic mechanisms of ischemia-related ventricular arrhythmias”. In: *Clinical Cardiology* 19.4 (Apr. 1996), pp. 325–331. ISSN: 01609289. DOI: 10.1002/clc.4960190409.

[25] Harry A. Fozzard. “Afterdepolarizations and triggered activity”. In: *Basic Research in Cardiology* 87.SUPPL. 2 (1992), pp. 105–113. ISSN: 03008428. DOI: 10.1007/978-3-642-72477-0_10.

[26] James N. Weiss, Alan Garfinkel, Hrayr S. Karagueuzian, Peng Sheng Chen, and Zhilin Qu. “Early afterdepolarizations and cardiac arrhythmias”. In: *Heart Rhythm* 7.12 (Dec. 2010), pp. 1891–1899. ISSN: 15475271. DOI: 10.1016/j.hrthm.2010.09.017.

[27] Charles Antzelevitch and Alexander Burashnikov. *Overview of Basic Mechanisms of Cardiac Arrhythmia*. 2011. DOI: 10.1016/j.ccep.2010.10.012.

[28] David E Krummen, Gordon Ho, Christopher T Villongco, Justin Hayase, and Amir A Schricker. *Ventricular fibrillation: Triggers, mechanisms and therapies*. May 2016. DOI: 10.2217/fca-2016-0001.

[29] Arthur C. Guyton and John E. Hall. “The Normal Electrocardiogram”. In: *Textbook of Medical Physiology*. Ed. by Arthur C. Guyton and John E. Hall. 11th ed. Elsevier Saunders, 2006. Chap. 11, pp. 123–130.

[30] David M. Mirvis and Ary L. Goldberger. “Electrocardiography”. In: *Braunwald’s Heart Disease: A Textbook of Cardiovascular Medicine*. Ed. by Robert O. Bonow, Douglas L. Mann, Dougles P. Zipes, and Peter Libby. 9th ed. Elsevier Saunders, 2012. Chap. 13, pp. 126–167.

[31] Russell K. Hobbie and Bradley J. Roth. *Intermediate physics for medicine and biology*. Biological and medical physics, biomedical engineering. Springer New York, 2007, pp. 1–616. ISBN: 038730942X. DOI: 10.1007/978-0-387-49885-0.

[32] Charles Antzelevitch. “Cellular basis for the repolarization waves of the ECG”. In: *Annals of the New York Academy of Sciences*. Vol. 1080. Blackwell Publishing Inc., 2006, pp. 268–281. ISBN: 1573316512. DOI: 10.1196/annals.1380.021.

[33] National Clinical Guideline Centre. “Myocardial Infarction with ST-Segment Elevation: The Acute Management of Myocardial Infarction with ST-Segment Elevation - PubMed - NCBI”. In: *Clinical guideline 167. Methods, evidence and recommendations* July (2013), pp. 1–130.

[34] Kristian Thygesen et al. “Fourth universal definition of myocardial infarction (2018)”. In: *European Heart Journal* 40.3 (2019), pp. 237–269. ISSN: 15229645. DOI: 10.1093/eurheartj/ehy462.

[35] Marc S. Sabatine and Christopher P. Cannon. “Approach to the Patient with Chest Pain”. In: *Braunwald’s Heart Disease: A Textbook of Cardiovascular Medicine*. Ed. by Robert O. Bonow, Douglas L. Mann, Douglas P. Zipes, and Peter Libby. 9th ed. Elsevier Saunders, 2012. Chap. 53, pp. 1076–1086.

[36] Elliott M. Antman. “ST-Segment Elevation Myocardial Infarction: Pathology, Pathophysiology, and Clinical Features”. In: *Braunwald’s Heart Disease: A Textbook of Cardiovascular Medicine*. Ed. by Robert O. Bonow, Douglas L. Mann, Douglas P. Zipes, and Peter Libby. 9th ed. Elsevier Saunders, 2012. Chap. 54, pp. 1087–1110.

[37] Elliott M. Antman and David A. Morrow. “ST-Segment Elevation Myocardial Infarction: Management”. In: *Braunwald’s Heart Disease: A Textbook of Cardiovascular Medicine*. Ed. by Robert O. Bonow, Douglas L. Mann, Douglas P. Zipes, and Peter Libby. 9th ed. Elsevier Saunders, 2012. Chap. 55, pp. 1111–1177.

[38] Christopher P. Cannon and Eugene Braunwald. “Unstable Angina and Non-ST Elevation Myocardial Infarction”. In: *Braunwald’s Heart Disease: A Textbook of Cardiovascular Medicine*. Ed. by Robert O. Bonow, Douglas L. Mann, Douglas P. Zipes, and Peter Libby. 9th ed. Elsevier Saunders, 2012. Chap. 56, pp. 1178–1209.

[39] Patrick T O Gara et al. “AHA Guidelines - STEMI”. In: *Circulation* 127.4 (Jan. 2013). ISSN: 0009-7322. DOI: 10.1161/CIR.0b013e3182742cf6.

[40] Borja Ibanez et al. “2017 ESC Guidelines for the management of acute myocardial infarction in patients presenting with ST-segment elevation”. In: *European Heart Journal* 39.2 (Jan. 2018), pp. 119–177. ISSN: 15229645. DOI: 10.1093/eurheartj/ehx393.

[41] Jorrit S. Lemkes et al. “Coronary angiography after cardiac arrest without ST-segment elevation”. In: *New England Journal of Medicine* 380.15 (Apr. 2019), pp. 1397–1407. ISSN: 15334406. DOI: 10.1056/NEJMoa1816897.

[42] Jose Victor Nable and William Brady. “The evolution of electrocardiographic changes in ST-segment elevation myocardial infarction”. In: *American Journal of Emergency Medicine* 27.6 (July 2009), pp. 734–746. ISSN: 07356757. DOI: 10.1016/j.ajem.2008.05.025.

[43] Francis Morris and William J Brady. “ABC of clinical electrocardiography Acute myocardial infarction-Part I”. In: *British Medical Journal* 324 (2002), pp. 831–834.

[44] Akira Tamura, Kimiaki Nagase, Yoshiaki Mikuriya, and Masaru Nasu. “Significance of spontaneous normalization of negative T waves in infarct-related leads during healing of anterior wall acute myocardial infarction”. In: *American Journal of Cardiology* 84.11 (Dec. 1999), pp. 1341–1344. ISSN: 00029149. DOI: 10.1016/S0002-9149(99)00569-X.

[45] W. D. Weaver, L. A. Cobb, D. Dennis, R. Ray, A. P. Hallstrom, and M. K. Copass. “Amplitude of ventricular fibrillation waveform and outcome after cardiac arrest”. In: *Annals of Internal Medicine* 102.1 (Jan. 1985), pp. 53–55. ISSN: 00034819. DOI: 10.7326/0003-4819-102-1-53.

[46] Matthew J. Reed, Gareth R. Clegg, and Colin E. Robertson. *Analysing the ventricular fibrillation waveform*. 2003. DOI: 10.1016/S0300-9572(02)00441-0.

[47] Jos Thannhauser et al. “Computerized analysis of the ventricular fibrillation waveform allows identification of myocardial infarction: a proof-of-concept study for smart defibrillator applications in cardiac arrest”. In: *Journal of the American Heart Association* (2020).

[48] C. K. Peng, S V Buldyrev, S. Havlin, M Simons, H E Stanley, and A. L. Goldberger. “Mosaic organization of DNA nucleotides”. In: *Physical Review E* 49.2 (1994), pp. 1685–1689. ISSN: 1063651X. DOI: 10.1103/PhysRevE.49.1685.

[49] C. K. Peng, Shlomo Havlin, H Eugene Stanley, and Ary L Goldberger. “Quantification of scaling exponents and crossover phenomena in nonstationary heartbeat time series”. In: *Chaos* 5.1 (1995), pp. 82–87. ISSN: 10541500. DOI: 10.1063/1.166141.

[50] Michael Callaham, Odelia Braun, Wesley Valentine, Douglas M Clark, and Claudia Zegans. “Prehospital cardiac arrest treated by urban first-responders: Profile of patient response and prediction of outcome by ventricular fibrillation waveform”. In: *Annals of Emergency Medicine* 22.11 (Nov. 1993), pp. 1664–1677. ISSN: 01960644. DOI: 10.1016/S0196-0644(05)81304-6.

[51] G W.N. Dalzell and A A.J. Adgey. “Determinants of successful transthoracic defibrillation and outcome in ventricular fibrillation”. In: *British Heart Journal* 65.6 (June 1991), pp. 311–316. ISSN: 00070769. DOI: 10.1136/hrt.65.6.311.

[52] Hans Ulrich Strohmenger, Karl H. Lindner, and Charles G. Brown. “Analysis of the ventricular fibrillation ECG signal amplitude and frequency parameters as predictors of countershock success in humans”. In: *Chest* 111.3 (Mar. 1997), pp. 584–589. ISSN: 00123692. DOI: 10.1378/chest.111.3.584.

[53] H. P. Povoas and J. Bisera. “Electrocardiographic waveform analysis for predicting the success of defibrillation”. In: *Critical Care Medicine* 28.11 SUPPL. (Nov. 2000), N210–1. ISSN: 00903493.

[54] Heitor P. Povoas, Max Harry Weil, Wanchun Tang, Joe Bisera, Kada Klouche, and Ann Barbatsis. “Predicting the success of defibrillation by electrocardiographic analysis”. In: *Resuscitation* 53.1 (Apr. 2002), pp. 77–82. ISSN: 03009572. DOI: 10.1016/S0300-9572(01)00488-9.

[55] Hans Ulrich Strohmenger. *Predicting defibrillation success*. 2008. DOI: 10.1097/MCC.0b013e3282fc9a9c.

[56] Clifton W Callaway and James J Menegazzi. “Waveform analysis of ventricular fibrillation to predict defibrillation”. In: *Curr Opin Crit Care* 11 (2005), pp. 192–199.

[57] Trygve Eftestol, Kjetil Sunde, Sven Ole Aase, John Håkon Husoy, and Petter Andreas Steen. “‘Probability of successful defibrillation’ as a monitor during CPR in out-of-hospital cardiac arrested patients”. In: *Resuscitation* 48.3 (Mar. 2001), pp. 245–254. ISSN: 03009572. DOI: 10.1016/S0300-9572(00)00266-5.

[58] Trygve Eftestøl, Kjetil Sunde, Sven Ole Aase, John Håkon Husøy, and Petter Andreas Steen. “Predicting outcome of defibrillation by spectral characterization and nonparametric classification of ventricular fibrillation in patients with out-of-hospital cardiac arrest”. In: *Circulation* 102.13 (Sept. 2000), pp. 1523–1529. ISSN: 00097322. DOI: 10.1161/01.CIR.102.13.1523.

[59] Julia H. Indik, Richard L. Donnerstein, Robert A. Berg, Ronald W. Hilwig, Marc D. Berg, and Karl B. Kern. “Ventricular fibrillation frequency characteristics are altered in acute myocardial infarction”. In: *Critical Care Medicine* 35.4 (Apr. 2007), pp. 1133–1138. ISSN: 00903493. DOI: 10.1097/01.CCM.0000259540.52062.99.

[60] Julia H. Indik et al. “Predictors of resuscitation outcome in a swine model of VF cardiac arrest: A comparison of VF duration, presence of acute myocardial infarction and VF waveform”. In: *Resuscitation* 80.12 (Dec. 2009), pp. 1420–1423. ISSN: 03009572. DOI: 10.1016/j.resuscitation.2009.08.023.

[61] Theresa M. Olasveengen, Trygve Eftestøl, Kenneth Gundersen, Lars Wik, and Kjetil Sunde. “Acute ischemic heart disease alters ventricular fibrillation waveform characteristics in out-of hospital cardiac arrest”. In: *Resuscitation* 80.4 (Apr. 2009), pp. 412–417. ISSN: 03009572. DOI: 10.1016/j.resuscitation.2009.01.012.

[62] Michiel Hulleman et al. “Predictive value of amplitude spectrum area of ventricular fibrillation waveform in patients with acute or previous myocardial infarction in out-of-hospital cardiac arrest”. In: *Resuscitation* 120 (Nov. 2017), pp. 125–131. ISSN: 18731570. DOI: 10.1016/j.resuscitation.2017.08.219.

[63] Julia H. Indik et al. “The influence of myocardial substrate on ventricular fibrillation waveform: A swine model of acute and postmyocardial infarction”. In: *Critical Care Medicine* 36.7 (July 2008), pp. 2136–2142. ISSN: 15300293. DOI: 10.1097/CCM.0b013e31817d798c.

[64] Julia H. Indik, Daniel Allen, Michael Gura, Christian Dameff, Ronald W. Hilwig, and Karl B. Kern. “Utility of the ventricular fibrillation waveform to predict a return of spontaneous circulation and distinguish acute from post myocardial infarction or normal swine in ventricular fibrillation cardiac arrest”. In: *Circulation: Arrhythmia and Electrophysiology* 4.3 (June 2011), pp. 337–343. ISSN: 19413149. DOI: 10.1161/CIRCEP.110.960419.

[65] Judith L. Bonnes et al. “Characteristics of ventricular fibrillation in relation to cardiac aetiology and shock success: A waveform analysis study in ICD-patients”. In: *Resuscitation* 86 (Jan. 2015), pp. 95–99. ISSN: 18731570. DOI: 10.1016/j.resuscitation.2014.10.003.

[66] Judith L. Bonnes et al. “Ventricular fibrillation waveform characteristics differ according to the presence of a previous myocardial infarction: A surface ECG study in ICD-patients”. In: *Resuscitation* 96 (Nov. 2015), pp. 239–245. ISSN: 18731570. DOI: 10.1016/j.resuscitation.2015.08.014.

[67] Julia H. Indik, Richard L. Donnerstein, Karl B. Kern, Steven Goldman, Mohamed A. Gaballa, and Robert A. Berg. “Ventricular fibrillation waveform characteristics are different in ischemic heart failure compared with structurally normal hearts”. In: *Resuscitation* 69.3 (June 2006), pp. 471–477. ISSN: 03009572. DOI: 10.1016/j.resuscitation.2005.10.017.

[68] Julia H. Indik et al. “Predictors of resuscitation in a swine model of ischemic and nonischemic ventricular fibrillation cardiac arrest: Superiority of amplitude spectral area and slope to predict a return of spontaneous circulation when resuscitation efforts are prolonged”. In: *Critical Care Medicine* 38.12 (Dec. 2010), pp. 2352–2357. ISSN: 15300293. DOI: 10.1097/CCM.0b013e3181fa01ee.

[69] Meghan McGovern, Daniel Allen, Fahd Chaudhry, Zacherie Conover, Ronald Hilwig, and Julia H. Indik. “The ventricular fibrillation waveform approach to direct postshock chest compressions in a swine model of VF arrest”. In: *Journal of Emergency Medicine* 48.3 (2015), pp. 373–381. ISSN: 07364679. DOI: 10.1016/j.jemermed.2014.09.057.

[70] Juan J. Sánchez-Muñoz et al. “Effects of the location of myocardial infarction on the spectral characteristics of ventricular fibrillation”. In: *PACE - Pacing and Clinical Electrophysiology* 31.6 (June 2008), pp. 660–665. ISSN: 01478389. DOI: 10.1111/j.1540-8159.2008.01068.x.

[71] Danelle Hidano et al. “Ventricular fibrillation waveform measures and the etiology of cardiac arrest”. In: *Resuscitation* (2016). ISSN: 18731570. DOI: 10.1016/j.resuscitation.2016.10.007.

[72] Andy Field. “Logistic regression”. In: *Discovering Statistics Using SPSS*. 3rd ed. SAGE Publications, 2009. Chap. 8, pp. 264–315. ISBN: 9781847879073.

[73] Rudolf J. Freund, William J. Wilson, and Donna L. Mohr. “Special Types of Regression”. In: *Statistical Methods* (2010), pp. 663–688. DOI: 10.1016/b978-0-12-374970-3.00013-5.

[74] G James, D Witten, T Hastie, and R Tibshirani. *An Introduction to Statistical Learning: with Applications in R*. 1st ed. Springer Texts in Statistics. Springer New York, 2013, p. 426. ISBN: 9781461471387.

[75] T Hastie, R Tibshirani, and J Friedman. *The Elements of Statistical Learning: Data Mining, Inference, and Prediction, Second Edition*. 2nd ed. Springer Series in Statistics. Springer New York, 2009, p. 745. ISBN: 9780387848587.

[76] Gh John, Ron Kohavi, and K Pfleger. “Irrelevant Features and the Subset Selection Problem”. In: *Machine Learning: Proceedings of the Eleventh International Conference* (1994), pp. 121–129. ISSN: 00189340.

[77] Max Kuhn and Kjell Johnson. *Applied Predictive Modeling with Applications in R*. 2013, p. 615. ISBN: 9781461468486.

[78] John Fox. *Applied Regression Analysis and Generalized Linear Models*. 3rd ed. SAGE Publications, 2016. ISBN: 9781483321318.

[79] V Vapnik. *The Nature of Statistical Learning Theory*. 2nd ed. Information Science and Statistics. Springer New York, 2000, p. 314. ISBN: 9781475732641.

[80] Christopher M Bishop. *Pattern Recognition and Machine Learning*. Ed. by M Jordan, J Kleinberg, and B Schölkopf. 1st ed. Information Science and Statistics. Springer, 2006, p. 738. ISBN: 9780387310732.

[81] Kevin P Murphy. *Machine Learning: A Probabilistic Perspective*. 1st ed. Adaptive Computation and Machine Learning series. MIT Press, 2012, p. 1067. ISBN: 9780262018029.

3 | Introducing the multi-electrode defibrillator patch: A novel approach to diagnose a myocardial infarction during ventricular fibrillation cardiac arrest

K.M. van der Sluijs[1], J. Thannhauser[2], M.A. Brouwer[2]
[1] Technical Medicine, University of Twente, Enschede, The Netherlands
[2] Department of Cardiology, Radboud University Medical Center, Nijmegen, The Netherlands

Abstract

Out-of-hospital cardiac arrest (OHCA) is a major healthcare problem and still has a low survival rate despite improvements over the past years. The defibrillator electrocardiogram (ECG) enables waveform analysis of ventricular fibrillation (VF), the most commonly found shockable rhythm. This offers an early, easily obtainable tool to gain insight into patient-specific information. Multiple applications of VF-waveform analysis have been reported, such as predicting defibrillation success. An application that requires further research is diagnosis of the disease underlying the arrhythmia. Diagnosis of acute myocardial infarction (AMI) is particularly relevant as it is the major cause of VF. Animal studies have already shown that AMI can be detected using the VF-waveform. Human studies have reported associations between the VF-waveform and AMI as well, but no evidence currently exists that AMI can be detected from the VF-waveform in the OHCA setting. This application may require a multi-lead ECG approach, as VF-waveform analysis of 12-lead ECGs acquired during implantable cardioverter-defibrillator testing suggests. Predictive models based on these data can help find the optimal lead combination needed to detect AMI during VF. This gives direction to further research to move towards clinical implementation of a multi-electrode defibrillator.

3.1 Current status

Out-of-hospital cardiac arrest (OHCA) is a major healthcare problem. It occurs frequently in the Netherlands with an annual incidence rate of about 37 per 100,000 inhabitants and yields a high mortality of approximately 77%[1]. OHCA can be regarded a complex and unique medical emergency, of which outcomes strongly rely on community factors in the first phase, such as arrest recognition, bystander cardiopulmonary resuscitation (CPR), activation of the emergency medical services and availability of automated external defibrillators. Adequate treatment by medical professionals in the subsequent phase consists of high-quality CPR, defibrillation, hospital transportation, treatment of the underlying cause and post-arrest care. Technological advances have optimised these factors over the past years which has led to a steady increase in OHCA survival[1–3].

The current treatment for OHCA is protocolised and lacks an approach optimised for the individual patient. The paddle electrocardiogram (ECG) obtained by the defibrillator is one of the few available tools during OHCA and can provide patient-specific information. With use of the paddle ECG, defibrillators can distinguish non-shockable from shockable cardiac rhythms and apply defibrillatory shocks in case of the latter[4]. Besides the defibrillator's therapeutic use, the paddle ECG has been investigated for its diagnostic value. Especially in case of ventricular fibrillation (VF), which is the shockable rhythm most commonly found in OHCA patients, the VF-waveform provides an early, easily obtainable tool to provide patient-specific information and has been the subject of study since the 1980s[5–7]. This paper provides an overview of the current knowledge on the VF-waveform and an outlook on how VF-waveform analysis may be used in the future to facilitate patient-tailored resuscitative strategies during OHCA.

3.2 The possibilities of the paddle electrocardiogram

One of the earliest analyses of the VF-waveform was in the 1980s when Weaver *et al.* described how the amplitude of the VF is associated to arrest duration and chance of survival[8]. Similarly, Brown *et al.* reported associations between the median frequency of VF in swine and arrest duration, which they later used to predict downtime in other swine[9,10]. Additionally, they reported a decrease in the median frequency of human VF as arrest duration increased[10]. More research on the VF-waveform followed, showing that the amplitude can predict the conversion to a stable rhythm, hospital admission, hospital discharge and survival[11,12].

New ventricular fibrillation waveform characteristics (VFWC) have been introduced over the years along with new applications[7]. Predicting defibrillation shock success is one of the most studied uses of the VF-waveform[13]. Strohmenger *et al.* reported associations between frequency-related VFWC in swine and shock success[14]. Later studies found that shock success can be predicted using the VF-waveform as well[15–18]. Povoas *et al.* achieved this by using the amplitude spectrum area (AMSA), a new measure quantifying the area of the amplitude spectrum derived by fast Fourier transform of the ECG signal[17]. Strohmenger *et al.* continued their work in humans and found associations similar to those found in swine[19]. In recent years, Ristagno *et al.* have conducted retrospective studies and were able to predict shock success in humans using the AMSA[20–22]. Their current randomised controlled trial investigates whether real-time AMSA analysis during CPR can predict defibrillation success and optimise defibrillation timing[23]. This illustrates that VF-waveform analysis is ready for application in the resuscitation setting and may thereby optimise treatment strategy.

Another relevant application for VFWC that is gaining interest is identification of the arrhythmic cause. Detecting acute myocardial infarction (AMI) is of particular interest since it is a frequent initiator of VF[24]. Given that a severe AMI can often be recognised on a sinus rhythm ECG, it is presumable that AMI alters the VF-waveform as well[25].

Animal studies performed by Indik *et al.* have indeed found associations between decreases

in VFWC such as AMSA and presence of AMI or old myocardial infarction (OMI)[26–28]. Furthermore, Sherman *et al.* showed that frequency-related VFWC were lower in ischaemic swine than in swine with electrically induced VF[29]. Later work by Indik *et al.* showed that the AMSA and slope of porcine VF can predict a return of spontaneous circulation and presence of AMI[30–32].

Extending these findings to humans, Olasveengen *et al.*, Bonnes *et al.* and Hulleman *et al.* associated decreases in AMSA and median slope to presence of AMI or OMI[33–35]. These associations suggest that real-time VF-waveform analysis may be used to detect AMI during out-of-hospital ventricular fibrillation (OHVF). This is relevant as it may alter treatment strategy. Early coronary angiography and percutaneous coronary intervention are associated with better survival in OHCA patients with a restored rhythm[36–41]. This suggests that OHVF patients with AMI whose rhythm has not been restored will benefit from cardiac catheterisation as well. Recent advances such as mechanical CPR and extracorporeal life support allow for transport and cardiac catheterisation of patients without a perfusing rhythm. Yannopoulos *et al.* have shown that such an aggressive treatment strategy may benefit coronary artery disease patients with refractory VF[42]. Early diagnosis of AMI during OHVF may therefore guide therapy and save lives of patients who would otherwise have a small chance of survival.

3.3 The added value of the 12-lead electrocardiogram

So far, no prospective studies have been conducted that use the VF-waveform to detect AMI during OHVF. However, Thannhauser *et al.* were able to detect OMI using VFWC recorded in the setting of implantable cardioverter-defibrillator (ICD) testing[43]. These results propose that AMI can be detected using VFWC as well, since Indik *et al.* showed that the VF-waveform is altered by AMI and OMI in the same way[28].

Noteworthy is that Thannhauser *et al.* had access to 12-lead ECGs of VF rather than the single paddle ECG lead. Defibrillation testing during ICD implantation offers a unique setting to acquire 12-lead ECGs of VF, which could never happen in regular clinical practice. These data have led to several insights other than detecting myocardial infarction. Bonnes *et al.* reported that the left ventricular mass and diameter affect the VF-waveform[44]. Furthermore, they showed that the decreases in VFWC caused by OMI only occurred in the ECG leads aimed at the infarcted site[34]. These findings suggest that the VF-waveform is patient-specific and that the severity and location of underlying diseases play a role in the shaping of the VF-waveform.

An electrocardiographic description of the entire heart is therefore needed to reliably detect an underlying disease such as AMI. Diagnosis of an anterior AMI during sinus rhythm with a 12-lead ECG requires inspection of the anterior leads. It is therefore likely that diagnosis of an anterior AMI during VF requires inspection of an anterior lead as well. Since the paddle ECG is limited to one direction, a multi-lead ECG seems necessary to detect all AMIs during VF.

Thannhauser *et al.* therefore used the VF-waveform of 12-lead ECGs as input for a support vector machine (SVM) to detect OMIs[43]. An SVM with the AMSA of all twelve leads was compared to the AMSA of lead II alone, which can be considered a surrogate for the paddle ECG. The 12-lead model was superior in detecting OMI, strengthening the hypothesis that a multi-lead ECG can improve AMI detection during OHVF. Another interesting finding of this study was that the discriminative ability of the 12-lead model was lower when multiple VFWC were used rather than the AMSA alone. This suggests that a selection of input features for the SVM yields better results than bluntly using all available VFWC.

3.4 The potential of a multi-electrode defibrillator patch

Presumably, a multi-lead ECG can detect AMI more accurately than the single lead of the paddle ECG. However, clinical implementation is a long way off. The necessary protocol adaptations require extensive testing to investigate the best way of acquiring a multi-lead ECG.

Extra electrodes besides the two defibrillator pads are needed to obtain a multi-lead ECG. A 12-lead ECG requires the time-consuming placement of ten electrodes, making it unfit for the resuscitation setting. A minimal number of extra electrodes is therefore desirable, which means that only certain leads can be obtained. These could be some of the twelve regular leads but could include other leads as well, derived from non-conventional electrode placement. A single patch containing multiple electrodes offers an attractive solution as the resuscitation setting demands quick and easy placement of the extra electrodes. Even if such a patch is developed, the question remains what the optimal number and position of additional electrodes is for detecting AMI. Furthermore, the limited possibilities to adapt resuscitation protocols need to be taken into consideration.

Analysis of 12-lead ECGs of VF acquired during ICD testing may help answer what the optimal number and locations of additional electrodes is. Using such data in their proof-of-concept study, Thannhauser *et al.* have demonstrated that basic use of an SVM can already detect an OMI with an area under the receiver operating characteristic curve of 0.75[43]. Optimisation of the SVM hyperparameters and substantiated selection of input features may improve this. Comparing the SVM performance to that of traditional multivariate logistic regression models is essential to establish whether an SVM approach is of added value at all.

Analysis using both traditional statistical methods and machine learning approaches may propose an optimal method to detect OMIs using multi-lead VFWC based on the 12-lead configuration. This gives direction to further research on non-conventional electrode placement, moving towards the goal of a multi-electrode defibrillator patch to diagnose AMI during OHVF.

3.5 Conclusion

The VF-waveform contains useful information that can optimise treatment strategy of OHCA. An ongoing trial on predicting shock success proves that real-time VF-waveform analysis to guide therapy is feasible. Diagnosing AMI is another relevant application that deserves attention. Recent results suggest that a multi-electrode ECG may facilitate this. Further research is needed to find the optimal configuration of a multi-electrode defibrillator patch for diagnosing AMI during OHVF.

References

[1] J.A. Zijlstra et al. “Overleving na een reanimatie buiten het ziekenhuis: vergelijking van de resultaten van 6 verschillende Nederlandse regio’s”. In: *Reanimatie in Nederland 2016*. Den Haag: Hartstichting, 2016. Chap. 1, pp. 9–24.

[2] Marieke T. Blom et al. “Improved survival after out-of-hospital cardiac arrest and use of automated external defibrillators”. In: *Circulation* 130.21 (2014), pp. 1868–1875. ISSN: 15244539. DOI: 10.1161/CIRCULATIONAHA.114.010905.

[3] J. Nas et al. “Changes in automated external defibrillator use and survival after out-of-hospital cardiac arrest in the Nijmegen area”. In: *Netherlands Heart Journal* 26.12 (Dec. 2018), pp. 600–605. ISSN: 18766250. DOI: 10.1007/s12471-018-1162-9.

[4] Gavin D. Perkins et al. “European Resuscitation Council Guidelines for Resuscitation 2015. Section 2. Adult basic life support and automated external defibrillation.” In: *Resuscitation* 95 (2015), pp. 81–99. ISSN: 18731570. DOI: 10.1016/j.resuscitation.2015.07.015.

[5] Jocelyn Berdowski, Robert A. Berg, Jan G P Tijssen, and Rudolph W. Koster. “Global incidences of out-of-hospital cardiac arrest and survival rates: Systematic review of 67 prospective studies”. In: *Resuscitation* 81.11 (Nov. 2010), pp. 1479–1487. ISSN: 03009572. DOI: 10.1016/j.resuscitation.2010.08.006.

[6] J. N. Herbschleb, R. M. Heethaar, I. van der Tweel, and F. L. Meijler. “Frequency Analysis of the Ecg Before and During Ventricular Fibrillation.” In: *Computers in Cardiology* (1980), pp. 365–368. ISSN: 02766574.

[7] Matthew J. Reed, Gareth R. Clegg, and Colin E. Robertson. *Analysing the ventricular fibrillation waveform*. 2003. DOI: 10.1016/S0300-9572(02)00441-0.

[8] W. D. Weaver, L. A. Cobb, D. Dennis, R. Ray, A. P. Hallstrom, and M. K. Copass. “Amplitude of ventricular fibrillation waveform and outcome after cardiac arrest”. In: *Annals of Internal Medicine* 102.1 (Jan. 1985), pp. 53–55. ISSN: 00034819. DOI: 10.7326/0003-4819-102-1-53.

[9] Charles G Brown, Roger Dzwonczyk, Howard A Werman, and Robert L Hamlin. “Estimating the duration of ventricular fibrillation”. In: *Annals of Emergency Medicine* 18.11 (Nov. 1989), pp. 1181–1185. ISSN: 01960644. DOI: 10.1016/S0196-0644(89)80056-3.

[10] Charles G. Brown, Roger Dzwonczyk, and Daniel R. Martin. “Physiologic measurement of the ventricular fibrillation ECG signal: Estimating the duration of ventricular fibrillation”. In: *Annals of Emergency Medicine* 22.1 (1993), pp. 70–74. ISSN: 01960644. DOI: 10.1016/S0196-0644(05)80253-7.

[11] G W.N. Dalzell and A A.J. Adgey. “Determinants of successful transthoracic defibrillation and outcome in ventricular fibrillation”. In: *British Heart Journal* 65.6 (June 1991), pp. 311–316. ISSN: 00070769. DOI: 10.1136/hrt.65.6.311.

[12] Michael Callaham, Odelia Braun, Wesley Valentine, Douglas M Clark, and Claudia Zegans. “Prehospital cardiac arrest treated by urban first-responders: Profile of patient response and prediction of outcome by ventricular fibrillation waveform”. In: *Annals of Emergency Medicine* 22.11 (Nov. 1993), pp. 1664–1677. ISSN: 01960644. DOI: 10.1016/S0196-0644(05)81304-6.

[13] Hans Ulrich Strohmenger. *Predicting defibrillation success*. 2008. DOI: 10.1097/MCC.0b013e3282fc9a9c.

[14] Hans Ulrich Strohmenger, Karl H. Lindner, Andreas Keller, Ingrid M. Lindner, and Ernst G. Pfenninger. “Spectral analysis of ventricular fibrillation and closed-chest cardiopulmonary resuscitation”. In: *Resuscitation* 33.2 (Dec. 1996), pp. 155–161. ISSN: 03009572. DOI: 10.1016/S0300-9572(96)01003-9.

[15] Marko Noc, Max Harry Weil, Wanchun Tang, Shijie Sun, Andrej Pernat, and Joe Bisera. *Electrocardiographic prediction of the success of cardiac resuscitation*. Apr. 1999. DOI: 10.1097/00003246-199904000-00021.

[16] A. Marn-Pernat, M. H. Weil, W. Tang, A. Pernat, and J. Bisera. “Optimizing timing of ventricular defibrillation”. In: *Critical Care Medicine* 29.12 (2001), pp. 2360–2365. ISSN: 00903493. DOI: 10.1097/00003246-200112000-00019.

[17] H. P. Povoas and J. Bisera. “Electrocardiographic waveform analysis for predicting the success of defibrillation”. In: *Critical Care Medicine* 28.11 SUPPL. (Nov. 2000), N210–1. ISSN: 00903493.

[18] Heitor P. Povoas, Max Harry Weil, Wanchun Tang, Joe Bisera, Kada Klouche, and Ann Barbatsis. “Predicting the success of defibrillation by electrocardiographic analysis”. In: *Resuscitation* 53.1 (Apr. 2002), pp. 77–82. ISSN: 03009572. DOI: 10.1016/S0300-9572(01)00488-9.

[19] Hans Ulrich Strohmenger, Karl H. Lindner, and Charles G. Brown. “Analysis of the ventricular fibrillation ECG signal amplitude and frequency parameters as predictors of countershock success in humans”. In: *Chest* 111.3 (Mar. 1997), pp. 584–589. ISSN: 00123692. DOI: 10.1378/chest.111.3.584.

[20] G. Ristagno, A. Gullo, G. Berlot, U. Lucangelo, F. Geheb, and J. Bisera. "Prediction of successful defibrillation in human victims of out-of-hospital cardiac arrest: A retrospective electrocardiographic analysis". In: *Anaesthesia and Intensive Care* 36.1 (Jan. 2008), pp. 46–50. ISSN: 0310057X. DOI: 10.1177/0310057x0803600108.

[21] Giuseppe Ristagno, Yongqin Li, Francesca Fumagalli, Andrea Finzi, and Weilun Quan. "Amplitude spectrum area to guide resuscitation-A retrospective analysis during out-of-hospital cardiopulmonary resuscitation in 609 patients with ventricular fibrillation cardiac arrest". In: *Resuscitation* 84.12 (Dec. 2013), pp. 1697–1703. ISSN: 03009572. DOI: 10.1016/j.resuscitation.2013.08.017.

[22] Giuseppe Ristagno et al. "Amplitude spectrum area to guide defibrillation a validation on 1617 patients with ventricular fibrillation". In: *Circulation* 131.5 (Feb. 2015), pp. 478–487. ISSN: 15244539. DOI: 10.1161/CIRCULATIONAHA.114.010989.

[23] Giuseppe Ristagno. *Real Time Amplitude Spectrum Area to Guide Defibrillation (AMSA)*. 2018.

[24] Robert J. Myerburg and Agustin Castellanos. "Cardiac Arrest and Sudden Cardiac Death". In: *Braunwald's Heart Disease: A Textbook of Cardiovascular Medicine*. Ed. by Robert O. Bonow, Douglas L. Mann, Douglas P. Zipes, and Peter Libby. 9th ed. Elsevier Saunders, 2012. Chap. 41, pp. 845–884. DOI: 10.1016/b978-1-4377-0398-6.00041-x.

[25] David M. Mirvis and Ary L. Goldberger. "Electrocardiography". In: *Braunwald's Heart Disease: A Textbook of Cardiovascular Medicine*. Ed. by Robert O. Bonow, Douglas L. Mann, Dougles P. Zipes, and Peter Libby. 9th ed. Elsevier Saunders, 2012. Chap. 13, pp. 126–167.

[26] Julia H. Indik, Richard L. Donnerstein, Karl B. Kern, Steven Goldman, Mohamed A. Gaballa, and Robert A. Berg. "Ventricular fibrillation waveform characteristics are different in ischemic heart failure compared with structurally normal hearts". In: *Resuscitation* 69.3 (June 2006), pp. 471–477. ISSN: 03009572. DOI: 10.1016/j.resuscitation.2005.10.017.

[27] Julia H. Indik, Richard L. Donnerstein, Robert A. Berg, Ronald W. Hilwig, Marc D. Berg, and Karl B. Kern. "Ventricular fibrillation frequency characteristics are altered in acute myocardial infarction". In: *Critical Care Medicine* 35.4 (Apr. 2007), pp. 1133–1138. ISSN: 00903493. DOI: 10.1097/01.CCM.0000259540.52062.99.

[28] Julia H. Indik et al. "The influence of myocardial substrate on ventricular fibrillation waveform: A swine model of acute and postmyocardial infarction". In: *Critical Care Medicine* 36.7 (July 2008), pp. 2136–2142. ISSN: 15300293. DOI: 10.1097/CCM.0b013e31817d798c.

[29] Lawrence D. Sherman, James T. Niemann, John P. Rosborough, and James J. Menegazzi. "The effect of ischemia on ventricular fibrillation as measured by fractal dimension and frequency measures". In: *Resuscitation* 75.3 (2007), pp. 499–505. ISSN: 03009572. DOI: 10.1016/j.resuscitation.2007.05.019.

[30] Julia H. Indik et al. "Predictors of resuscitation outcome in a swine model of VF cardiac arrest: A comparison of VF duration, presence of acute myocardial infarction and VF waveform". In: *Resuscitation* 80.12 (Dec. 2009), pp. 1420–1423. ISSN: 03009572. DOI: 10.1016/j.resuscitation.2009.08.023.

[31] Julia H. Indik et al. "Predictors of resuscitation in a swine model of ischemic and nonischemic ventricular fibrillation cardiac arrest: Superiority of amplitude spectral area and slope to predict a return of spontaneous circulation when resuscitation efforts are prolonged". In: *Critical Care Medicine* 38.12 (Dec. 2010), pp. 2352–2357. ISSN: 15300293. DOI: 10.1097/CCM.0b013e3181fa01ee.

[32] Julia H. Indik, Daniel Allen, Michael Gura, Christian Dameff, Ronald W. Hilwig, and Karl B. Kern. "Utility of the ventricular fibrillation waveform to predict a return of spontaneous circulation and distinguish acute from post myocardial infarction or normal swine in ventricular fibrillation cardiac arrest". In: *Circulation: Arrhythmia and Electrophysiology* 4.3 (June 2011), pp. 337–343. ISSN: 19413149. DOI: 10.1161/CIRCEP.110.960419.

[33] Theresa M. Olasveengen, Trygve Eftestøl, Kenneth Gundersen, Lars Wik, and Kjetil Sunde. "Acute ischemic heart disease alters ventricular fibrillation waveform characteristics in out-of hospital cardiac arrest". In: *Resuscitation* 80.4 (Apr. 2009), pp. 412–417. ISSN: 03009572. DOI: 10.1016/j.resuscitation.2009.01.012.

[34] Judith L. Bonnes et al. "Ventricular fibrillation waveform characteristics differ according to the presence of a previous myocardial infarction: A surface ECG study in ICD-patients". In: *Resuscitation* 96 (Nov. 2015), pp. 239–245. ISSN: 18731570. DOI: 10.1016/j.resuscitation.2015.08.014.

[35] Michiel Hulleman et al. "Predictive value of amplitude spectrum area of ventricular fibrillation waveform in patients with acute or previous myocardial infarction in out-of-hospital cardiac arrest". In: *Resuscitation* 120 (Nov. 2017), pp. 125–131. ISSN: 18731570. DOI: 10.1016/j.resuscitation.2017.08.219.

[36] Philippe Garot et al. "Six-month outcome of emergency percutaneous coronary intervention in resuscitated patients after cardiac arrest complicating ST-elevation myocardial infarction". In: *Circulation* 115.11 (2007), pp. 1354–1362. ISSN: 00097322. DOI: 10.1161/CIRCULATIONAHA.106.657619.

[37] Florence Dumas et al. “Immediate percutaneous coronary intervention is associated with better survival after out-of-hospital cardiac arrest: Insights from the PROCAT (Parisian Region Out of Hospital Cardiac Arrest) registry”. In: *Circulation: Cardiovascular Interventions* 3.3 (June 2010), pp. 200–207. ISSN: 19417640. DOI: 10.1161/CIRCINTERVENTIONS.109.913665.

[38] Clifton W. Callaway et al. “Early coronary angiography and induced hypothermia are associated with survival and functional recovery after out-of-hospital cardiac arrest”. In: *Resuscitation* 85.5 (2014), pp. 657–663. ISSN: 18731570. DOI: 10.1016/j.resuscitation.2013.12.028.

[39] Anthony C. Camuglia, Varinder K. Randhawa, Shahar Lavi, and Darren L. Walters. “Cardiac catheterization is associated with superior outcomes for survivors of out of hospital cardiac arrest: Review and meta-analysis”. In: *Resuscitation* 85.11 (2014), pp. 1533–1540. ISSN: 18731570. DOI: 10.1016/j.resuscitation.2014.08.025.

[40] Santiago Garcia et al. “Early access to the cardiac catheterization laboratory for patients resuscitated from cardiac arrest due to a shockable rhythm: The Minnesota Resuscitation Consortium Twin Cities Unified Protocol”. In: *Journal of the American Heart Association* 5.1 (Jan. 2016). ISSN: 20479980. DOI: 10.1161/JAHA.115.002670.

[41] Florence Dumas et al. “Emergency Percutaneous Coronary Intervention in Post-Cardiac Arrest Patients Without ST-Segment Elevation Pattern: Insights from the PROCAT II Registry”. In: *JACC: Cardiovascular Interventions* 9.10 (May 2016), pp. 1011–1018. ISSN: 18767605. DOI: 10.1016/j.jcin.2016.02.001.

[42] Demetris Yannopoulos et al. “Coronary Artery Disease in Patients With Out-of-Hospital Refractory Ventricular Fibrillation Cardiac Arrest”. In: *Journal of the American College of Cardiology* 70.9 (Aug. 2017), pp. 1109–1117. ISSN: 15583597. DOI: 10.1016/j.jacc.2017.06.059.

[43] Jos Thannhauser et al. “Computerized analysis of the ventricular fibrillation waveform allows identification of myocardial infarction: a proof-of-concept study for smart defibrillator applications in cardiac arrest”. In: *Journal of the American Heart Association* (2020).

[44] Judith L. Bonnes et al. “Ventricular fibrillation waveform characteristics of the surface ECG: Impact of the left ventricular diameter and mass”. In: *Resuscitation* 115 (June 2017), pp. 82–89. ISSN: 18731570. DOI: 10.1016/j.resuscitation.2017.03.029.

4 | Detecting myocardial infarction using ventricular fibrillation waveform analysis: A multi-lead machine learning approach

K.M. van der Sluijs[1], J. Thannhauser[2], H.J. Zwart [3], M.A. Brouwer[2]
[1] Technical Medicine, University of Twente, Enschede, The Netherlands
[2] Department of Cardiology, Radboud University Medical Center, Nijmegen, The Netherlands
[3] Faculty of Electrical Engineering, Mathematics and Computer Sciences, Department of Applied Mathematics, University of Twente, Enschede, The Netherlands

Abstract

Background: Out-of-hospital cardiac arrest has meagre survival rates despite improvements in resuscitative care. Detection of acute myocardial infarction (MI) by ventricular fibrillation (VF)-waveform analysis may facilitate individualised treatment strategies. In follow-up on previous machine learning studies, optimisation of input features in terms of electrocardiogram (ECG) leads and VF-waveform characteristics (VFWC) is needed. This study aimed to investigate the effect of feature selection on the performance of machine learning models detecting old MI.

Methods: Adult patients were included from a prospective observational registry of implantable cardioverter-defibrillator implantations (June 2010 - July 2017). Sets were created with 17, 391 and 51 VFWC from lead II, all twelve leads and lead II + V_1 respectively. These sets were used as input features for models discriminating between patients with and without old MI. Feature selection was applied to reduce the number of VFWC in each set, after which reduced models were created. Model performance was assessed by receiver operating characteristic analysis.

Results: Of the 242 included patients, 137 had an old MI. Patients with MI were older and more often male. The models based on lead II, all twelve leads and lead II + V_1 reached an area under the curve (AUC) of 0.61, 0.78 and 0.71 respectively before feature selection. Feature selection reduced the number of VFWC to 3, 10 and 5 and the resulting models reached AUCs of 0.58, 0.83 and 0.76 respectively.

Conclusions: Machine learning models for the detection of old MI based on multiple ECG leads for which feature selection was applied reached numerically higher AUCs than the models for which no feature selection was performed. Optimised models with input features selected from two leads reached acceptable discriminative ability. The optimisation methods presented in this study are promising and should be investigated in the out-of-hospital setting for the detection of acute MI.

4.1 Introduction

Out-of-hospital cardiac arrest (OHCA) is a major healthcare problem. In the Netherlands, the incidence rate of out-of-hospital resuscitation is approximately 37 per 100,000 inhabitants, of which only 23% survives to hospital discharge[1]. The current treatment of OHCA by the emergency medical services is protocolised and does not take the underlying disease of the individual patient into account. In case of ventricular fibrillation (VF), the most common shockable rhythm, the most frequent underlying cause is acute myocardial infarction (AMI)[2–4]. A recent study showed that novel, aggressive treatment strategies using mechanical cardiopulmonary resuscitation and extracorporeal life support may facilitate transport and intervention of AMI patients with refractory VF, increasing the chance of successful resuscitation[4]. In-field identification of AMI during OHCA may therefore save lives.

The paddle electrocardiogram (ECG) of the defibrillator is an early, easily obtainable tool that can provide patient-specific information. Its current use is limited to distinguishing non-shockable from shockable rhythms so that defibrillatory shocks can be applied as needed. More useful information can be obtained by analysing the VF-waveform[5]. It has been used to predict defibrillation shock success and good neurological outcome in OHCA[6,7]. An ongoing randomised controlled trial uses VF-waveform analysis to guide defibrillation and shows that real-time analysis is feasible[8]. Furthermore, the VF-waveform may hold information about underlying disease of the heart[9,10]. As such, it may offer a way to detect the cause of the arrest.

Animal studies have shown that the VF-waveform, quantified by ventricular fibrillation waveform characteristics (VFWC), is affected by AMI[11–15]. Similar associations have been reported in humans in case of old myocardial infarction (OMI), which is the rationale behind the use of OMI as a surrogate for AMI in VF-waveform studies[9,12,16–18]. A recent proof-of-concept study on waveform analysis of VF induced for implantable cardioverter-defibrillator (ICD) testing showed that OMI could be detected using machine learning models[19]. Notably, models based on twelve ECG leads could detect OMI more accurately than models based on lead II alone. Moreover, a model based on the amplitude spectrum area (AMSA) alone led to better results than a model created using all available VFWC, suggesting that feature selection is beneficial.

In follow-up on the aforementioned proof-of-concept study, optimisation of input features might improve the performance of diagnostic models detecting OMI. The aim of this thesis was therefore to investigate the effect of established feature selection methods and hyperparameter optimisation on the ability of multi-lead machine learning models to distinguish patients with OMI from patients without OMI.

4.2 Methods

4.2.1 Study population

The study population was derived from a prospective observational registry of first ICD or cardiac resynchronisation therapy-defibrillator (CRT-D) implantations with defibrillation testing performed at the Radboud University Medical Center (Radboudumc). Adult patients (age $\geq$ 18) who received an ICD or CRT-D in the period between June 2010 and July 2017 were included. Exclusion criteria were congenital heart disease and absence of an analysable 12-lead ECG recording of the induced VF.

4.2.2 Data acquisition

Clinical characteristics

Clinical characteristics and the patient's medical history were obtained from their medical records. Data were obtained independently by at least two researchers to ensure inter-observer validity.

A third reviewer checked in case of disagreement.

Ventricular fibrillation waveform characteristics

After the implantation procedure, VF was induced by T-wave shock, direct current pulses or 50 Hz burst pacing to assess if the device could adequately sense the arrhythmia and terminate it by means of defibrillation. The approximately thirty-second period before, during and after the induced VF was recorded with a 12-lead surface ECG using the BARD® LabSystem™ Pro (Lowell, MA, USA) with a sampling frequency of 1000 Hz and a 16 bit A/D converter.

The data were analysed using MATLAB® (version 2020a, MathWorks®, Natick, MA, USA). The 4.1-second segment (4096 samples) of VF prior to first shock delivery was selected manually and pre-processed with a fourth order Butterworth bandpass filter with cut-off frequencies of 1 and 48 Hz. Visually identified artefacts were removed and replaced by linear interpolation. The VFWC of the segment were computed for all twelve leads; a total of 391 VFWC were computed per patient. An overview and mathematical description of each of the VFWC can be found in subsection 2.2.1.

Study groups

Patients were divided into two groups based on whether or not they had an OMI. Reports in their medical charts were evaluated for presence of an OMI, using the third universal definition of myocardial infarction (MI) by the European Society of Cardiology[20].

4.2.3 Descriptive analysis

Clinical and VF-waveform characteristics were compared between the two study groups. Continuous variables were reported as median [Q1-Q3] and categorical variables as number (percentage). Continuous variables were analysed using Mann-Whitney U tests and categorical variables using Fisher's Exact Test. A p-value of <0.05 was considered significant. All statistical analyses were performed with IBM SPSS® Statistics software (IBM Corp. Released 2017. IBM SPSS Statistics for Windows, Version 25.0. Armonk, NY: IBM Corp).

4.2.4 Predictive analysis

Set composition

Eight sets of VFWC were composed, each including a different combination of VFWC of different ECG leads. Figure 4.1 shows how the eight sets 1A-8A were composed.

First, a selection of leads was made: lead II (sets 1A and 2A), all twelve leads (sets 3A through 6A) or lead II + lead V_1 (sets 7A and 8A). Lead II alone was studied because it resembles the defibrillator lead. All twelve leads together were studied to evaluate all available information combined. The combination of leads II and V_1 was used to investigate the potential of a selection of leads and followed the preliminary research presented in appendix A.1.

The first four sets 1A-4A contained only regular VFWC. The last four sets 5A-8A contained both regular and ΔV_1 VFWC. Therefore, sets 1A and 2A contained only regular VFWC of lead II. Sets 3A and 4A contained only regular VFWC of all twelve leads. Sets 5A and 6A contained both regular and ΔV_1 VFWC of all twelve leads. Sets 7A and 8A contained both regular and ΔV_1 VFWC of leads II and V_1.

The final distinction within these pairs followed Mann-Whitney U tests that compared the VFWC between the patients with and without OMI. The even-numbered sets included only those VFWC with a p-value of <0.1. The odd-numbered sets were not subjected to this filter type of feature selection and also contained VFWC with larger p-values.

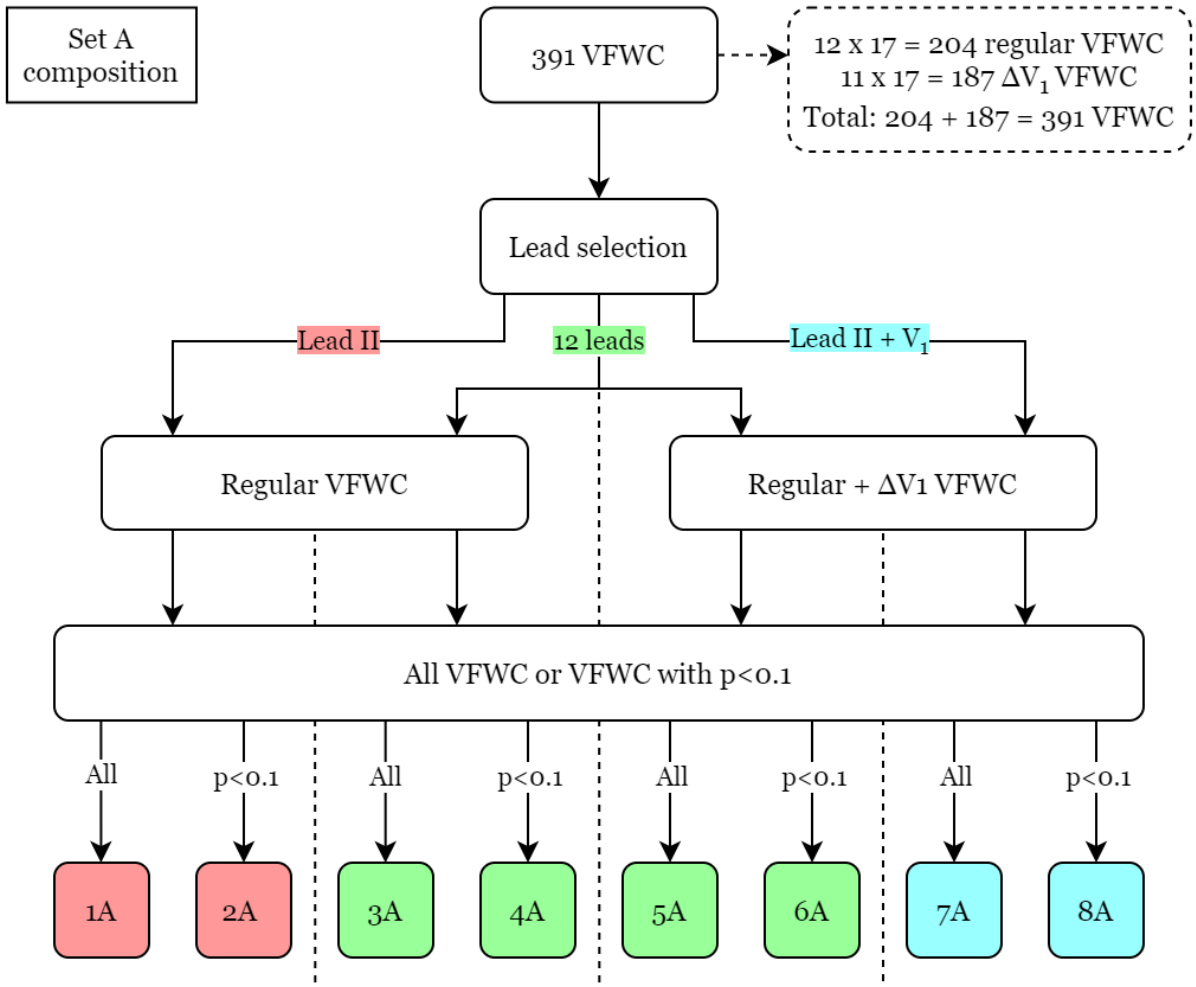

Figure 4.1: Composition of sets 1A-8A. VFWC: ventricular fibrillation waveform characteristics.

Prediction models

The eight sets were used as input features for models detecting OMI. Both a traditional statistical approach of multivariate logistic regression (MVR) and a machine learning approach with a support vector machine (SVM) was used. An overview of how the sets were used as input features for the different models can be seen in figure 4.2.

Sets 1A through 8A were used as input for eight MVR models as well as eight SVM A models. Only a selection of the VFWC in each set A was included in the MVR model, since a forward stepwise method was used to enter variables. This wrapper type of feature selection resulted in eight new sets named 1B through 8B, which formed the input for another eight SVM B models. The hyperparameters of each of the sixteen SVMs were optimised according to the algorithm explained in subsection 2.2.3. Moreover, all SVMs were subjected to five-fold cross-validation before their performance was evaluated.

The effect of feature selection was studied for the lead II models, the 12-lead models and the lead II + V_1 models, with specific focus on the *SVMs of sets 1, 5 and 7*. The set 7B SVM was studied in more detail to evaluate the potential of an SVM with a selection of VFWC from two leads.

The SVM A models of the three sets were compared to the corresponding SVM B models to investigate the effect of the wrapper type feature selection of using fewer, more relevant input features rather than using all of them. The comparison between the SVM B models of the three sets and the corresponding MVR models was made to evaluate the added value of

machine learning over a traditional statistical method. The wrapper type of feature selection was expected to be of more influence on model performance than the filter type. The comparison between the odd-numbered and even-numbered models to study the effect of the filter type selection was therefore exploratory.

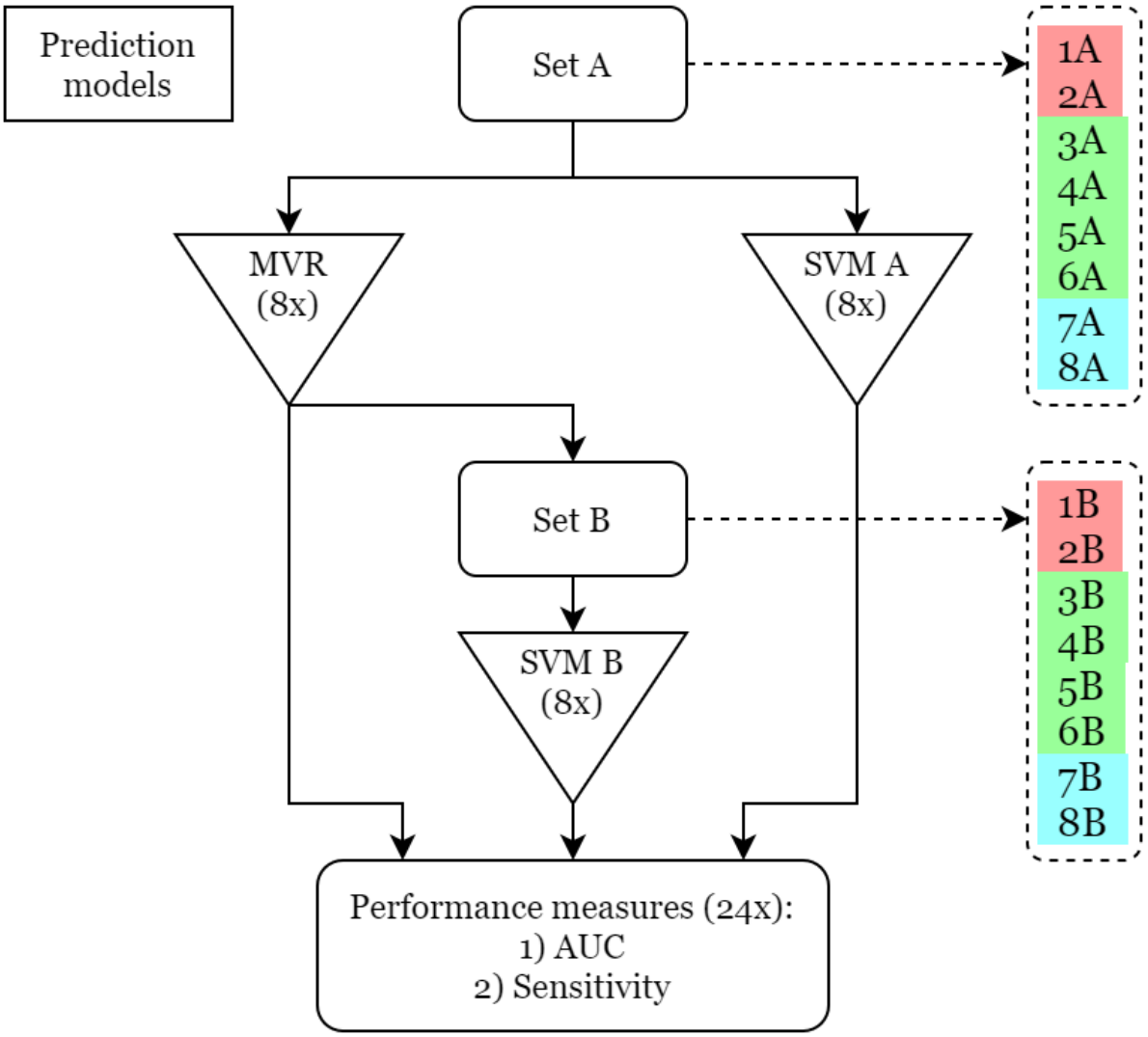

Figure 4.2: Overview of the prediction models and the performance measures. AUC: area under the curve, MVR: multivariate logistic regression, SVM: support vector machine.

Outcome measures

Two outcome measures were used to assess the discriminative ability of the twenty-four models, with a specific focus on the set 1, 5 and 7 SVMs: the area under the curve (AUC) of the receiver operating characteristic (ROC) and the sensitivity.

For the MVR models, the 95% confidence interval of the AUC was acquired from a non-parametric estimation of the standard error of the AUC. The confidence interval of the AUC of the SVMs was computed using a bootstrap procedure with 1000 replicas.

The sensitivity was measured at a level of 80% specificity. A high specificity for detecting MI is desirable for future use during a resuscitation. In this setting, unnecessary transport of false-positive AMI patients is more detrimental than refraining from transport of false-negative AMI patients. A threshold with a high specificity was therefore used to measure the sensitivity.

4.2.5 Subgroup analysis

In order to explore which clinical factors were associated to the classification by an SVM created with only VFWC as input features, a subgroup analysis was performed using the set 7B SVM. The patients were divided into tertiles based on their classification score, a measure of the likelihood of having OMI. The three subgroups thereby represented low, intermediate and high risk patients. Baseline characteristics related to cardiac mass or function that could be of influence on the VF-waveform were compared between the subgroups.

Continuous variables were reported as median [Q1-Q3] and compared using Kruskal-Wallis tests. In case of significant differences, pairwise comparisons with Bonferroni correction were performed. Categorical variables were reported as number (percentage) and compared using the Mantel-Haenszel test for linear-by-linear association. A p-value of <0.05 was considered significant.

4.3 Results

4.3.1 Study population

A total of 378 patients who underwent an ICD or CRT-D implantation between June 2010 and July 2017 were registered. A 12-lead ECG of the period around the induced VF was captured in 250 patients, of which 8 could not be analysed due to artefacts. Figure 4.3 shows an example ECG of lead II. In total, 242 patients were analysed, of which 105 (43.4%) did not have an OMI and 137 (56.6%) did. Figure 4.4 shows a flowchart with the amounts of patients registered and analysed.

4.3.2 Descriptive analysis

Clinical characteristics

The median age of the 242 patients was 64.0 years [55.0-72.0] and 185 (76.4%) were male. Compared to the patients without OMI, the patients with OMI were older (67.0 vs. 59.0 years, $p<0.001$) and a larger proportion of them was male (82.5% vs. 68.6%, $p=0.014$). Out of the 137 patients with OMI, 52 (38.0%) had an anterior MI, 67 (48.9%) had an inferior MI, 10 (7.3%) had both and the MI location was unknown for the last 8 patients (5.8%). Patients in the OMI group received antiplatelet and cholesterol reducer medication more often than patients without OMI ($p<0.001$ for both). Table 4.1 shows all baseline characteristics of the study population.

Ventricular fibrillation waveform characteristics

Mann-Whitney U tests were performed to investigate differences in VFWC of all leads between the groups of patients with and without OMI. Appendix A.2 contains tables A.3 and A.4 that show the p-values of all 391 VFWC and table A.5 summarises their contents.

The VFWC with the most pronounced differences between the groups were the mean absolute amplitude, median slope, AMSA and power spectrum area, as well as their ΔV_1 variants. Most VFWC were decreased in case of OMI.

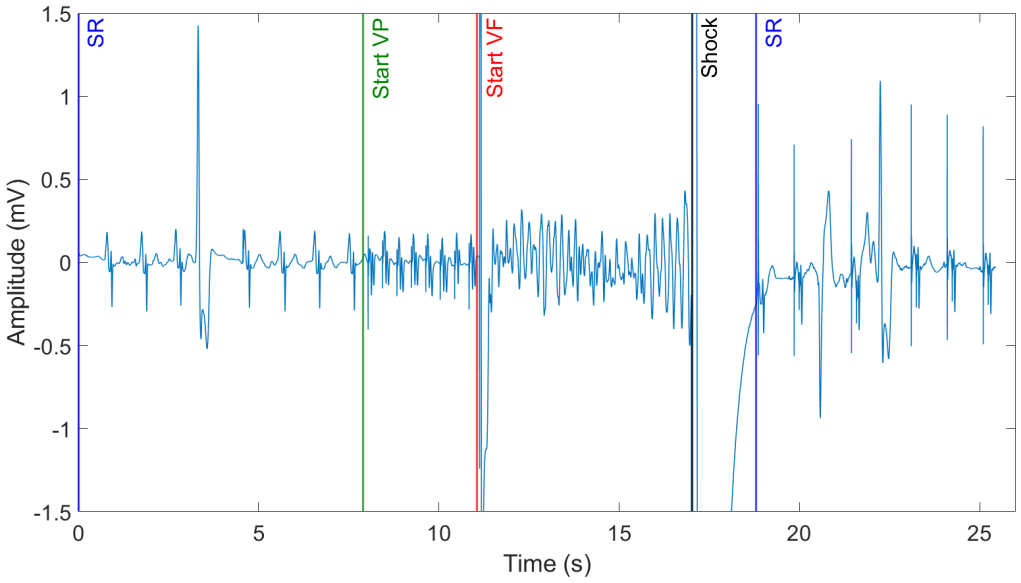

Figure 4.3: A lead II electrocardiogram of ventricular fibrillation acquired during defibrillation testing. Initially, sinus rhythm is present. Then ventricular pacing starts and a direct current shock is applied. This is induces ventricular fibrillation which is terminated by a defibrillation shock after which sinus rhythm returns. SR: sinus rhythm, VF: ventricular fibrillation, VP: ventricular pacing.

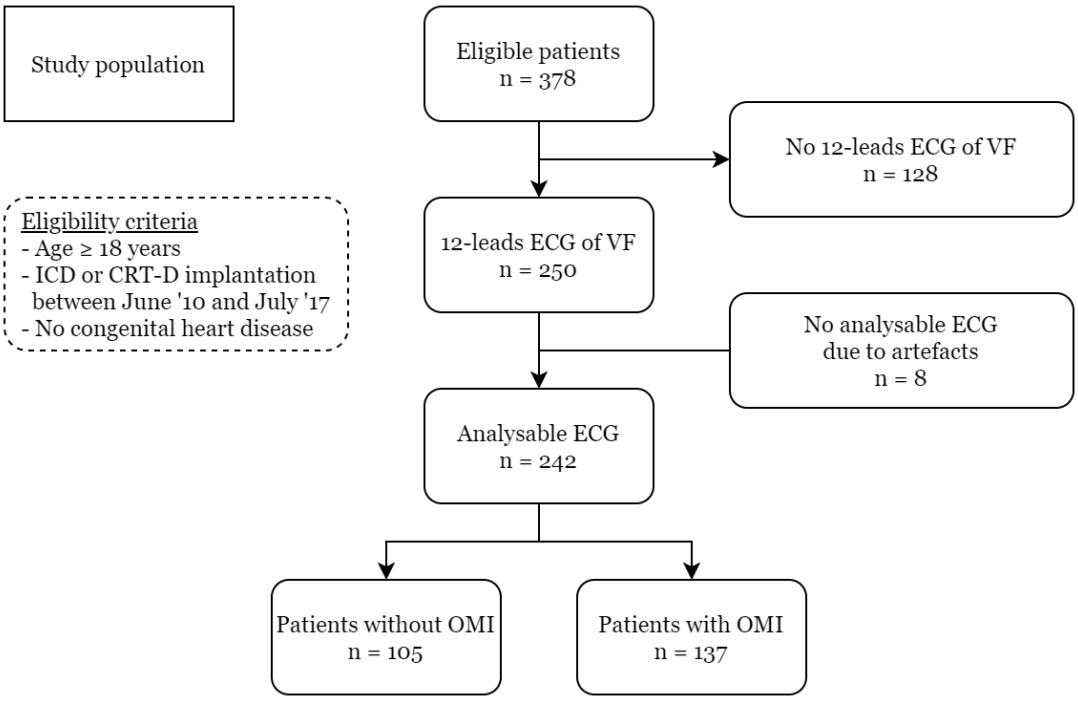

Figure 4.4: Flowchart of the patient inclusion process. CRT-D: cardiac resynchronisation therapy-defibrillator, ECG: electrocardiogram, ICD: implantable cardioverter-defibrillator, OMI: old myocardial infarction, VF: ventricular fibrillation.

4.3.3 Predictive analysis

Set composition

The number of VFWC in each of the sets 1A-8A as determined by figure 4.1 can be seen in figure 4.5. The wrapper type of feature selection of forward stepwise entry by MVR reduced the number of VFWC to compose sets 1B-8B. Sets 1A, 5A and 7A with 17, 391 and 51 VFWC respectively were reduced to sets 1B, 5B and 7B containing 3, 10 and 5 VFWC. An overview of the VFWC in each set can be found in appendix A.3.

Prediction models

The sets were used to create twenty-four prediction models in total, eight models of MVR, SVM A and SVM B each. The optimised hyperparameters of the SVM A and SVM B models can be found in table A.7 in appendix A.4. Figure 4.6 shows the areas under the ROC-curves of the twenty-four prediction models. The 95% confidence interval is depicted using error bars. Figure 4.7 shows the sensitivities of the models measured at the level of 80% specificity.

Lead II models

The lead II models reached AUCs around 0.6 and sensitivities around 0.3. The SVMs of sets 1A and 1B achieved AUCs of 0.61 and 0.58 with sensitivities of 0.26 and 0.24 respectively.

12-lead models

The set 3 and 4 models based on twelve leads without ΔV_1 VFWC reached AUCs just below 0.8; sensitivities around 0.6 were observed. The set 5 and 6 models of twelve leads with ΔV_1 VFWC had AUCs just above 0.8 and sensitivities just above 0.65. The set 5A and 5B SVMs had AUCs of 0.78 and 0.83 respectively. The corresponding sensitivities were 0.66 and 0.68.

Lead II + V_1 models

The models with VFWC from leads II and V_1 had AUCs around 0.75 and sensitivities just above 0.5. The set 7A SVM had an AUC of 0.71 and a sensitivity of 0.53. The ROC-curve of the set 7B SVM is shown in figure 4.8. This model reached an AUC of 0.76 and a sensitivity of 0.55.

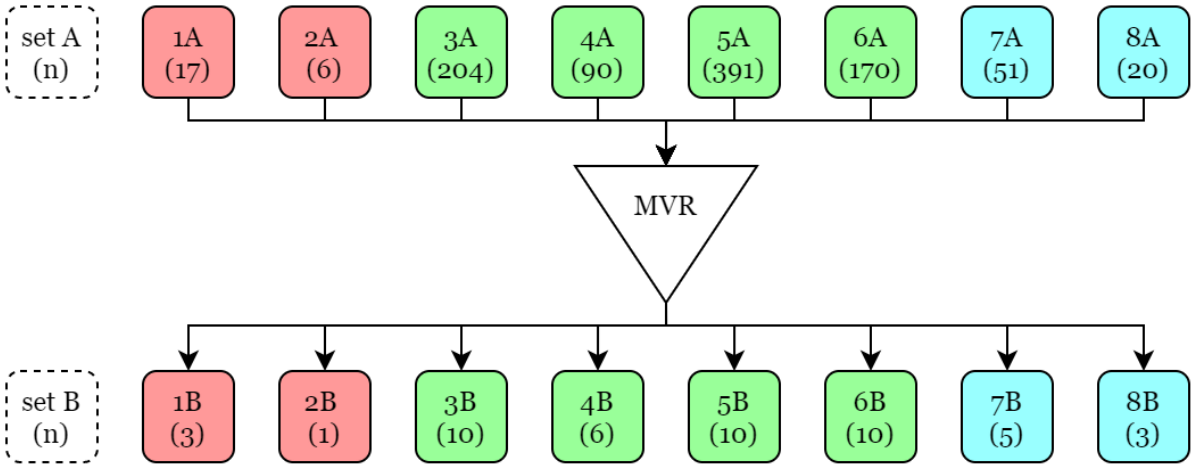

Figure 4.5: Overview of the number of ventricular fibrillation waveform characteristics in sets 1A-8A and 1B-8B. The forward stepwise entry method of multivariate logistic regression was used to create subselections of sets A that composed sets B. MVR: multivariate logistic regression.

Table 4.1: Baseline characteristics of the study population. Continuous variables are medians [Q1-Q3], categorical variables are n (%). Significant p-values are printed in bold.

	All patients n=242	**No OMI** n=105	**OMI** n=137	***p*-value**
Age (years)	64.0 [55.0-72.0]	59.0 [48.0-68.0]	67.0 [61.0-74.0]	**<0.001**
Male gender	185 (76.4)	72 (68.6)	113 (82.5)	**0.014**
OMI	137 (56.6)	0 (0)	137 (100)	-
Anterior	*52 (21.5)*	-	*52 (38.0)*	-
Inferior	*67 (27.7)*	-	*67 (48.9)*	-
Both	*10 (4.1)*	-	*10 (7.3)*	-
Unknown	*8 (3.3)*	-	*8 (5.8)*	-
BMI (kg/m^2)	26.2 [23.9-29.0]	25.6 [23.0-28.8]	26.6 [24.5-29.1]	**0.039**
Hypertension	100 (41.5)	37 (35.2)	63 (46.3)	0.088
Diabetes mellitus	53 (22.0)	18 (17.1)	35 (25.7)	0.119
Atrial fibrillation	70 (28.9)	28 (26.7)	42 (30.7)	0.568
Primary prevention	152 (62.8)	72 (68.6)	80 (58.4)	0.110
CRT-D	67 (27.7)	35 (33.3)	32 (23.4)	0.051
QRS duration (ms)	118 [100-140]	120 [101-150]	116 [99-136]	0.372
LVEF (%)	35.0 [28.0-45.3]	35.0 [27.0-46.0]	35.0 [28.0-45.0]	0.730
LVIDd index (cm/m^2)	3.00 [2.70-3.30]	3.00 [2.69-3.26]	3.00 [2.70-3.30]	0.996
LV dilation	40 (17.9)	18 (19.1)	22 (17.1)	0.726
LV mass index (g/m^2)	113.0 [91.1-134.1]	113.8 [87.0-136.0]	111.1 [95.0-132.7]	0.919
Creatinine (μmol/L)	85 [72-104]	85 [71-101]	87 [74-106]	0.348
Beta blocker	217 (90.0)	91 (86.7)	126 (92.6)	0.135
ACEI or ARB	204 (84.6)	84 (80.0)	120 (88.2)	0.104
Aldosteron antagonist	96 (39.8)	40 (38.1)	56 (41.2)	0.691
Diuretics	117 (48.5)	48 (45.7)	69 (50.7)	0.516
Antiplatelet	143 (59.3)	38 (36.2)	105 (77.2)	**<0.001**
Anticoagulation	98 (40.7)	40 (38.1)	58 (42.6)	0.510
Cholesterol reducer	163 (67.6)	43 (41.0)	120 (88.2)	**<0.001**
Amiodarone	30 (12.4)	10 (9.5)	20 (14.7)	0.245

ACEI: angiotension converting enzyme inhibitor, ARB: angiotensin receptor blocker, BMI: body mass index, CRT-D: cardiac resynchronisation therapy-defibrillator, LV: left ventricular, LVEF: left ventricular ejection fraction, LVIDd: left ventricular internal diastolic diameter, OMI: old myocardial infarction.

4.3.4 Subgroup analysis

The classification scores of the set 7B SVM are shown in figure 4.9 and were used to create subgroups. The baseline characteristics of the three subgroups are shown in table 4.2. The weight of the patients was different between the three groups ($p<0.008$). Low risk patients had lower weights than high risk patients ($p<0.003$). Furthermore, diuretics use showed a linear trend between the subgroups ($p<0.011$). Higher classification scores were accompanied by more diuretics use.

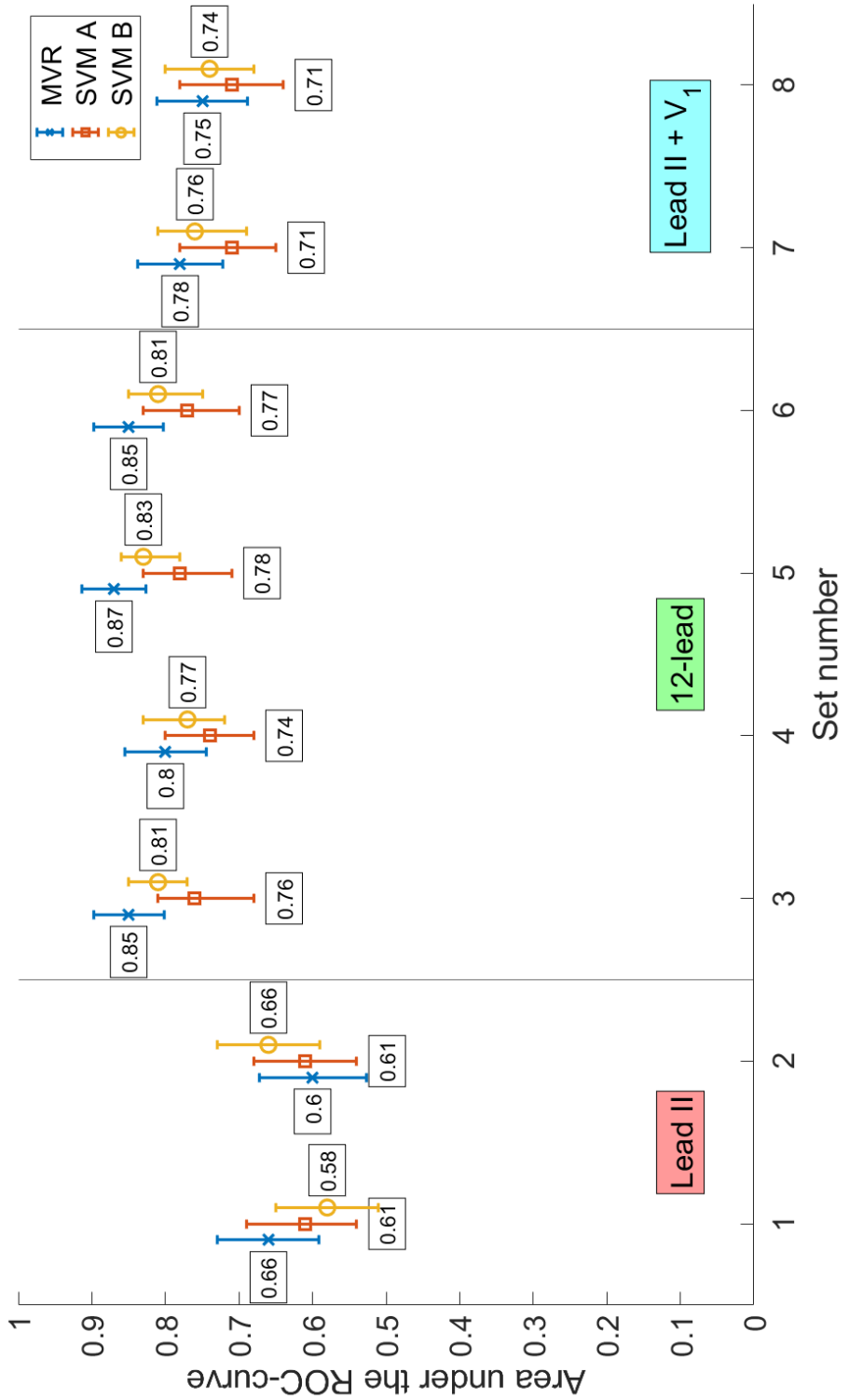

Figure 4.6: The areas under the ROC-curves of the twenty-four prediction models of types MVR, SVM A and SVM B. The labels represent the areas, the error bars visualise the 95% confidence intervals. MVR: multivariate logistic regression, ROC: receiver operating characteristic, SVM: support vector machine.

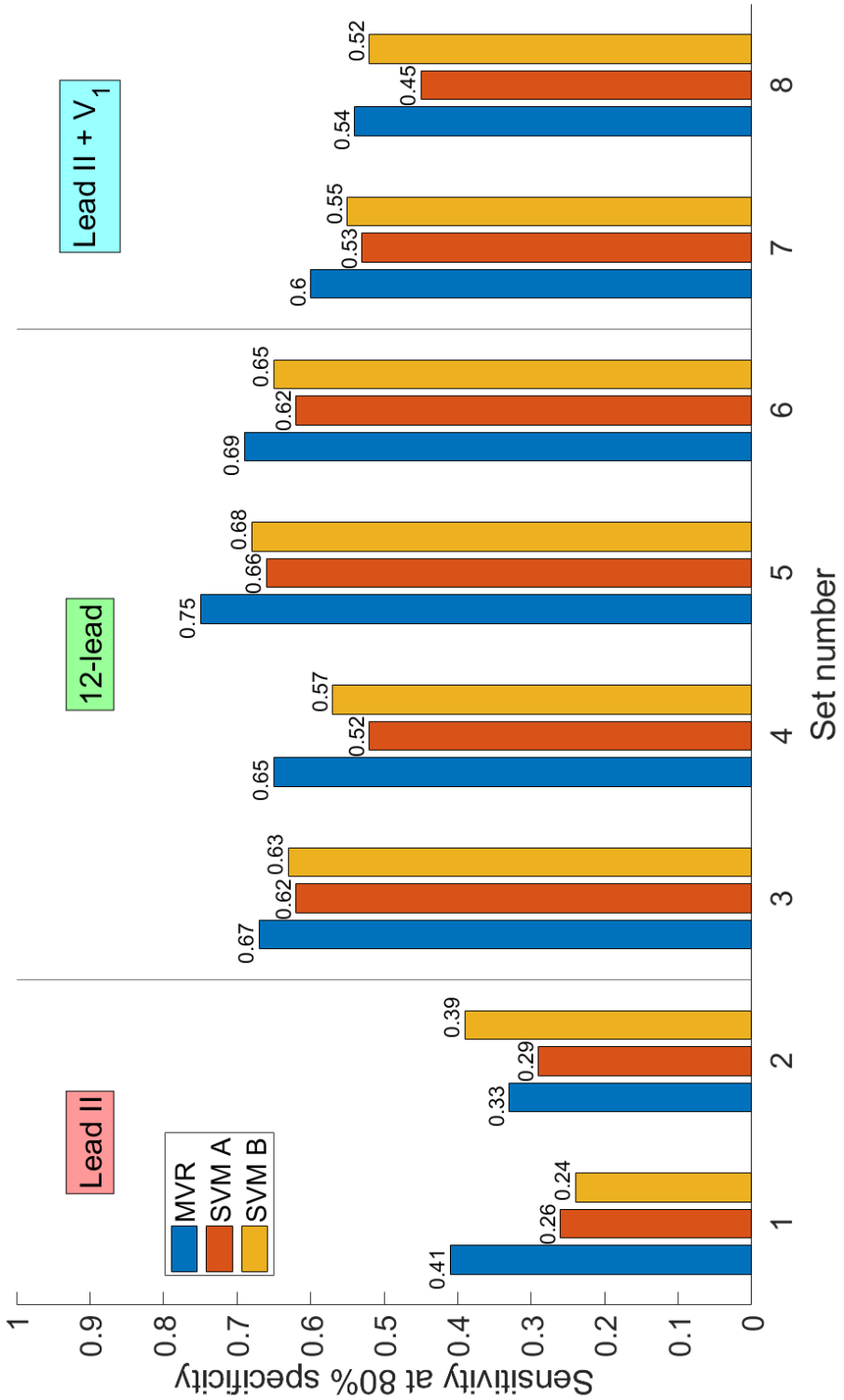

Figure 4.7: The sensitivities of the twenty-four prediction models of types MVR, SVM A and SVM B, measured at the level of 80% specificity. MVR: multivariate logistic regression, SVM: support vector machine.

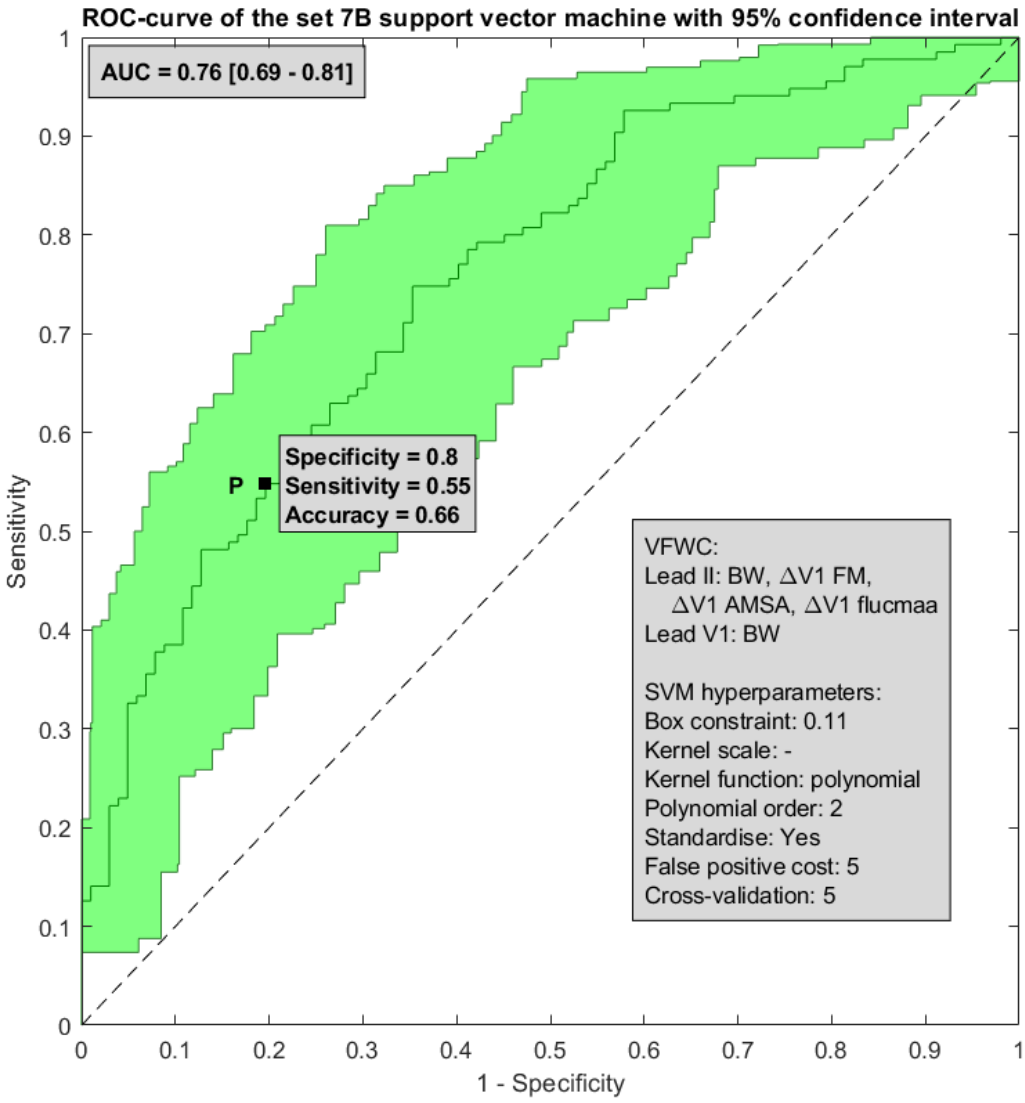

Figure 4.8: Receiver operating characteristic curve of the set 7B support vector machine with VFWC of leads II and V_1. The green shaded area represents the 95% confidence interval of the area under the curve, which is presented in the upper-left corner as AUC [lower bound - upper bound]. Point P represents the working point set at a specificity of 80% and displays the corresponding sensitivity and accuracy. AMSA: amplitude spectrum area, AUC: area under the curve, BW: bandwidth, FM: median frequency, ROC: receiver operating characteristic, SVM: support vector machine, VFWC: ventricular fibrillation waveform characteristics.

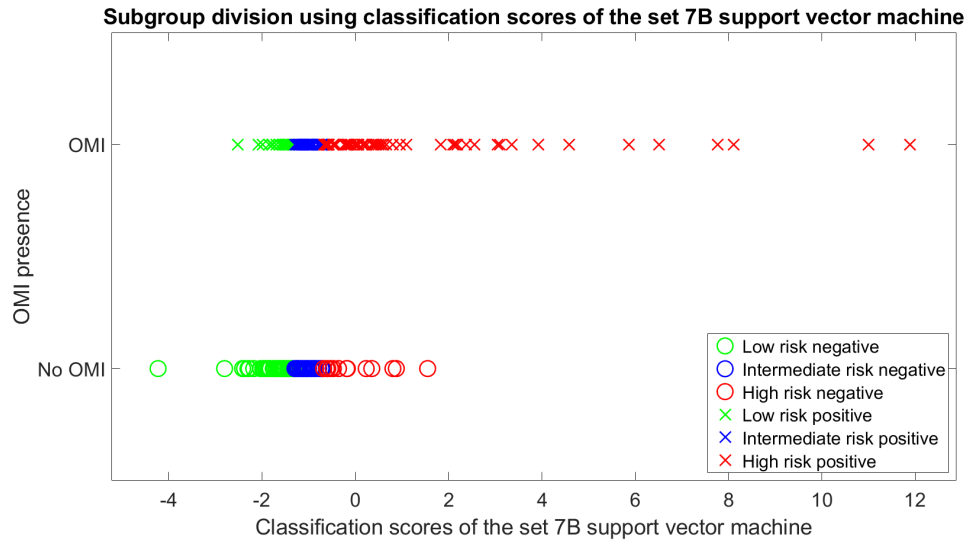

Figure 4.9: The classification scores of the set 7B support vector machine shown for the two study groups of patients without ('o') and with old myocardial infarction ('x'). All patients were divided into tertiles based on their classification scores which led to three subgroups. The threshold between the low risk and intermediate risk subgroups is at -1.30; the threshold between the intermediate risk and high risk subgroups is at -0.68. OMI: old myocardial infarction.

Table 4.2: Baseline characteristics of the subgroups based on tertiles of the classification scores of the set 7B support vector machine. The threshold between the low risk and intermediate risk subgroups is at -1.30; the threshold between the intermediate risk and high risk subgroups is at -0.68. Continuous variables are medians [Q1-Q3], categorical variables are n (%). Significant p-values are printed in bold. Significant post-hoc test results are indicated by an asterisk (*).

	Low risk	**Intermediate risk**	**High risk**	***p*-value**
Demographics				
Age (years)	62.0 [55.0-70.0]	65.0 [51.0-74.0]	67.0 [58.0-72.0]	0.064
Weight (kg)	75 [66-87]*	82 [71-90]	83 [74-91]*	**0.008**
Hypertension	29 (36.7)	35 (44.9)	35 (44.3)	0.376
Diabetes mellitus	11 (13.9)	22 (28.2)	20 (25.3)	0.105
Primary prevention	49 (62.0)	45 (57.0)	55 (69.6)	0.366
LV mass related				
LV mass index (g/m^2)	118.8 [84.6-136.6]	113.0 [97.6-134.2]	110.5 [90.1-132.0]	0.937
LV mass index (cat.)				0.525
Low mass	24 (37.5)	20 (28.6)	23 (33.8)	
Medium mass	15 (23.4)	25 (35.7)	27 (39.7)	
High mass	25 (39.1)	25 (35.7)	18 (26.5)	
Heart failure related				
QRS duration (ms)	116 [99-148]	112 [98-130]	125 [102-152]	0.142
LVEF (%)	35 [28-50]	35 [28-48]	33 [27-41]	0.105
CRT-D	21 (26.6)	20 (25.3)	25 (31.6)	0.536
LV dilation	15 (21.1)	11 (15.3)	14 (18.7)	0.750
ACEI or ARB	62 (78.5)	68 (86.1)	69 (88.5)	0.100
Diuretics	32 (40.5)	35 (44.3)	48 (61.5)	**0.011**
Antiarrhytmic drugs				
Beta blocker	71 (89.9)	69 (87.3)	73 (93.6)	0.504
Amiodarone	9 (11.4)	11 (13.9)	10 (12.8)	0.812

ACEI: angiotensin converting enzyme inhibitor, ARB: angiotensin receptor blocker, CRT-D: cardiac resynchronisation therapy-defibrillator, LV: left ventricular, LVEF: left ventricular ejection fraction.

4.4 Discussion

4.4.1 Main findings

In this study, the effect of feature optimisation on the performance of multi-lead machine learning models was studied. SVMs with as input VFWC of lead II, all twelve leads and leads II + V_1 reached AUCs of 0.61, 0.78 and 0.71 respectively before feature selection was applied. Feature selection reduced the number of VFWC from 17 to 3, from 391 to 10 and from 51 to 5. The models based on these reduced sets of input features reached AUCs of 0.58, 0.83 and 0.76. Overall, the 12-lead models reached the highest AUCs and sensitivities, followed by the lead II + V_1 models and the lead II models. Moreover, the SVM B models reached numerically higher AUCs and sensitivities than the corresponding SVM A models. The highest AUCs and sensitivities were observed for the MVR type models.

Since the 12-lead models were created with the most data, it is not surprising that these models reached the highest outcomes. Interestingly, the SVM B based on leads II and V_1 reached an AUC of 0.76, which can be considered acceptable[21]. This AUC was closer to the AUCs of the 12-lead models than those of the lead II models. This suggests that not all twelve leads contributed evenly to the discriminative ability of those models. Presumably, relatively unique and uncorrelated information is offered by leads II and V_1 because of their nearly orthogonal configuration within the patient. This could explain why the addition of lead V_1 resulted in models with markedly higher AUCs. It demonstrates that using multiple leads is a sensible way of gaining more insight into the underlying disease.

Notably, the SVM B models reached higher AUCs than their SVM A counterparts. Since all SVMs were subjected to an optimisation of hyperparameters, this contrast is likely attributable to differences in input features. The wrapper method of forward stepwise variable entry therefore appeared to be effective. Applying the filter method prior to the wrapper method seemed to remove valuable information as the even-numbered models reached lower outcomes than the odd-numbered variants.

The observed AUCs of the MVR models were higher than those of the SVM models. A possible explanation for this is that the SVM models were subjected to five-fold cross-validation whereas the MVR models were not cross-validated. The MVR models might therefore have been overfitted and might have produced worse results when unseen test data had been used to evaluate the performance. In order to estimate the size of this effect, the SVMs were once recreated without cross-validation; these models have not been reported here. The models reached AUCs markedly higher than those of the cross-validated SVMs and MVR models. The performance of the MVR models observed in this study is therefore likely overestimated. Further research with cross-validated MVR models is required to confirm this hypothesis.

4.4.2 Comparison to previous studies

The relationship between MI presence and the VF-waveform has been described numerously before. Early work in swine models showed that OMI and AMI change the VF-waveform in a similar way[11–15]. Human studies have demonstrated that AMI alters VFWC in the setting of OHCA as well[17,18]. The data used in the current study show similar changes of the VF-waveform caused by OMI and have been reported before[9,10].

This study exploited these VF-waveform changes to produce models for the detection of OMI. It is thereby a follow-up on the earlier proof-of-concept study on VF-waveform analysis of 12-lead ECGs with a machine learning approach[19]. In comparison, the current study employed a more thorough method for the optimisation of SVM hyperparameters and included models with new lead combinations. In addition, this study focused on the effect of established feature selection methods on model performance[22,23]. The approach of applying univariate analysis to identify potential predictors for a multivariate model is considered a filter method. This was

done in the current study by using the *p*-values of Mann-Whitney U tests on VFWC to compose the even-numbered sets of input features. The forward stepwise method for variable entry utilised by MVR could be considered a wrapper method, comparing the performance of models with different input features to determine the best combination. The employed methods of feature selections resulted in a lead II + V_1 model with an AUC comparable to those of the 12-lead models described in the proof-of-concept study. These methods of feature selection thus appeared to be effective.

4.4.3 Implications

The results of this study are in line with the findings of the proof-of-concept study mentioned earlier on detection of OMI using machine learning analysis of the VF-waveform[19]. The current study has shown that fine-tuning of the SVM hyperparameters and input features might improve the discriminative ability of the models. A wrapper method such as forward stepwise variable entry appears to be an effective way of removing redundant variables. Combining multiple feature selection methods may result in an excessive removal of predictor variables and a decrease of performance, however.

Similar to the proof-of-concept study, the ability of the models to detect OMI was better when using multiple ECG leads[19]. Given that the waveform changes imposed by OMI and AMI are similar, multi-lead models may facilitate AMI detection in the OHCA setting. Developing such models is a future prospect, however, as clinical trials are required to obtain multi-lead out-of-hospital VF data. Moreover, this study and previous work have shown that single lead models can detect OMI as well[19]. A first step would therefore be to translate the methods of this study to the out-of-hospital setting with the paddle ECG being the only available lead. This would give insight into the potential of diagnostic machine learning models for in-field detection of AMI and could warrant future research on the development and implementation of a multi-lead defibrillator ECG.

Furthermore, the subgroup analysis of this study has given insight into how an SVM with only VF-waveform based input features discriminates between patients with and without OMI. Nearly none of the clinical factors was different between the subgroups based on the SVM classification scores. This implies that the information in the VF-waveform is different from the information given by these clinical characteristics. This offers possibilities, as adding clinical factors to the model, such as age or gender, will supply unique information that might improve its discriminative ability.

4.4.4 Limitations

A limitation of the current study is that VF was induced electrically. Differences in waveform characteristics have been known to exist between electrically induced VF and spontaneous VF[24–26]. Moreover, this study attempted to detect OMI whereas the OHCA setting requires a method to detect AMI. This questions the generalisability of the current approach to the out-of-hospital setting with spontaneous VF caused by AMI. However, animal and human studies have suggested that the VF-waveform changes imposed by OMI are more abundant in case of AMI[12,15,18,27]. This suggests that the machine learning approach of VF-waveform analysis for the detection of OMI may perform better in the OHCA setting for the detection of AMI.

Moreover, in the current study only the initial phase of VF was analysed. The data did therefore not contain information about how the VF-waveform evolves over time. This lack of temporal information may have limited the performance of the models presented here. This means, however, that the current results may underestimate the performance of future in-field models that will have the possibility to analyse the VF-waveform over time. Detection of AMI in the out-of-hospital setting might therefore in the future be more accurate than this study in experimental setting suggests.

Considering that machine learning approaches are most suitable for large data sets, the small amount of patients in this study poses another limitation. Nonetheless, the SVMs reached acceptable discriminative abilities based on the AUCs. Future research with a larger study population might improve the accuracy of the models.

4.4.5 Conclusion

This study has demonstrated that feature selection and optimisation of hyperparameters might improve the performance of multi-lead machine learning models for the detection of OMI. Optimised models with input features selected from two leads reached acceptable discriminative abilities, performing on par with models based on twelve leads described in earlier work. These results are promising and warrant exploration of multi-lead models in clinical trials. Further research should investigate the effect of the proposed optimisation process on models detecting AMI in the setting of OHCA.

References

[1] J.A. Zijlstra et al. “Overleving na een reanimatie buiten het ziekenhuis: vergelijking van de resultaten van 6 verschillende Nederlandse regio’s”. In: *Reanimatie in Nederland 2016*. Den Haag: Hartstichting, 2016. Chap. 1, pp. 9–24.

[2] Robert J. Myerburg and Agustin Castellanos. “Cardiac Arrest and Sudden Cardiac Death”. In: *Braunwald’s Heart Disease: A Textbook of Cardiovascular Medicine*. Ed. by Robert O. Bonow, Douglas L. Mann, Douglas P. Zipes, and Peter Libby. 9th ed. Elsevier Saunders, 2012. Chap. 41, pp. 845–884. DOI: 10.1016/b978-1-4377-0398-6.00041-x.

[3] Guillaume Debaty et al. *Prognostic factors for extracorporeal cardiopulmonary resuscitation recipients following out-of-hospital refractory cardiac arrest. A systematic review and meta-analysis*. Mar. 2017. DOI: 10.1016/j.resuscitation.2016.12.011.

[4] Demetris Yannopoulos et al. “Coronary Artery Disease in Patients With Out-of-Hospital Refractory Ventricular Fibrillation Cardiac Arrest”. In: *Journal of the American College of Cardiology* 70.9 (Aug. 2017), pp. 1109–1117. ISSN: 15583597. DOI: 10.1016/j.jacc.2017.06.059.

[5] Matthew J. Reed, Gareth R. Clegg, and Colin E. Robertson. *Analysing the ventricular fibrillation waveform*. 2003. DOI: 10.1016/S0300-9572(02)00441-0.

[6] Giuseppe Ristagno et al. “Amplitude spectrum area to guide defibrillation a validation on 1617 patients with ventricular fibrillation”. In: *Circulation* 131.5 (Feb. 2015), pp. 478–487. ISSN: 15244539. DOI: 10.1161/CIRCULATIONAHA.114.010989.

[7] Julia H Indik et al. “Amplitude-spectral area and chest compression release velocity independently predict hospital discharge and good neurological outcome in ventricular fibrillation out-of-hospital cardiac arrest ”. In: *Resuscitation* 92 (2015), pp. 122–128. ISSN: 0300-9572. DOI: 10.1016/j.resuscitation.2015.05.002.

[8] Giuseppe Ristagno. *Real Time Amplitude Spectrum Area to Guide Defibrillation (AMSA)*. 2018.

[9] Judith L. Bonnes et al. “Ventricular fibrillation waveform characteristics differ according to the presence of a previous myocardial infarction: A surface ECG study in ICD-patients”. In: *Resuscitation* 96 (Nov. 2015), pp. 239–245. ISSN: 18731570. DOI: 10.1016/j.resuscitation.2015.08.014.

[10] Judith L. Bonnes et al. “Ventricular fibrillation waveform characteristics of the surface ECG: Impact of the left ventricular diameter and mass”. In: *Resuscitation* 115 (June 2017), pp. 82–89. ISSN: 18731570. DOI: 10.1016/j.resuscitation.2017.03.029.

[11] Julia H. Indik, Richard L. Donnerstein, Robert A. Berg, Ronald W. Hilwig, Marc D. Berg, and Karl B. Kern. “Ventricular fibrillation frequency characteristics are altered in acute myocardial infarction”. In: *Critical Care Medicine* 35.4 (Apr. 2007), pp. 1133–1138. ISSN: 00903493. DOI: 10.1097/01.CCM.0000259540.52062.99.

[12] Julia H. Indik et al. “The influence of myocardial substrate on ventricular fibrillation waveform: A swine model of acute and postmyocardial infarction”. In: *Critical Care Medicine* 36.7 (July 2008), pp. 2136–2142. ISSN: 15300293. DOI: 10.1097/CCM.0b013e31817d798c.

[13] Julia H. Indik et al. “Predictors of resuscitation outcome in a swine model of VF cardiac arrest: A comparison of VF duration, presence of acute myocardial infarction and VF waveform”. In: *Resuscitation* 80.12 (Dec. 2009), pp. 1420–1423. ISSN: 03009572. DOI: 10.1016/j.resuscitation.2009.08.023.

[14] Julia H. Indik et al. “Predictors of resuscitation in a swine model of ischemic and nonischemic ventricular fibrillation cardiac arrest: Superiority of amplitude spectral area and slope to predict a return of spontaneous circulation when resuscitation efforts are prolonged”. In: *Critical Care Medicine* 38.12 (Dec. 2010), pp. 2352–2357. ISSN: 15300293. DOI: 10.1097/CCM.0b013e3181fa01ee.

[15] Julia H. Indik, Daniel Allen, Michael Gura, Christian Dameff, Ronald W. Hilwig, and Karl B. Kern. “Utility of the ventricular fibrillation waveform to predict a return of spontaneous circulation and distinguish acute from post myocardial infarction or normal swine in ventricular fibrillation cardiac arrest”. In: *Circulation: Arrhythmia and Electrophysiology* 4.3 (June 2011), pp. 337–343. ISSN: 19413149. DOI: 10.1161/CIRCEP.110.960419.

[16] Julia H. Indik, Richard L. Donnerstein, Karl B. Kern, Steven Goldman, Mohamed A. Gaballa, and Robert A. Berg. “Ventricular fibrillation waveform characteristics are different in ischemic heart failure compared with structurally normal hearts”. In: *Resuscitation* 69.3 (June 2006), pp. 471–477. ISSN: 03009572. DOI: 10.1016/j.resuscitation.2005.10.017.

[17] Theresa M. Olasveengen, Trygve Eftestøl, Kenneth Gundersen, Lars Wik, and Kjetil Sunde. “Acute ischemic heart disease alters ventricular fibrillation waveform characteristics in out-of hospital cardiac arrest”. In: *Resuscitation* 80.4 (Apr. 2009), pp. 412–417. ISSN: 03009572. DOI: 10.1016/j.resuscitation.2009.01.012.

[18] Michiel Hulleman et al. “Predictive value of amplitude spectrum area of ventricular fibrillation waveform in patients with acute or previous myocardial infarction in out-of-hospital cardiac arrest”. In: *Resuscitation* 120 (Nov. 2017), pp. 125–131. ISSN: 18731570. DOI: 10.1016/j.resuscitation.2017.08.219.

[19] Jos Thannhauser et al. “Computerized analysis of the ventricular fibrillation waveform allows identification of myocardial infarction: a proof-of-concept study for smart defibrillator applications in cardiac arrest”. In: *Journal of the American Heart Association* (2020).

[20] Kristian Thygesen et al. “Third universal definition of myocardial infarction”. In: *European Heart Journal* 33.20 (2012), pp. 2551–2567. ISSN: 0195668X. DOI: 10.1093/eurheartj/ehs184.

[21] D W Hosmer and S Lemeshow. *Applied Logistic Regression*. Applied Logistic Regression. Wiley, 2004. ISBN: 9780471654025.

[22] Gh John, Ron Kohavi, and K Pfleger. “Irrelevant Features and the Subset Selection Problem”. In: *Machine Learning: Proceedings of the Eleventh International Conference* (1994), pp. 121–129. ISSN: 00189340.

[23] Max Kuhn and Kjell Johnson. *Applied Predictive Modeling with Applications in R*. 2013, p. 615. ISBN: 9781461468486.

[24] Nigel A. Lever, Emma G. Newall, and Peter D. Larsen. “Differences in the characteristics of induced and spontaneous episodes of ventricular fibrillation”. In: *Europace* 9.11 (2007), pp. 1054–1058. ISSN: 10995129. DOI: 10.1093/europace/eum194.

[25] Juan José Sánchez-Muñoz et al. “Spectral analysis of intracardiac electrograms during induced and spontaneous ventricular fibrillation in humans”. In: *Europace* 11.3 (2009), pp. 328–331. ISSN: 10995129. DOI: 10.1093/europace/eun366.

[26] Lawrence D. Sherman, James T. Niemann, John P. Rosborough, and James J. Menegazzi. “The effect of ischemia on ventricular fibrillation as measured by fractal dimension and frequency measures”. In: *Resuscitation* 75.3 (2007), pp. 499–505. ISSN: 03009572. DOI: 10.1016/j.resuscitation.2007.05.019.

[27] Michiel Hulleman, Marieke Blom, and David Salcido. “Changes in ventricular fibrillation quantitative waveform measures in out-of-hospital cardiac arrest in relation to acute myocardial infarction”. In: *Resuscitation* 106 (2016), e1. ISSN: 03009572. DOI: 10.1016/j.resuscitation.2016.07.009.

5 | A machine learning approach for detection of acute myocardial infarction in out-of-hospital cardiac arrest using ventricular fibrillation waveform analysis

K.M. van der Sluijs[1], J. Thannhauser[2], H.J. Zwart [3], M.A. Brouwer[2]
[1] Technical Medicine, University of Twente, Enschede, The Netherlands
[2] Department of Cardiology, Radboud University Medical Center, Nijmegen, The Netherlands
[3] Faculty of Electrical Engineering, Mathematics and Computer Sciences, Department of Applied Mathematics, University of Twente, Enschede, The Netherlands

Abstract

Background: Out-of-hospital ventricular fibrillation (VF) has dismal survival rates despite improvements in resuscitative care. Detection of acute myocardial infarction (AMI) by VF-waveform analysis may facilitate patient-tailored treatment strategies. This study aimed to identify predictors and assess the discriminative ability of machine learning models for the detection of AMI.

Methods: Adult patients with non-traumatic out-of-hospital VF transported to the Radboud University Medical Center were included (November 2005 - January 2011). VF-waveform characteristics (VFWC) were computed for the last three seconds before the first and second defibrillation shock. Selections of VFWC from the first, second, or both segments combined were used as input for models discriminating between patients with and without AMI. Model performance was assessed by receiver operating characteristic analysis.

Results: A total of 102 patients was included, of which 62 had an AMI. The VFWC amplitude spectrum area, detrended fluctuation analysis $\alpha 2$, median slope and flucvar were predictors for AMI. Models with VFWC of the first and second VF segment as input features had an area under the curve (AUC) of 0.74 and 0.72 respectively. Models with VFWC of both segments combined reached an AUC of 0.76.

Conclusions: Amplitude and organisation-related VFWC were predictors for AMI. Machine learning models with selections of VFWC had acceptable discriminative ability for detecting AMI. The proposed machine learning approach is promising and may facilitate an individualised treatment strategy by identifying patients with AMI during out-of-hospital VF.

5.1 Introduction

Ventricular fibrillation (VF) is the presenting cardiac rhythm in about 30% of all out-of-hospital cardiac arrest (OHCA) and carries dismal survival despite improvements in the chain of care[1,2]. Various initiatives have been taken over the last years that have increased the rate of lay person cardiopulmonary resuscitation (CPR) and automated external defibrillator (AED) use, yet there still is room for improvement[3,4].

In the quest towards patient-tailored therapeutic options, early recognition and treatment of the underlying arrest cause have been suggested[5,6]. Recent case series demonstrated a potential benefit of early transportation and intervention in patients with refractory VF, in case the underlying cause was acute myocardial infarction (AMI)[7]. However, diagnosis of AMI is currently restricted to patients in whom return of spontaneous circulation (ROSC) is achieved, precluding early aetiology-driven resuscitative interventions[8,9]. A more timely diagnosis of a reversible arrest cause such as an AMI, may pave the way for individualised treatment strategies, potentially improving outcomes.

A possible way for in-field identification of AMI patients may be by analysing the VF-waveform of the defibrillator electrocardiogram (ECG). Animal and human studies have demonstrated that both old myocardial infarction (OMI) and AMI affect morphological characteristics of the VF-waveform[10–13]. A recent human study on induced VF showed that a machine learning diagnostic approach with VF-waveform information as input enables detection of an OMI[14]. The study presented in chapter 4 of this thesis demonstrated that optimisation of input features improved the performance of those models. Although VF-morphology may differ between electrically induced and spontaneous VF, these studies showed the promising potential of VF-waveform analysis for diagnostic purposes[15,16].

As of yet, it is unknown whether the aforementioned results for detecting OMI in induced VF and optimisation of input features apply for early, in-field detection of AMI and spontaneous VF. It is also unknown which ventricular fibrillation waveform characteristics (VFWC) are essential for such discriminative models. Therefore, this study focused on identification of patients with an AMI as the underlying cause of OHCA in a real-world cohort using the VF-waveform. The aim was to identify predictors and to assess the discriminative ability of machine learning models for the detection of AMI using optimised input features.

5.2 Methods

5.2.1 Study population

All consecutive OHCA patients resuscitated between November 2005 and January 2011 by the emergency medical services (EMS) of region Gelderland-Zuid (The Netherlands) were registered. Adult patients (age $\geq$ 18) with VF as the first observed rhythm who were transported to the Radboud University Medical Center (Radboudumc) in Nijmegen were eligible for inclusion. Exclusion criteria were traumatic OHCA, a defibrillation shock delivered by an AED or implantable cardioverter-defibrillator (ICD) before EMS arrival, prematurely stopped resuscitation, absence of an analysable ECG recording and lack of clinical information to determine the arrest aetiology.

5.2.2 Data acquisition

Clinical characteristics

Demographic, clinical and arrest characteristics according to the 2004 Utstein-style definitions were collected using EMS and hospital records[17]. ECG tracings were recorded during resuscitation using the paddles of a LIFEPAK 12 defibrillator (Physio-Control, Redmond, WA, USA) with

a sampling frequency of 125 Hz. Biphasic shocks were delivered manually at energy levels of 200-360-360 Joule.

Ventricular fibrillation waveform characteristics

ECG recordings were pre-processed with a fourth order Butterworth bandpass filter with cut-off frequencies of 1 and 48 Hz. A graphical user interface developed in MATLAB® (version 2020a, MathWorks®, Natick, MA, USA) was used to review each ECG and select periods of VF without chest compressions.

Two segments were derived from these periods, each with a duration of three seconds (375 samples): the last segment before the first defibrillation shock (VF_1) and if availble the last segment before the second defibrillation shock (VF_2). Both VF_1 and VF_2 had to occur within a maximum of thirty seconds before the shock. Patients who received only one defibrillation shock did not have a VF_2 segment.

Seventeen VFWC were computed for both segments to quantify the VF-waveform. Details on the computation of the VFWC can be found in subsection 2.2.1. Additionally, the differences between the VFWC of VF_1 and VF_2 ($\Delta_{1,2}$) were computed, resulting in seventeen extra VFWC. Patients with two or more defibrillation shocks therefore had a total of 51 VFWC while patients with one shock had 17.

Study groups

Patients were divided into two groups based on whether or not they had an AMI at the time of resuscitation. Only patients for whom it was nearly certain that the AMI was the underlying cause of the arrest were included in the AMI group in order to avoid false-positives. For this study, AMI was therefore defined as presence of myocardial infarction according to the third universal definition, as well as presence of an acute coronary occlusion according to either of the following two criteria[18]. The first criterion was new ST-segment elevation of $\geq$0.1 mV on a post-arrest ECG with organised rhythm. A higher cut-off was applied for leads V_2 and V_3: $\geq$0.15 mV for women and $\geq$0.2 mV or $\geq$0.25 mV for men older or younger than 40 years old respectively. The second criterion was an intracoronary thrombus or acute occlusion identified by an experienced interventional cardiologist on an acute coronary angiography or by a pathologist on autopsy.

5.2.3 Descriptive analysis

Clinical and VF-waveform characteristics were compared between the two study groups. Continuous variables were reported as median [Q1-Q3] and categorical variables as number (percentage). Continuous variables were compared using Mann-Whitney U tests and categorical variables using Fisher's Exact Test. A p-value of <0.05 was considered significant.

Additionally, the median and [Q1-Q3] of some commonly used VFWC were reported side by side for the current study population as well as the study population described in chapter 4. The waveform characteristics of this population described VF induced electrically during ICD implantation procedures. They were reported in this study to demonstrate waveform differences between electrically induced VF and spontaneous VF caused by ischaemia.

All statistical analyses were performed with IBM SPSS® Statistics software (IBM Corp. Released 2017. IBM SPSS Statistics for Windows, Version 25.0. Armonk, NY: IBM Corp).

5.2.4 Predictive analysis

Set composition

Six sets of VFWC were composed, each including a different combination of VFWC of different VF segments. Figure 5.1 shows how the six sets 1A through 6A were composed.

First, a selection of segments was made: VF_1 alone (sets 1A and 2A), VF_2 alone (sets 3A and 4A) or $VF_1 + VF_2 + \Delta_{1,2}$ combined (sets 5A and 6A). The two segments alone were studied to assess the value of the VF-waveform at the two different moments. The segments and their differences combined were studied to investigate if combining information about different phases of the resuscitation would improve discriminative ability.

The distinction between the two sets within the three pairs was based on Mann-Whitney U tests that compared the VFWC between the patients with and without AMI. The even-numbered sets included only those VFWC with a *p*-value of <0.1. The odd-numbered sets contained VFWC with larger *p*-values as well.

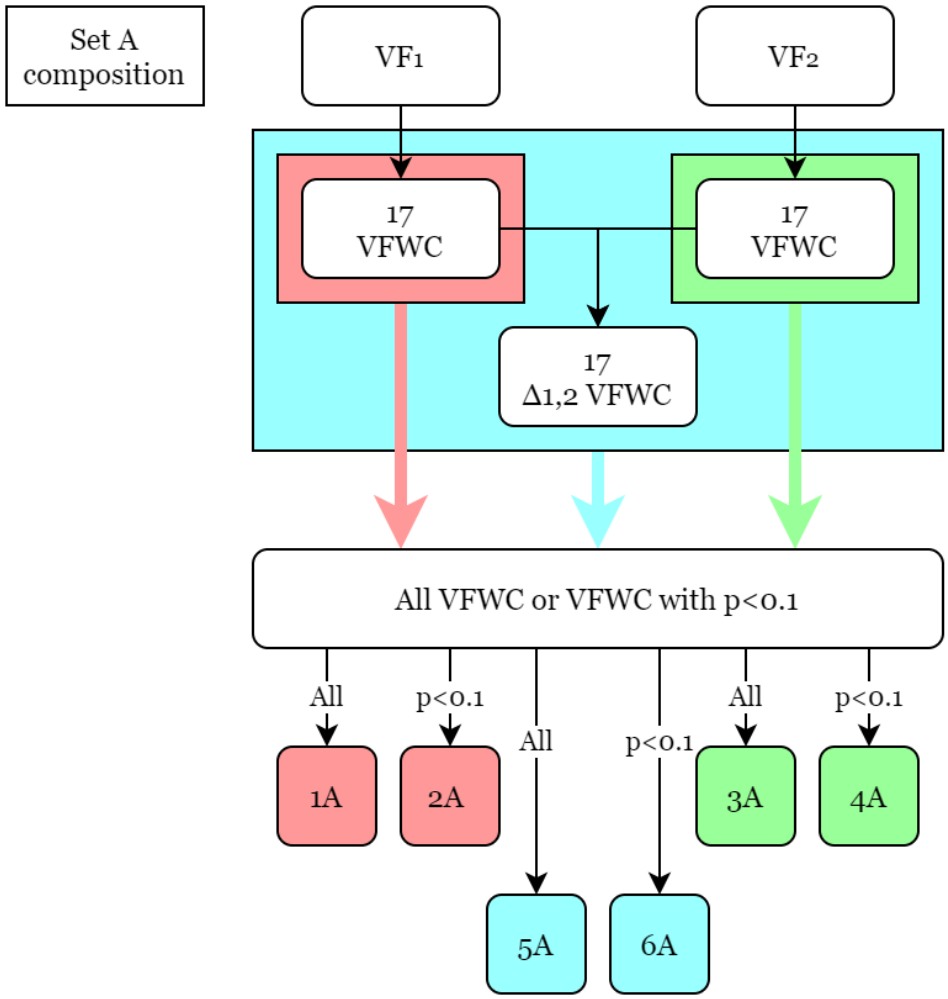

Figure 5.1: Composition of sets 1A-6A. VF_1: the last segment before the first defibrillation shock, VF_2: the last segment before the second defibrillation shock, VFWC: ventricular fibrillation waveform characteristics, $\Delta_{1,2}$: the differences between the ventricular fibrillation waveform characteristics of VF_1 and VF_2.

Prediction models

The six sets A were used as input features for six support vector machine (SVM) A models and six multivariate logistic regression (MVR) models. The wrapper type feature selection of forward stepwise entry reduced the number of variables included in the MVR models. The included variables composed the six sets B, which were used as input for the corresponding six SVM B models. The hyperparameters of the twelve SVMs were optimised according to the algorithm explained in subsection 2.2.3. Figure 5.2 shows an overview of how the sets were used as input features for the different models. The SVMs were subjected to five-fold cross-validation.

The results of the study presented in chapter 4 suggested that a wrapper type of feature selection applied on an SVM produces the most accurate models. The performances of the odd-numbered SVM B models were therefore considered the main results. The set 1B, 3B and 5B SVMs were evaluated to study the performance of models created from different VF segments. The other models were created from an exploratory perspective to investigate if the optimal method of feature selection proposed in chapter 4 applied to data of an OHCA cohort as well.

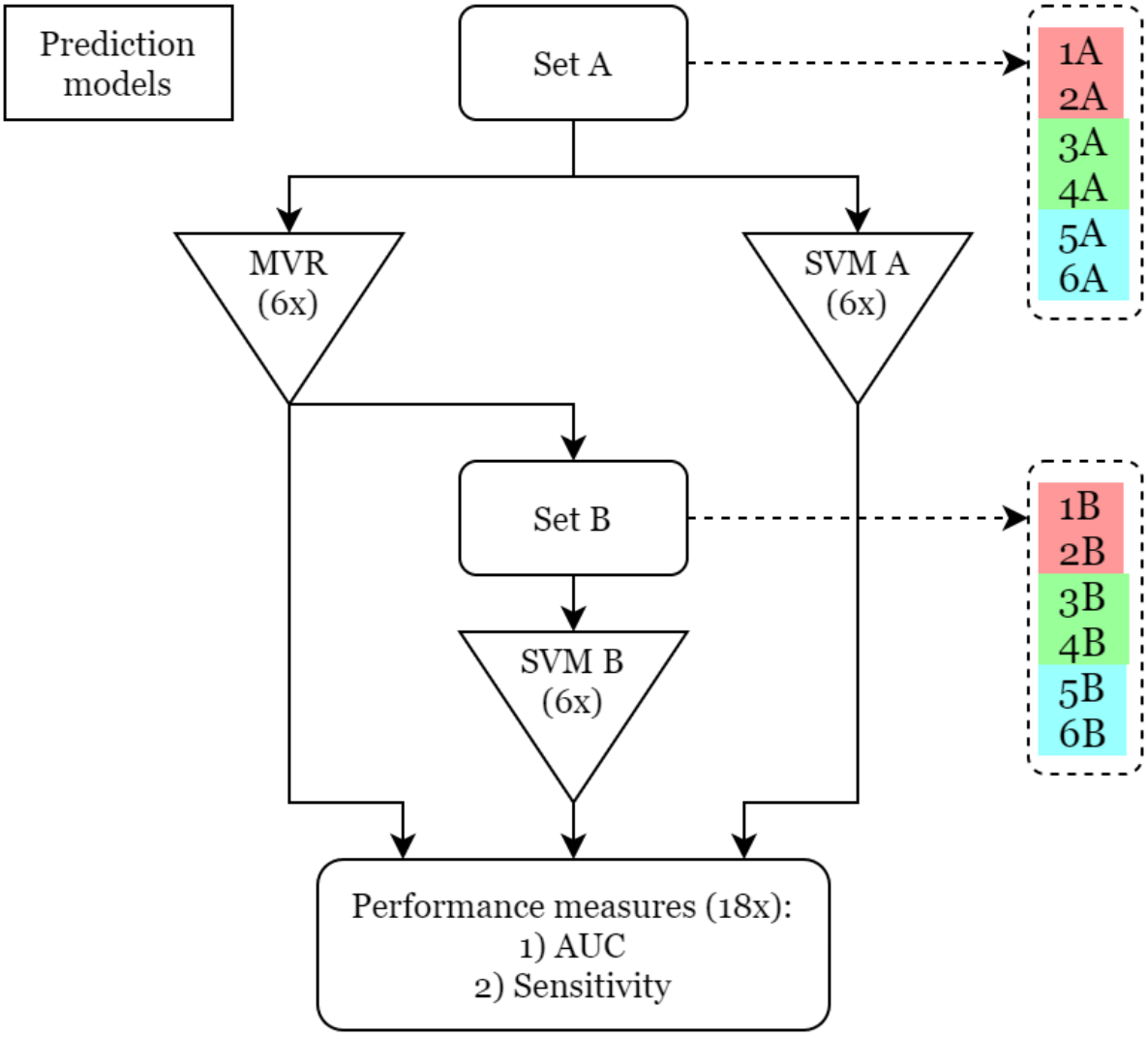

Figure 5.2: Overview of the prediction methods and the performance measures. AUC: area under the curve, MVR: multivariate logistic regression, SVM: support vector machine.

Outcome measures

Two outcome measures were used to assess the discriminative ability of each of the models: the area under the curve (AUC) of the receiver operating characteristic (ROC)-curve and the sensitivity at the level of 80% specificity. The rationale behind using these two outcome measures was the same as in chapter 4.

5.3 Results

5.3.1 Study population

In the period between November 2005 and January 2011, 253 patients were eligible for inclusion of which 151 were excluded for various reasons. Of the 102 included patients, 40 (39.2%) did not have an AMI and 62 (60.8%) did. Figure 5.3 shows an overview of the amount of patients in each stage of inclusion.

The VF_2 segment could be determined for 72 (70.6%) of the included patients as they received two or more defibrillation shocks during resuscitation. Figure 5.4 shows two phases of the defibrillator ECG of one of the included patients recorded during OHCA.

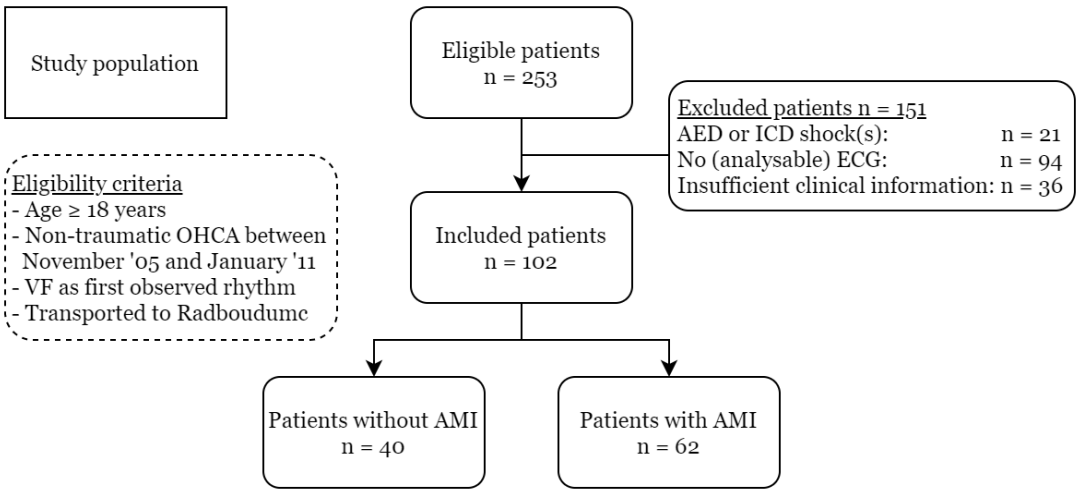

Figure 5.3: Flowchart of the patient inclusion process. AED: automated external defibrillator, AMI: acute myocardial infarction, ECG: electrocardiogram, ICD: implantable cardioverter-defibrillator, OHCA: out-of-hospital cardiac arrest, VF: ventricular fibrillation.

5.3.2 Descriptive analysis

Clinical characteristics

The median age of the 102 patients was 61.5 years [51.0-71.3] and 73 (71.6%) were male. The patients with AMI were younger and a larger proportion was male compared to the patients without AMI, but the differences were not significant. No differences existed in the arrest characteristics except for the response time, which was shorter for patients without AMI (7.0 vs. 8.0 minutes, p=0.038). Regarding outcome, patients without AMI more often had ROSC upon arrival at the emergency department (90.0% vs. 72.6%, p=0.045). Survival to hospital discharge was similar for the two groups. Table 5.1 shows all the baseline characteristics of the study population.

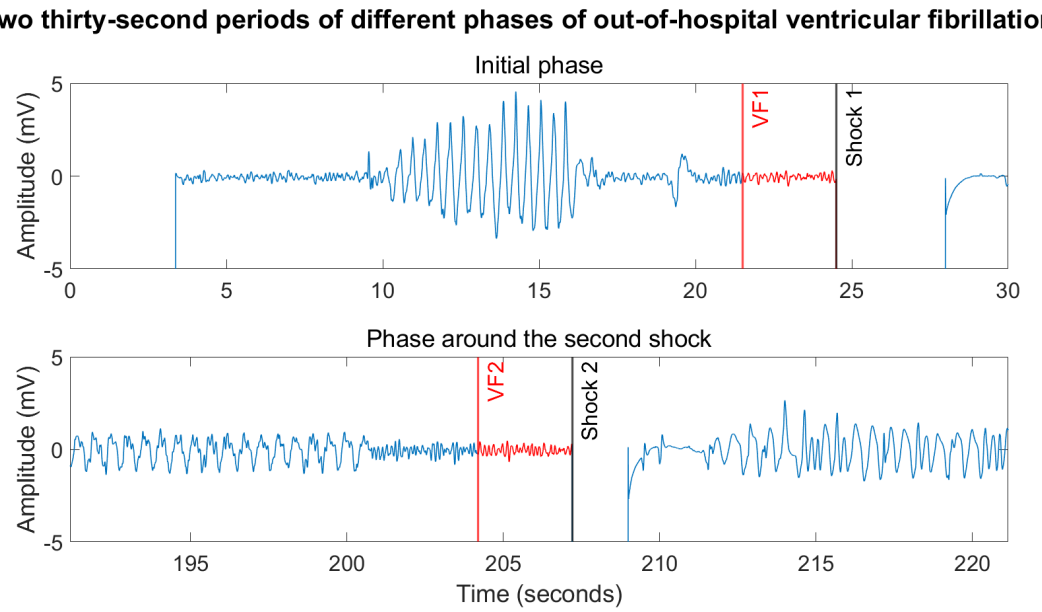

Figure 5.4: Example electrocardiogram recorded during out-of-hospital ventricular fibrillation. The upper panel shows the initial thirty seconds of the resuscitation with the last segment before the first shock (VF_1) marked in red. The lower panel shows the recording three minutes into the resuscitation with the last segment before the second shock (VF_2) in red.

Table 5.1: Baseline characteristics of the study population. Continuous variables are medians [Q1-Q3], categorical variables are n (%). Significant p-values are printed in bold.

	All patients n=102	**No AMI** n=40	**AMI** n=62	***p*-value**
Patient characteristics				
Age (years)	61.5 [51.0-71.3]	62.0 [53.5-71.8]	60.5 [49.0-71.3]	0.641
Male gender	73 (71.6)	26 (65.0)	47 (75.8)	0.266
Arrest characteristics				
Public location arrest	44 (43.1)	17 (42.5)	27 (43.5)	1.000
Witnessed arrest	86 (86.9)	33 (84.6)	53 (88.3)	0.762
Bystander	84 (84.8)	33 (84.6)	51 (85.0)	1.000
EMS	2 (2.0)	0 (0.0)	2 (3.3)	0.518
Bystander CPR	66 (66.7)	25 (64.1)	41 (68.3)	0.669
Response time (minutes)	8.0 [6.0-10.0]	7.0 [5.0-9.0]	8.0 [6.0-10.8]	**0.038**
Number of EMS shocks	3.0 [1.0-6]	2.5 [1.0-4.0]	3.0 [1.0-6.0]	0.272
Amiodarone	64 (65.3)	21 (55.3)	43 (71.7)	0.128
Adrenaline	79 (79.8)	30 (76.9)	49 (81.7)	0.614
Outcome characteristics				
ROSC at arrival ED	81 (79.4)	36 (90.0)	45 (72.6)	**0.045**
Survival to discharge	49 (48.0)	21 (52.5)	28 (45.2)	0.544

AMI: acute myocardial infarction, CPR: cardiopulmonary resuscitation, ED: emergency department, EMS: emergency medical services, ROSC: return of spontaneous circulation.

Ventricular fibrillation waveform characteristics

Mann-Whitney U tests were performed to investigate the differences of the VF_1, VF_2 and the $\Delta_{1,2}$ VFWC between the groups of patients with and without AMI. Table 5.2 shows the corresponding p-values.

VFWC with differences between the groups for both the VF segments were the mean absolute amplitude ($p \leq 0.024$), median slope ($p \leq 0.013$), amplitude spectrum area (AMSA) ($p \leq 0.011$) and power spectrum area ($p \leq 0.039$).

VFWC observed in this study are reported in table 5.3 alongside the VFWC of the study population described in chapter 4, obtained from electrically induced VF. Differences were observed between the two types of VF ($p = 0.002$ for AMSA, $p < 0.001$ for the other VFWC). Both the amplitude and frequency-related characteristics were higher for the electrically induced VF; the AMSA was lower. Furthermore, electrically induced VF had a smaller bandwidth and a larger organisation index and detrended fluctuation analysis (DFA) scaling exponents.

5.3.3 Predictive analysis

Set composition

The amount of VFWC in each of the sets 1A-6A as determined by figure 5.1 can be seen in figure 5.5. The forward stepwise entry method of MVR reduced the number of VFWC to compose sets 1B-6B. These sets contained one or two VFWC. A more elaborate description of the set compositions is given in appendix A.5.

Prediction models

Eighteen sets were created, six models of MVR, SVM A and SVM B each. The optimised hyperparameters of the SVMs can be found in table A.9 in A.6. Figure 5.6 shows the areas under the ROC-curves with the 95% confidence intervals depicted using error bars. Figure 5.7 shows the sensitivities of the models at the level of 80% specificity.

The set 1B SVM based on the AMSA and DFA$\alpha 2$ of the VF_1 segment had an AUC and sensitivity of 0.74 and 0.58 respectively. The SVM of set 3B with the median slope of segment VF_2 as input feature had an AUC of 0.72 and a sensitivity of 0.40. The SVM of set 5B with the flucvar of the VF_1 segment and the median slope of the VF_2 segment as input features reached an AUC of 0.76 and a sensitivity of 0.55.

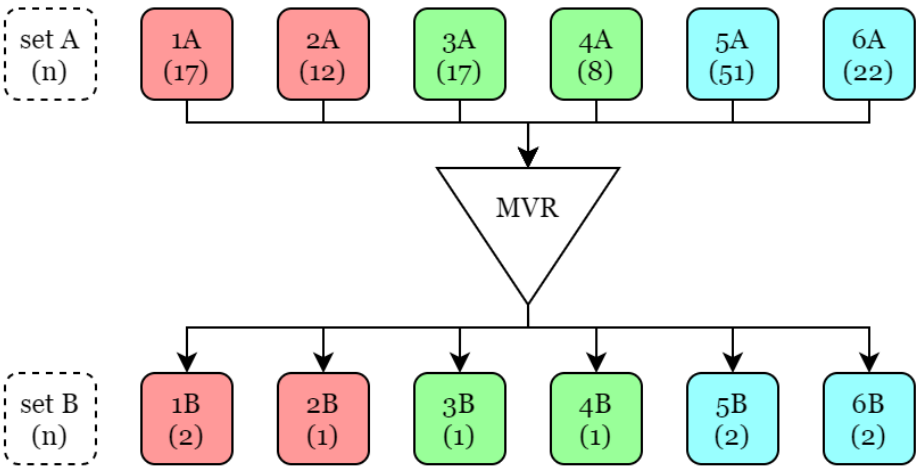

Figure 5.5: Overview of the number of ventricular fibrillation waveform characteristics in sets 1A-6A and 1B-6B. The forward stepwise entry method of multivariate logistic regression was used to create subselections of sets A that compose sets B. MVR: multivariate logistic regression.

Table 5.2: The p-values of Mann-Whitney U tests of the ventricular fibrillation waveform characteristics between the groups with and without acute myocardial infarction. Green cells indicate p-values <0.05, yellow cells indicate p-values <0.1. Underlined values indicate that the waveform characteristic was larger for the group with acute myocardial infarction.

	VF_1	VF_2	$\Delta_{1,2}$
MAA	0.016	0.024	0.386
MS	0.013	0.004	0.349
FM	0.062	0.175	0.687
FD	0.052	0.228	0.608
BW	0.631	0.037	0.088
AMSA	0.006	0.011	0.940
AMSAlf	0.011	0.028	0.821
AMSAhf	0.005	0.007	0.875
AMSAratio	0.967	0.688	0.785
PSA	0.008	0.039	0.529
flucmean	0.151	0.053	0.966
flucvar	0.184	0.850	0.422
flucrms	0.025	0.570	0.259
flucmaa	0.044	0.530	0.526
OI	0.060	0.399	0.070
DFAα1	0.033	0.207	0.839
DFAα2	0.219	0.838	0.885
Total p<0.1	12	8	2

AMSA: amplitude spectrum area, $AMSA_{hf}$: AMSA high frequencies, $AMSA_{lf}$: AMSA low frequencies, BW: bandwidth, DFA: detrended fluctuation analysis, FD: dominant frequency, FM: median frequency, MAA: mean absolute amplitude, MS: median slope, OI: organisation index, PSA: power spectrum area, VF_1: the last segment before the first defibrillation shock, VF_2: the last segment before the second defibrillation shock, $\Delta_{1,2}$: the differences between the ventricular fibrillation waveform characteristics of VF_1 and VF_2.

Table 5.3: Medians and [Q1-Q3] of a selection of ventricular fibrillation waveform characteristics. The OHCA column contains waveform characteristics of the last segment before the first defibrillation shock measured during out-of-hospital cardiac arrest in the study population described in the current study. The ICD column contains waveform characteristics of lead II of ventricular fibrillation induced electrically during implantable cardioverter-defibrillator testing in the study population described in chapter 4. Significant p-values are printed in bold.

	OHCA	**ICD**	***p*-value**
Mean absolute amplitude	0.12 [0.10-0.16]	0.15 [0.11-0.24]	**<0.001**
Median slope	3.05 [1.83-4.88]	4.65 [3.52-7.10]	**<0.001**
Dominant frequency	4.39 [2.93-6.35]	5.13 [4.88-5.62]	**<0.001**
Bandwidth	2.20 [1.46-2.99]	0.49 [0.24-0.73]	**<0.001**
Amplitude spectrum area	14.23 [9.70-20.80]	11.28 [9.06-16.01]	**0.002**
Power spectrum area	0.06 [0.02-0.16]	0.18 [0.10-0.42]	**<0.001**
Organisation index	0.47 [0.34-0.63]	0.69 [0.55-0.78]	**<0.001**
Detrended fluctuation analysis α1	1.39 [1.26-1.49]	1.97 [1.95-1.98]	**<0.001**
Detrended fluctuation analysis α2	0.07 [0.05-0.10]	0.26 [0.22-0.31]	**<0.001**

ICD: implantable cardioverter-defibrillator, OHCA: out-of-hospital cardiac arrest.

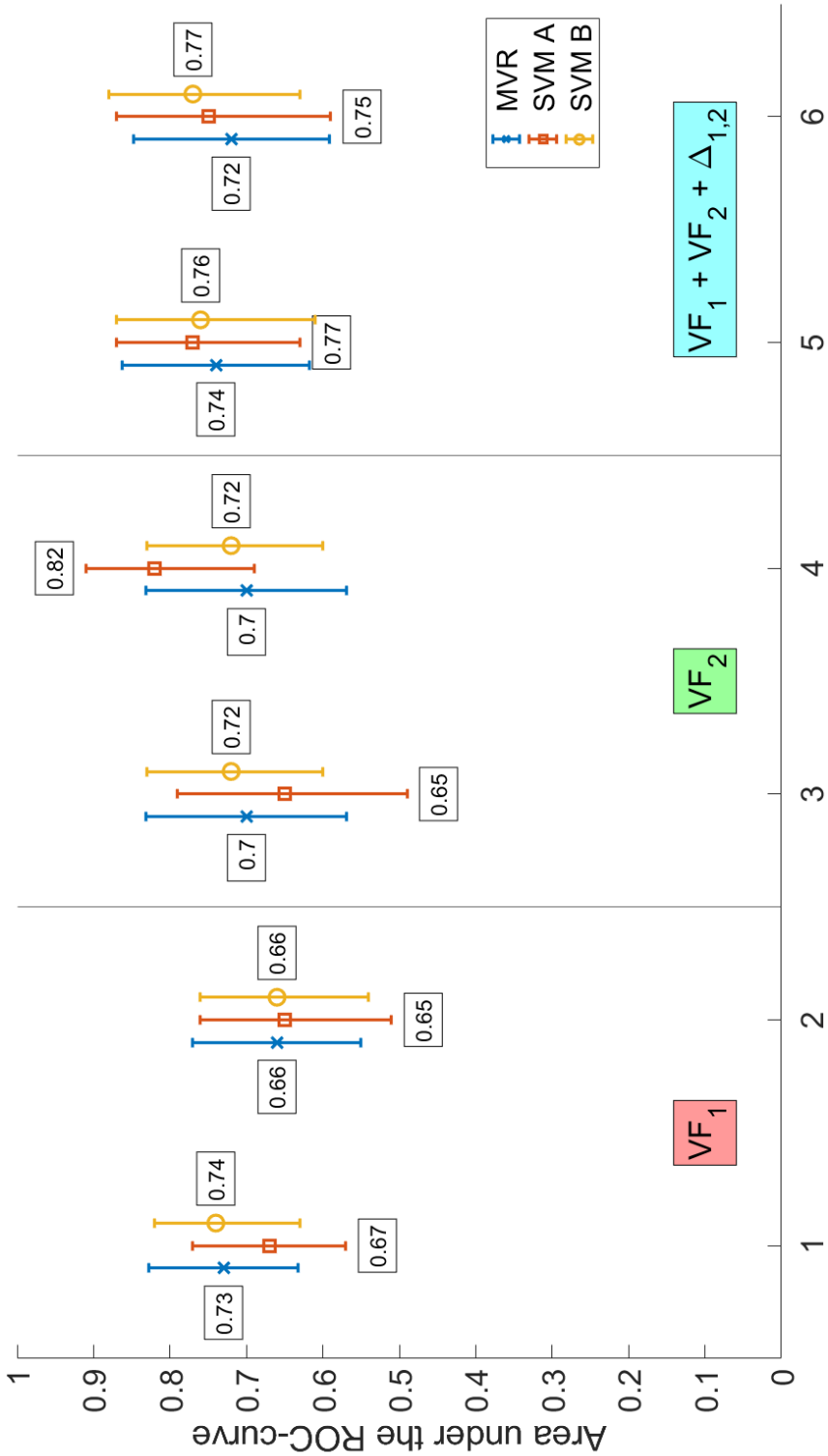

Figure 5.6: The areas under the ROC-curves of the eighteen prediction models of types MVR, SVM A and SVM B. The labels represent the areas, the error bars visualise the 95% confidence intervals. MVR: multivariate logistic regression, ROC: receiver operating characteristic, SVM: support vector machine, VF_1: the last segment before the first defibrillation shock, VF_2: the last segment before the second defibrillation shock, $\Delta_{1,2}$: the differences between the waveform characteristics of segments VF_1 and VF_2.

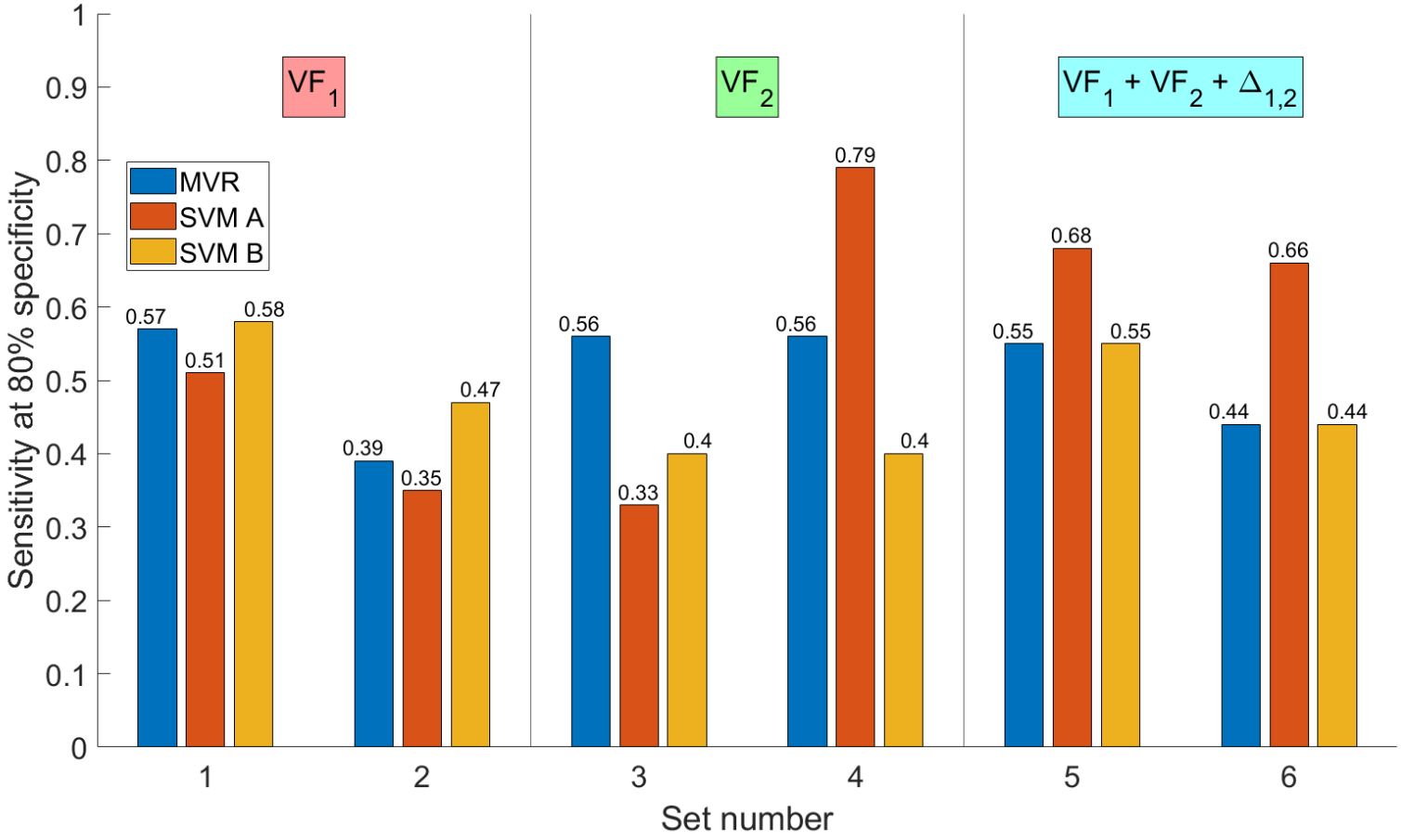

Figure 5.7: The sensitivities of the eighteen prediction models of types MVR, SVM A and SVM B, measured at the level of 80% specificity. MVR: multivariate logistic regression, SVM: support vector machine, VF_1: the last segment before the first defibrillation shock, VF_2: the last segment before the second defibrillation shock, $\Delta_{1,2}$: the differences between the waveform characteristics of segments VF_1 and VF_2.

5.4 Discussion

5.4.1 Main findings

The aim of this study was to identify predictors and to assess the discriminative ability of machine learning models for detecting AMI using optimised input features from different segments of the resuscitation. The VFWC that were predictors in the SVM B models were the AMSA, DFAα2, median slope and flucvar. The SVM models created using VFWC of the first and second VF segment reached an AUC of 0.74 and 0.72 respectively. The model with input features from both segments combined had an AUC of 0.76. All three models had a discriminative ability that can be considered acceptable[19]. Considering the other models, the highest AUCs were reached when VFWC of both segments were used.

Combining input features from different phases of the resuscitation seemed to result in models with the best ability to discriminate between patients with and without AMI. This is understandable, as these models were created with more information than the single segment models. This finding suggests that there was a difference between the two patient groups in the way the VF-waveform evolved over time. While the amplitude-related measures were consistently lower in patients with AMI, the organisation-related measures evolved differently for the two groups. The VF of patients without AMI underwent a decrease in bandwidth over time, indicating an increase of signal organisation. Conversely, the organisation index of patients with AMI decreased over time, indicating a decrease of signal organisation. The signal organisation thus seemed to decrease in case of AMI, while it increased in absence of AMI.

One factor that may have overestimated the discriminative abilities of the current models is that the response time was higher for the patients with AMI. Previous research has shown that amplitude-related VFWC, such as AMSA, decrease over the course of the arrest[13]. This suggests that the lower amplitude-related VFWC observed in the AMI group may partially have been caused by the longer response time, rather than by presence of AMI alone. Since it is unlikely that a longer response time in itself increased the likelihood of AMI, response time was not considered to be a confounder and its effect was assumed to be limited. Nonetheless, the discriminative abilities of the current models might have been overestimated and might have been worse if equal response times had been observed for the two study groups.

The comparison between the waveform characteristics of spontaneous VF recorded in the OHCA setting and electrically induced VF obtained during ICD testing showed clear differences. Both amplitude and frequency-related measures were smaller during OHCA. This could have been caused by the acute nature of the myocardial infarctions, which are known to have a stronger effect on the VF-waveform than OMIs[10,13]. The longer time period between the onset and recording of VF in the OHCA cohort could have caused smaller amplitude and frequency measures as well. Surprisingly, the AMSA was higher for these patients, while it is a combined amplitude-frequency measure. Inspection of the power spectra showed that spontaneous VF indeed had a lower dominant frequency, but also had a higher bandwidth. This increased dispersion of power over the frequency range presumably amounted to a higher AMSA. On the same note, the higher bandwidth in the OHCA group was accompanied by a lower organisation index, as compared to the ICD group. Besides lower amplitude and frequency measures, spontaneous VF therefore also appeared to have a lower degree of signal organisation than electrically induced VF.

5.4.2 Comparison to previous studies

Analysing changes in the VF-waveform to detect AMI has been described before. Swine studies showed that the AMSA and median slope are decreased in case of AMI[10,20,21]. Human studies found similar results, suggesting that VF-waveform analysis may be used to detect AMI during OHCA[12,13]. This study extended these findings and showed that the AMSA and median slope in

addition to other VFWC may be used to detect AMI with an acceptable accuracy.

The use of a machine learning approach to detect AMI is relatively new. A proof-of-concept study on electrically induced VF acquired during ICD testing first demonstrated this practice for the detection of OMI[14]. The study reported in chapter 4 of this thesis improved the method by performing an optimisation of input features. The current study applied the same machine learning approach on a real-world OHCA cohort with spontaneous VF. The AUCs that were achieved are similar to those described in the earlier studies on the detection of OMI. Those studies used models based on VFWC of two or even twelve leads, however. In contrast, the models in the current study were created with input features from the defibrillator ECG lead alone.

The similar performance achieved with a single ECG lead instead of multiple leads may be explained by the relevance of the organisation-related VFWC for the detection of AMI. These waveform measures played a more important role in the OHCA setting for differentiating between patients with and without AMI than in the experimental setting for the detection of OMI. This increased variety of predictors may have led to similar model performances, despite the fact that all input features originated from a single ECG lead.

5.4.3 Implications

This study has demonstrated that analysing the out-of-hospital VF-waveform over time improves the ability of a model to detect AMI. Gathering these data from the first possible moment in a resuscitation is therefore key, once in-field VF-waveform analysis becomes available.

Furthermore, organisation-related measures seemed to play a role in distinguishing between patients with and without AMI. The discriminative value of these VFWC was not apparent in earlier studies on the detection of OMI in electrically induced VF. The differences observed in this study between these VFWC measured in spontaneous and electrically induced VF might explain why the discriminative role is limited to the OHCA setting; organisation-related measures might therefore be more valuable than previously thought. An in-field application for AMI detection would likely benefit from a wide range of VFWC and include these measures besides the more commonly used measures, such as AMSA.

The amplitude and frequency-related VFWC were found to be different between the spontaneous and electrically induced VF as well. These differences prevent a direct translation of earlier results found in the experimental setting to the out-of-hospital setting. Future research on in-field identification of AMI should therefore be based on out-of-hospital data.

A further improvement of the AMI detection method may be facilitated by analysis of multiple ECG leads. A previous study has shown that multi-lead VF-waveform analysis improves the detection of OMI[14]. This method has only been applied in an experimental setting; the effect of a multi-lead approach in the OHCA setting is still unknown and should be investigated. Multi-lead machine learning models might detect AMI more accurately than the models presented in this study. Since such models require data, a first step would be to set up a prospective registry to systematically record out-of-hospital VF data in multiple leads.

5.4.4 Limitations

One limitation of this study is that selection bias may have occurred in the inclusion of patients. Only patients that were transported to the hospital were included as patients for whom resuscitation was terminated did not meet the eligibility criteria. The included patients might have constituted a more homogeneous sample than the study population they represented. The generalisability of the current results to the entire out-of-hospital population might therefore be questioned.

Furthermore, the number of included patients was relatively small for machine learning purposes. The best performing models were created with even a smaller number as the VF_2

segment was not recorded for all patients. The amount of predictor variables for the SVM A models was therefore likely to be too large, following the one in ten rule[22,23]. This might have caused overfitting, which questions the discriminative ability on unseen test data. Cross-validation was applied to prevent this, however. In addition, the MVR and SVM B models were composed of only one or two predictor variables. The results might therefore still be representative.

Another limitation of this study is that only the VF_1 and VF_2 segments were analysed, which were both recorded in the early phase of the resuscitation. Using additional VF segments recorded later in the resuscitation would provide extra information and possibly increase model performance. This would introduce bias, however, as long duration resuscitation attempts that usually have poor outcomes would be overrepresented. The current combination of VF segments before the first and second defibrillation shock might therefore represent the OHCA population more accurately.

5.4.5 Conclusion

This study found that both amplitude and organisation-related VFWC were predictors for AMI in the OHCA setting. Machine learning models based on optimised sets of these VFWC were able to detect AMI with acceptable discriminative ability. Combining VFWC recorded in different phases of the resuscitation seemed to improve detection. Further research should investigate the discriminative ability of multi-lead models in the out-of-hospital setting. Implementation of a multi-lead machine learning model in clinical practice may in the future facilitate early, in-field identification of AMI during OHCA.

References

[1] Jocelyn Berdowski, Robert A. Berg, Jan G P Tijssen, and Rudolph W. Koster. "Global incidences of out-of-hospital cardiac arrest and survival rates: Systematic review of 67 prospective studies". In: *Resuscitation* 81.11 (Nov. 2010), pp. 1479–1487. ISSN: 03009572. DOI: 10.1016/j.resuscitation.2010.08.006.

[2] Mohamud R. Daya et al. "Out-of-hospital cardiac arrest survival improving over time: Results from the Resuscitation Outcomes Consortium (ROC)". In: *Resuscitation* 91 (June 2015), pp. 108–115. ISSN: 18731570. DOI: 10.1016/j.resuscitation.2015.02.003.

[3] Myron L. Weisfeldt et al. "Survival After Application of Automatic External Defibrillators Before Arrival of the Emergency Medical System. Evaluation in the Resuscitation Outcomes Consortium Population of 21 Million". In: *Journal of the American College of Cardiology* 55.16 (Apr. 2010), pp. 1713–1720. ISSN: 07351097. DOI: 10.1016/j.jacc.2009.11.077.

[4] J. Nas et al. "Changes in automated external defibrillator use and survival after out-of-hospital cardiac arrest in the Nijmegen area". In: *Netherlands Heart Journal* 26.12 (Dec. 2018), pp. 600–605. ISSN: 18766250. DOI: 10.1007/s12471-018-1162-9.

[5] Christian M. Spaulding et al. "Immediate coronary angiography in survivors of out-of-hospital cardiac arrest". In: *New England Journal of Medicine* 336.23 (June 1997), pp. 1629–1633. ISSN: 00284793. DOI: 10.1056/NEJM199706053362302.

[6] Florence Dumas et al. "Immediate percutaneous coronary intervention is associated with better survival after out-of-hospital cardiac arrest: Insights from the PROCAT (Parisian Region Out of Hospital Cardiac Arrest) registry". In: *Circulation: Cardiovascular Interventions* 3.3 (June 2010), pp. 200–207. ISSN: 19417640. DOI: 10.1161/CIRCINTERVENTIONS.109.913665.

[7] Demetris Yannopoulos et al. "Coronary Artery Disease in Patients With Out-of-Hospital Refractory Ventricular Fibrillation Cardiac Arrest". In: *Journal of the American College of Cardiology* 70.9 (Aug. 2017), pp. 1109–1117. ISSN: 15583597. DOI: 10.1016/j.jacc.2017.06.059.

[8] Florence Dumas et al. "Can early cardiac troponin i measurement help to predict recent coronary occlusion in out-of-hospital cardiac arrest survivors?" In: *Critical Care Medicine* 40.6 (2012), pp. 1777–1784. ISSN: 00903493. DOI: 10.1097/CCM.0b013e3182474d5e.

[9] Patrick J Coppler and Cameron Dezfulian. "The quest continues to identify coronary occlusion in OHCA without ST elevation". In: *Resuscitation* 0.0 (Nov. 2019). ISSN: 03009572. DOI: 10.1016/j.resuscitation.2019.10.024.

[10] Julia H. Indik, Daniel Allen, Michael Gura, Christian Dameff, Ronald W. Hilwig, and Karl B. Kern. "Utility of the ventricular fibrillation waveform to predict a return of spontaneous circulation and distinguish acute from post myocardial infarction or normal swine in ventricular fibrillation cardiac arrest". In: *Circulation: Arrhythmia and Electrophysiology* 4.3 (June 2011), pp. 337–343. ISSN: 19413149. DOI: 10.1161/CIRCEP.110.960419.

[11] Judith L. Bonnes et al. "Ventricular fibrillation waveform characteristics differ according to the presence of a previous myocardial infarction: A surface ECG study in ICD-patients". In: *Resuscitation* 96 (Nov. 2015), pp. 239–245. ISSN: 18731570. DOI: 10.1016/j.resuscitation.2015.08.014.

[12] Theresa M. Olasveengen, Trygve Eftestøl, Kenneth Gundersen, Lars Wik, and Kjetil Sunde. "Acute ischemic heart disease alters ventricular fibrillation waveform characteristics in out-of hospital cardiac arrest". In: *Resuscitation* 80.4 (Apr. 2009), pp. 412–417. ISSN: 03009572. DOI: 10.1016/j.resuscitation.2009.01.012.

[13] Michiel Hulleman et al. "Predictive value of amplitude spectrum area of ventricular fibrillation waveform in patients with acute or previous myocardial infarction in out-of-hospital cardiac arrest". In: *Resuscitation* 120 (Nov. 2017), pp. 125–131. ISSN: 18731570. DOI: 10.1016/j.resuscitation.2017.08.219.

[14] Jos Thannhauser et al. "Computerized analysis of the ventricular fibrillation waveform allows identification of myocardial infarction: a proof-of-concept study for smart defibrillator applications in cardiac arrest". In: *Journal of the American Heart Association* (2020).

[15] Nigel A. Lever, Emma G. Newall, and Peter D. Larsen. "Differences in the characteristics of induced and spontaneous episodes of ventricular fibrillation". In: *Europace* 9.11 (2007), pp. 1054–1058. ISSN: 10995129. DOI: 10.1093/europace/eum194.

[16] Juan José Sánchez-Muñoz et al. "Spectral analysis of intracardiac electrograms during induced and spontaneous ventricular fibrillation in humans". In: *Europace* 11.3 (2009), pp. 328–331. ISSN: 10995129. DOI: 10.1093/europace/eun366.

[17] Ian Jacobs et al. *Cardiac arrest and cardiopulmonary resuscitation outcome reports: Update and simplification of the Utstein templates for resuscitation registries. A statement for healthcare professionals from a task force of the International Liaison Committee on Resusci*. Nov. 2004. DOI: 10.1161/01.CIR.0000147236.85306.15.

[18] Kristian Thygesen et al. “Third universal definition of myocardial infarction”. In: *European Heart Journal* 33.20 (2012), pp. 2551–2567. ISSN: 0195668X. DOI: 10.1093/eurheartj/ehs184.

[19] D W Hosmer and S Lemeshow. *Applied Logistic Regression*. Applied Logistic Regression. Wiley, 2004. ISBN: 9780471654025.

[20] Julia H. Indik et al. “Predictors of resuscitation outcome in a swine model of VF cardiac arrest: A comparison of VF duration, presence of acute myocardial infarction and VF waveform”. In: *Resuscitation* 80.12 (Dec. 2009), pp. 1420–1423. ISSN: 03009572. DOI: 10.1016/j.resuscitation.2009.08.023.

[21] Julia H. Indik et al. “Predictors of resuscitation in a swine model of ischemic and nonischemic ventricular fibrillation cardiac arrest: Superiority of amplitude spectral area and slope to predict a return of spontaneous circulation when resuscitation efforts are prolonged”. In: *Critical Care Medicine* 38.12 (Dec. 2010), pp. 2352–2357. ISSN: 15300293. DOI: 10.1097/CCM.0b013e3181fa01ee.

[22] Frank E. Harrell, Kerry L. Lee, and Daniel B. Mark. “Multivariable prognostic models: Issues in developing models, evaluating assumptions and adequacy, and measuring and reducing errors”. In: *Statistics in Medicine* 15.4 (Feb. 1996), pp. 361–387. ISSN: 02776715. DOI: 10.1002/(SICI)1097-0258(19960229)15:4<361::AID-SIM168>3.0.CO;2-4.

[23] Peter Peduzzi, John Concato, Elizabeth Kemper, Theodore R. Holford, and Alvan R. Feinstem. “A simulation study of the number of events per variable in logistic regression analysis”. In: *Journal of Clinical Epidemiology* 49.12 (Dec. 1996), pp. 1373–1379. ISSN: 08954356. DOI: 10.1016/S0895-4356(96)00236-3.

6 | General discussion

In search of individualised out-of-hospital cardiac arrest (OHCA) care to improve survival, this thesis investigated machine learning methods for the detection of acute myocardial infarction (AMI) as the underlying cause of the arrest using ventricular fibrillation (VF)-waveform analysis.

The study presented in chapter 4 focused on detection of old myocardial infarction (OMI) in patients with VF induced electrically in the setting of implantable cardioverter-defibrillator testing. The VF-waveform changes caused by OMI were studied here using twelve electrocardiogram (ECG) leads and were considered a surrogate for the VF-waveform changes imposed by AMI. The aim was to investigate the effect of established feature selection methods on the discriminative ability of machine learning models for the detection of OMI. Selections of ventricular fibrillation waveform characteristics (VFWC) of lead II, all twelve leads or lead II + V_1 were used as input features for support vector machine models. These models reached an area under the curve (AUC) of 0.58, 0.83 and 0.76 respectively. This study has demonstrated that feature selection and use of multiple ECG leads improved the discriminative ability of the machine learning models. Interestingly, the model based on leads II and V_1 was able to reach acceptable discrimination between patients with and without OMI with an AUC of 0.76. This is comparable to the performance of 12-lead models created using the same data described in the aforementioned proof-of-concept study. These promising results indicate that an optimised model based on two leads may have diagnostic value in clinical practice and requires exploration. The main limitation of this study was that VF was induced electrically, questioning the generalisability to the OHCA setting where VF arises spontaneously.

The study reported in chapter 5 therefore investigated the VF-waveform in an OHCA cohort of which some patients had AMI. The aim was to find predictors and to assess the discriminative ability of machine learning models for the detection of AMI. Amplitude and organisation-related VFWC were found to be predictors of AMI. Support vector machine models were created using selections of VFWC from a single VF segment or a combination of two segments. The single segment models reached AUCs of 0.74 and 0.72 and the model with VFWC of both segments had an AUC of 0.76. Thus, acceptable discrimination between patients with and without AMI was achieved with models based on the defibrillator ECG alone. Especially the models based on both segments performed well, as they incorporated the evolution of the VF-waveform over time. The results have shown that optimisation of input features is beneficial in the out-of-hospital setting as well. Because of the added discriminative value of the organisation-related VFWC in the out-of-hospital setting, the performances of the single lead models were comparable to those of the 12-lead models described in the earlier proof-of-concept study and to those of the lead II + V_1 models reported in chapter 4. This suggests that the potential of VF-waveform analysis is larger for detecting AMI in spontaneous VF than for detecting OMI in electrically induced VF. In conjunction with the results of chapter 4, this implies that machine learning models with optimised input features of multiple ECG leads may facilitate accurate in-field detection of AMI during OHCA.

Altogether, this thesis has shown that VF-waveform analysis for the detection of AMI in the OHCA setting using machine learning is promising. Feature selection, use of organisation-related VFWC and analysing the VF-waveform over time improves the discriminative ability of these models. Using multiple ECG leads to record the VF-waveform seems to have the most potential to improve the detection of AMI. Further research should focus on setting up a prospective OHCA registry to systematically record multi-lead ECGs of VF. This will enable optimisation of the machine learning models so they can be evaluated in clinical practice. This paves the way for clinical implementation of a smart, multi-lead defibrillator with in-field AMI detection capabilities that enables individualised OHCA treatment strategies and improves survival chances.

Appendices

A.1 Multivariate logistic regression for selection of the two leads used in sets 7 and 8 for the detection of old myocardial infarction

A.1.1 Introduction

Ventricular fibrillation (VF)-waveform analysis of multiple electrocardiogram (ECG) leads may improve detection of old myocardial infarction (OMI)[1,2]. Chapter 4 of this thesis aimed to investigate the effect of feature selection methods on the ability of multi-lead machine learning models to detect OMI. The preliminary research presented in this appendix using multivariate logistic regression (MVR) was conducted to investigate which combination of two leads would be worth exploring more thoroughly in chapter 4.

A.1.2 Methods

Information about the study population can be found in chapter 4, details on the data acquisition and computation of the ventricular fibrillation waveform characteristics (VFWC) can be found in subsection 2.2.1 and the mathematical background of MVR is given in subsection 2.2.2.

Numerous MVR models based on different lead combinations were created to gain insight in which of the twelve leads play a role in distinguishing between patients with and without OMI. Single models of each lead alone were created first and were named models 1 through 12. Models 13 through 25 were created to investigate combinations of leads. Lead II was included in these models since it resembles the paddle ECG; the best performing limb lead was used as well. One of the precordial leads V_1, V_3, V_5 or V_6 was added so that leads covering the entire thorax were included in the combined models. The best performing model with lead II was elaborated on, since it has the most potential for application in clinical practice.

The forward stepwise method based on the likelihood ratio statistic was used to enter VFWC into the models. A p-value of <0.1 was used as a threshold for entry or removal of variables. Model performance was assessed using the classification accuracy at a cut-off level of 0.5. All statistical analyses were performed with IBM SPSS® Statistics software (IBM Corp. Released 2017. IBM SPSS Statistics for Windows, Version 25.0. Armonk, NY: IBM Corp).

A.1.3 Results

Table A.1 shows an overview of the lead combinations used to create the models and the accuracies of these models. The lead aVR model reached the highest accuracy of the limb lead models. The lead V_6 model reached the highest accuracy of the precordial lead models. For the combined models, the highest accuracy was reached by leads aVR and V_1.

The model with leads II and V_1 performed equivalently and was investigated in more detail. The parameters of the model are shown in table A.2. All three included variables contributed significantly to the model ($p \leq 0.001$). The V_1 bandwidth and V_1 amplitude spectrum area (AMSA) showed odds ratios ($exp(b)$) greater than one. Conversely, the lead II low frequency AMSA ($AMSA_{lf}$) had an odds ratio of less than one.

Table A.1: Overview of the lead combinations and the number of ventricular fibrillation waveform characteristics of the multivariate logistic regression models and their accuracies at a cut-off level of 0.5. Accuracies are displayed as a percentage.

Model no.	Limb lead	Precordial lead	no. of VFWC	Accuracy
Limb lead models				
1	I	-	2	60.3
2	II	-	1	60.2
3	III	-	1	58.3
4	aVR	-	1	63.2
5	aVL	-	2	57.9
6	aVF	-	1	58.7
Precordial lead models				
7	-	V_1	3	63.7
8	-	V_2	1	64.0
9	-	V_3	4	65.3
10	-	V_4	1	60.6
11	-	V_5	2	62.3
12	-	V_6	1	66.4
Combined models				
13	II & aVR	-	1	63.1
14	II	V_1	3	69.0
15	II	V_3	6	64.8
16	II	V_5	3	67.4
17	II	V_6	1	66.0
18	aVR	V_1	3	70.0
19	aVR	V_3	5	66.5
20	aVR	V_5	3	64.8
21	aVR	V_6	1	66.4
22	II & aVR	V_1	3	69.5
23	II & aVR	V_3	6	67.0
24	II & aVR	V_5	3	67.4
25	II & aVR	V_6	1	66.4

VFWC: ventricular fibrillation waveform characteristics.

Table A.2: Parameters of the multivariate logistic regression model with ventricular fibrillation waveform characteristics of leads II and V_1.

	b	SE	Wald	df	*p*-value	$exp(b)$ [95% CI]
V_1 bandwidth	0.844	0.262	10.415	1	0.001	2.327 [1.393-3.886]
II $AMSA_{lf}$	-0.253	0.056	20.290	1	<0.001	0.776 [0.695-0.867]
V_1 AMSA	0.138	0.034	16.208	1	<0.001	1.148 [1.073-1.227]
Constant (b_0)	-0.203	0.451	0.202	1	0.653	0.817

AMSA: amplitude spectrum area, $AMSA_{lf}$: low frequency AMSA, b: constant b_0 or regression coefficient b_i, CI: confidence interval, df: degrees of freedom, SE: standard error of b.

A.1.4 Discussion

The model with leads aVR and V_1 reached the highest accuracy. The model with leads II and V_1 performed equivalently, making it an interesting combination since it would be easier to achieve in clinical practice. The combination of the three variables included in this model appeared to have the most discriminative value for the detection of OMI. With odds ratios greater than one, an increase of the V_1 bandwidth and V_1 AMSA would mean a higher likelihood of the patient having an OMI. Oppositely, an increase of lead II $AMSA_{lf}$ would mean a decrease of the likelihood of having an OMI.

It is surprising that the combination of leads II and V_1 delivered one of the best models: among the single lead models, lead aVR seemed to perform better than lead II and lead V_6 reached a higher accuracy than lead V_1. Apparently, combining leads II and V_1 supplied more unique and uncorrelated information about the presence of OMI than the other leads alone or combined. This might be caused by the near orthogonality of the two leads within the patient.

A limitation of the current approach is that the models were assessed only at a cut-off level of 0.5. Possibly, other lead combinations would have performed better when another threshold had been used. The models could have been analysed more thoroughly by evaluating the entire receiver operating characteristic curve.

Furthermore, the differences in accuracies of the models were only a few percent. These minor differences might not fully substantiate the decision to continue further work with the combination of leads II and V_1. However, the three best performing models all included lead V_1. Since lead II resembles the paddle ECG, adding lead V_1 seems sensible.

Concluding, the combination of leads II and V_1 produced an MVR model with reasonable accuracy for the detection of OMI. This lead combination will be used in further research reported in chapter 4 of this thesis.

A.2 Mann-Whitney U test results of ventricular fibrillation waveform characteristics of electrocardiograms acquired during implantable cardioverter-defibrillator testing

Tables A.3 and A.4 contain the p-values of the Mann-Whitney U test performed for all VFWC between the groups with and without an OMI. Table A.5 summarises these findings and shows the amount of VFWC with a significant difference between the two groups. The left half for a p-value of <0.05; the right half for a p-value of <0.1. The p-value of <0.1 is presented besides the conventional p-value of <0.05 since this level of significance was used to determine the composition of the even-numbered sets A.

Table A.3: The p-values of Mann-Whitney U tests of the regular ventricular fibrillation waveform characteristics between the groups with and without old myocardial infarction. Green cells indicate p-values <0.05, yellow cells indicate p-values <0.1. Underlined values indicate that the waveform characteristic was larger for the group with old myocardial infarction.

	I	II	III	aVR	aVL	aVF	V_1	V_2	V_3	V_4	V_5	V_6
MAA	0.075	0.012	0.056	0.012	0.113	0.024	0.898	0.055	0.002	0.001	<0.001	<0.001
MS	0.015	0.007	0.019	0.010	0.080	0.009	0.584	0.030	0.002	0.001	<0.001	<0.001
FM	0.015	0.210	0.153	0.060	0.067	0.231	0.238	0.455	0.099	0.158	0.138	0.044
FD	0.016	0.234	0.235	0.146	0.043	0.283	0.266	0.247	0.066	0.122	0.051	0.025
BW	0.481	0.117	0.321	0.064	0.777	0.684	0.014	0.106	0.015	0.066	0.026	0.125
AMSA	0.209	0.028	0.083	0.028	0.206	0.052	0.024	0.943	0.087	0.001	<0.001	<0.001
$AMSA_{lf}$	0.103	0.006	0.037	0.005	0.122	0.021	0.187	0.282	0.011	0.001	<0.001	<0.001
$AMSA_{hf}$	0.665	0.201	0.223	0.294	0.428	0.197	0.004	0.051	0.702	0.011	<0.001	<0.001
AMSAratio	0.175	0.001	0.112	0.001	0.302	0.024	0.025	<0.001	<0.001	0.007	0.023	0.004
PSA	0.063	0.006	0.022	0.006	0.120	0.011	0.775	0.068	0.002	<0.001	<0.001	<0.001
flucmean	0.138	0.708	0.258	0.259	0.036	0.480	0.941	0.027	0.158	0.829	0.248	0.922
flucvar	0.086	0.604	0.639	0.377	0.165	0.905	0.127	0.931	0.633	0.468	0.706	0.840
flucrms	0.280	0.683	0.719	0.436	0.645	0.535	0.120	0.144	0.336	0.826	0.245	0.139
flucmaa	0.271	0.324	0.621	0.746	0.851	0.309	0.083	0.219	0.302	0.615	0.208	0.235
OI	0.485	0.218	0.789	0.087	0.531	0.293	0.169	0.016	0.008	0.289	0.157	0.012
DFAα1	0.213	0.105	0.437	0.054	0.862	0.317	0.008	0.161	0.021	0.126	0.138	0.333
DFAα2	0.102	0.435	0.351	0.339	0.321	0.287	0.667	0.980	0.281	0.245	0.081	0.092
Total p<0.1	6	6	5	10	4	6	6	7	11	8	10	11

AMSA: amplitude spectrum area, $AMSA_{hf}$: AMSA high frequencies, $AMSA_{lf}$: AMSA low frequencies, BW: bandwidth, DFA: detrended fluctuation analysis, FD: dominant frequency, FM: median frequency, MAA: mean absolute amplitude, MS: median slope, OI: organisation index, PSA: power spectrum area.

Table A.4: The p-values of Mann-Whitney U tests of the ΔV_1 ventricular fibrillation waveform characteristics between the groups with and without old myocardial infarction. Green cells indicate p-values <0.05, yellow cells indicate p-values <0.1. Underlined values indicate that the waveform characteristic was larger for the group with old myocardial infarction.

	I	II	III	aVR	aVL	aVF	V_1	V_2	V_3	V_4	V_5	V_6
ΔV_1 MAA	0.038	<0.001	0.017	0.002	0.094	0.003	XXXXX	0.010	<0.001	<0.001	<0.001	<0.001
ΔV_1 MS	0.026	0.001	0.011	0.007	0.056	0.005	XXXXX	0.007	<0.001	<0.001	<0.001	<0.001
ΔV_1 FM	0.023	0.973	0.566	0.267	0.178	0.722	XXXXX	0.494	0.324	0.898	0.636	0.062
ΔV_1 FD	0.023	0.797	0.958	0.605	0.500	0.816	XXXXX	0.835	0.262	0.624	0.171	0.076
ΔV_1 BW	0.199	0.629	0.263	0.802	0.052	0.234	XXXXX	0.493	0.855	0.980	0.906	0.555
ΔV_1 AMSA	0.001	<0.001	<0.001	<0.001	0.001	<0.001	XXXXX	0.209	0.001	<0.001	<0.001	<0.001
ΔV_1 $AMSA_{lf}$	0.004	<0.001	0.001	<0.001	0.007	<0.001	XXXXX	0.011	<0.001	<0.001	<0.001	<0.001
ΔV_1 $AMSA_{hf}$	0.001	<0.001	<0.001	<0.001	<0.001	<0.001	XXXXX	0.574	0.030	<0.001	<0.001	<0.001
ΔV_1 AMSAratio	0.377	0.905	0.350	0.436	0.300	0.488	XXXXX	0.046	0.104	0.928	0.918	0.902
ΔV_1 PSA	0.010	<0.001	0.004	0.002	0.021	<0.001	XXXXX	0.008	<0.001	<0.001	<0.001	<0.001
ΔV_1 flucmean	0.273	0.957	0.361	0.250	0.257	0.496	XXXXX	0.072	0.459	0.839	0.613	0.635
ΔV_1 flucvar	0.576	0.458	0.167	0.684	0.528	0.291	XXXXX	0.166	0.033	0.034	0.508	0.159
ΔV_1 flucrms	0.620	0.051	0.057	0.335	0.309	0.040	XXXXX	0.805	0.402	0.207	0.519	0.896
ΔV_1 flucmaa	0.458	0.017	0.029	0.107	0.259	0.016	XXXXX	0.503	0.426	0.333	0.574	0.746
ΔV_1 OI	0.830	0.967	0.576	0.369	0.550	0.880	XXXXX	0.290	0.212	0.899	0.543	0.076
ΔV_1 DFAα1	0.286	0.367	0.149	0.882	0.122	0.255	XXXXX	0.526	0.941	0.319	0.729	0.439
ΔV_1 DFAα2	0.126	0.843	0.839	0.758	0.720	0.848	XXXXX	0.335	0.734	0.709	0.349	0.294
Total	8	8	8	6	7	8	XXXXX	6	7	7	6	9

AMSA: amplitude spectrum area, $AMSA_{hf}$: AMSA high frequencies, $AMSA_{lf}$: AMSA low frequencies, BW: bandwidth, DFA: detrended fluctuation analysis, FD: dominant frequency, FM: median frequency, MAA: mean absolute amplitude, MS: median slope, OI: organisation index, PSA: power spectrum area.

Table A.5: The amount of ventricular fibrillation waveform characteristics with a significant difference between the groups with and without old myocardial infarction per lead, for the significance levels of p<0.05 and p <0.1.

	p<0.05			*p<0.1*		
	Regular (n = 17)	ΔV_1 (n = 17)	Total (n = 34)	Regular (n = 17)	ΔV_1 (n = 17)	Total (n = 34)
I	3	8	11	6	8	14
II	6	7	13	6	8	14
III	3	7	10	5	8	13
aVR	6	6	12	10	6	16
aVL	2	4	6	4	7	11
aVF	5	8	13	6	8	14
V_1	5	-	5	6	-	6
V_2	4	5	9	7	6	13
V_3	8	7	15	11	7	18
V_4	7	7	14	8	7	15
V_5	8	6	14	10	6	16
V_6	10	6	16	11	9	20
Total	67	71	138	90	80	170

A.3 Ventricular fibrillation waveform characteristics in sets 1B-8B of electrocardiograms acquired during implantable cardioverter-defibrillator testing

Table A.6 shows an overview of the VFWC in sets 1B through 8B of ECGs acquired during implantable cardioverter-defibrillator testing. These sets of input features were used to detect OMI using support vector machines (SVMs).

As is described in chapter 4, the stepwise entry method for MVR resulted in the composition of sets 1B through 8B. Chapter 2 covers how the stepwise entry method works. The method used in chapter 4 was slightly expanded with regard to the removal of variables in order to prevent overfitting. These extra steps are explained in the following section.

A.3.1 Rationale

Overfitting may occur when the number of input variables for MVR is too large. Even when a stepwise entry method is used, the amount of included variables may exceed the one in ten rule. This is a rule of thumb which states that a maximum of one predictor variable can be used per ten events to prevent overfitting[3,4]. In this thesis, one patient of the smallest of the two groups is considered an event. Since the smallest group, the group with no OMI, contains approximately 100 patients, the one in ten rule dictates that a maximum of ten predictor variables should be used in MVR to minimise the risk of overfitting.

A.3.2 Method

Sets 3A, 5A and 6A contained a large amount of input variables: 204, 391 and 170 respectively. This likely contributed to a number of variables in the initial sets 3B, 5B and 6B exceeding the one in ten rule: 16, 28 and 14 respectively. Three new MVR models were created using these selections of variables. The stepwise entry method once again proposed subsets, thereby reducing the number of included variables. These reduced numbers of variables were used to create new models yet again and this process was repeated until no more variables were removed. The new sets 3B, 5B and 6B contained a smaller number of variables: 13, 20 and 11 respectively. Nonetheless, these amounts still exceeded the one in ten rule that imposed a maximum of ten predictor variables to minimise the risk of overfitting. Therefore, the final sets 3B, 5B and 6B were obtained by including only the first ten variables that were added during stepwise inclusion. As such, the final sets B contained a maximum of ten predictor variables. Table A.6 gives an overview of the variables included in each of the sets 1B through 8B.

Table A.6: The ventricular fibrillation waveform characteristics in sets 1B-8B of electrocardiograms acquired during implantable cardioverter-defibrillator testing, in order of inclusion. These sets were used for detecting old myocardial infarction.

	1B (n = 3)	2B (n = 1)	3B (n = 10)	4B (n = 6)	5B (n = 10)	6B (n = 10)	7B (n = 5)	8B (n = 3)
1	II, PSA	II, PSA	V_6, MS	V_6, MS	V_6, ΔV_1 AMSA	V_6, ΔV_1 AMSA	II, ΔV_1 AMSA	II, ΔV_1 flucmaa
2	II, flucmaa		V_2, AMSAratio	V_2, AMSAratio	aVF, ΔV_1 flucmaa	V_2, AMSAratio	II, ΔV_1 flucmaa	V_1, BW
3	II, BW		V_1, $AMSA_{lf}$	V_1, AMSA	II, BW	V_1, BW	V_1, BW	II, ΔV_1 PSA
4			V_4, flucvar	V_1, BW	V_1, BW	II, ΔV_1 MAA	II, BW	
5			V_1, BW	II, AMSA	V_3, ΔV_1 PSA	aVF, ΔV_1 flucmaa	II, ΔV_1 FM	
6			II, AMSA	III, MAA	V_2, ΔV_1 $AMSA_{hf}$	V_6, ΔV_1 OI		
7			II, flucmaa		aVL, flucmean	V_3, ΔV_1 flucvar		
8			II, BW		V_2, $AMSA_{lf}$	aVL, flucmean		
9			III, flucmean		V_2, DFAα1	V_3, OI		
10			V_5, FD		V_3, ΔV_1 OI	V_1, flucmaa		

AMSA: amplitude spectrum area, $AMSA_{hf}$: AMSA high frequencies, $AMSA_{lf}$: AMSA low frequencies, BW: bandwidth, DFA: detrended fluctuation analysis, FD: dominant frequency, FM: median frequency, MAA: mean absolute amplitude, MS: median slope, OI: organisation index, PSA: power spectrum area.

A.4 Optimised hyperparameters of support vector machines for detecting old myocardial infarction

Table A.7: Optimised hyperparameters of the sixteen support vector machines for detecting old myocardial infarction.

Set	no. of VFWC	Min. objective	Box constraint	Kernel scale	Kernel function	Polynomial order	Standardisation	False-positive cost
				SVM A				
1A	17	0.3750	0.035	-	Linear	-	False	1
2A	6	0.3760	2.381	-	Linear	-	True	5
3A	204	0.2832	21.870	51.724	Gaussian	-	True	2.5
4A	90	0.2783	0.011	-	Linear	-	True	1
5A	391	0.2876	0.007	-	Linear	-	True	2.5
6A	170	0.2599	0.008	-	Linear	-	True	1
7A	51	0.3165	663.709	93.024	Gaussian	-	False	2.5
8A	20	0.3080	0.001	-	Polynomial	2	False	1
				SVM B				
1B	3	0.3792	2.382	-	Polynomial	4	True	1
1B	1	0.3554	13.496	0.034	Gaussian	-	False	1
3B	10	0.2869	528.688	24.741	Gaussian	-	False	1
4B	6	0.3792	2.382	-	Polynomial	4	True	1
5B	10	0.2381	995.447	55.158	Gaussian	-	True	5
6B	10	0.2424	11.547	13.709	Gaussian	-	True	2.5
7B	5	0.2658	0.110	-	Polynomial	2	True	5
8B	3	0.2869	1.685	-	Linear	-	False	1

SVM: support vector machine, VFWC: ventricular fibrillation waveform characteristics.

A.5 Ventricular fibrillation waveform characteristics in sets 1B-6B of electrocardiograms acquired during out-of-hospital cardiac arrest

Table A.8 shows an overview of the VFWC in sets 1B through 6B of ECGs acquired during out-of-hospital cardiac arrest. These sets of input features were used to detect acute myocardial infarction using SVMs.

Table A.8: The ventricular fibrillation waveform characteristics in sets 1B-6B of electrocardiograms acquired during out-of-hospital cardiac arrest, in order of inclusion. These sets were used for detecting acute myocardial infarction.

	1B (n = 2)	2B (n = 1)	3B (n = 1)	4B (n = 1)	5B (n = 2)	6B (n = 2)
1	VF_1, AMSA	VF_1, AMSA	VF_2, MS	VF_2, MS	VF_2, MS	VF_2, MS
2	VF_1, DFAα2				VF_1, flucvar	$\Delta_{1,2}$, BW

AMSA: amplitude spectrum area, BW: bandwidth, DFA: detrended fluctuation analysis, MS: median slope, VF_1: the last segment before the first defibrillation shock, VF_2: the last segment before the second defibrillation shock, $\Delta_{1,2}$: the differences between the waveform characteristics of segments VF_1 and VF_2.

A.6 Optimised hyperparameters of support vector machines for detecting acute myocardial infarction

Table A.9: Optimised hyperparameters of the twelve support vector machines for detecting acute myocardial infarction.

Set	no. of VFWC	Min. objective	Box constraint	Kernel scale	Kernel function	Polynomial order	Standardisation	False-positive cost
				SVM A				
1A	17	0.3663	0.047	-	Linear	-	True	1
2A	12	0.2970	6.897	-	Polynomial	2	False	5
3A	17	0.2727	0.282	-	Linear	-	True	1
4A	8	0.2424	525.832	1.247	Gaussian	-	True	5
5A	51	0.2154	0.005	-	Polynomial	2	True	2.5
6A	22	0.2615	1.605	3.257	Gaussian	-	True	20
				SVM B				
1B	2	0.2843	411.533	14.430	Gaussian	-	False	10
1B	1	0.2843	53.384	1.603	Gaussian	-	True	10
3B	1	0.3056	195.997	-	Polynomial	3	False	2.5
4B	1	0.3056	195.997	-	Polynomial	3	False	2.5
5B	2	0.2535	0.585	-	Polynomial	3	True	1
6B	2	0.2083	0.005	-	Polynomial	4	False	1

SVM: support vector machine, VFWC: ventricular fibrillation waveform characteristics.

References

[1] Judith L. Bonnes et al. “Ventricular fibrillation waveform characteristics differ according to the presence of a previous myocardial infarction: A surface ECG study in ICD-patients”. In: *Resuscitation* 96 (Nov. 2015), pp. 239–245. ISSN: 18731570. DOI: 10.1016/j.resuscitation.2015.08.014.

[2] Jos Thannhauser et al. “Computerized analysis of the ventricular fibrillation waveform allows identification of myocardial infarction: a proof-of-concept study for smart defibrillator applications in cardiac arrest”. In: *Journal of the American Heart Association* (2020).

[3] Frank E. Harrell, Kerry L. Lee, and Daniel B. Mark. “Multivariable prognostic models: Issues in developing models, evaluating assumptions and adequacy, and measuring and reducing errors”. In: *Statistics in Medicine* 15.4 (Feb. 1996), pp. 361–387. ISSN: 02776715. DOI: 10.1002/(SICI)1097-0258(19960229)15:4<361::AID-SIM168>3.0.CO;2-4.

[4] Peter Peduzzi, John Concato, Elizabeth Kemper, Theodore R. Holford, and Alvan R. Feinstem. “A simulation study of the number of events per variable in logistic regression analysis”. In: *Journal of Clinical Epidemiology* 49.12 (Dec. 1996), pp. 1373–1379. ISSN: 08954356. DOI: 10.1016/S0895-4356(96)00236-3.